THESIS

COMMANDEERING OF THE CELLULAR HUR PROTEIN BY ALPHAVIRUSES AFFECTS THE REGULATION OF HOST POST-TRANSCRIPTIONAL GENE EXPRESSION

Submitted by

Michael D. Barnhart

Graduate Degree Program in Cell and Molecular Biology

In partial fulfillment of the requirements

For the Degree of Master of Science

Colorado State University

Fort Collins, Colorado

Spring 2013

Master's Committee:

Advisor: Jeffrey Wilusz

Paul J. Laybourn
Carol J. Wilusz

ABSTRACT

COMMANDEERING OF THE CELLULAR HUR PROTEIN BY ALPHAVIRUSES AFFECTS THE REGULATION OF HOST POST-TRANSCRIPTIONAL GENE EXPRESSION

It was previously shown that cellular HuR protein binds to a U-rich region in the 3'UTR of Sindbis virus RNA resulting in stabilization of viral transcripts and increased replication efficiency. While the presence of this U-rich region is generally conserved among alphaviruses, a subset lacks a typical U-rich region. The 3'UTR of two alphaviruses – Ross River virus and Chikungunya virus – that do not contain a typical U-rich region were tested for HuR interactions by Electrophoretic Mobility Shift Assay. HuR protein bound these 3'UTRs with nanomolar affinities, similar to what was observed for the U-rich region of Sindbis virus. These observations demonstrate that the critical role for HuR-mediated viral RNA stabilization is likely a conserved property of most, if not all, members of the virus family. By analyzing deletion derivatives, we mapped the novel HuR binding sites in these two viruses to specific regions in their 3'UTR.

Next, we uncovered four novel aspects of virus-host interaction and pathogenesis related to the high affinity interaction between the 3'UTR of alphaviruses and the cellular HuR protein. First, HuR protein, which is usually localized predominantly to the nucleus, dramatically accumulates in the cytoplasm during Sindbis virus (SinV) infection. Studies involving the transfection of constructs that express viral 3'UTR RNA fragments indicated that the mechanism of induction of HuR accumulation to the cytoplasm in infected cells is due to the viral RNA acting as a sponge for the protein. Second, HuR interaction with numerous cellular mRNAs was

found to be drastically decreased during a SinV infection and was associated with dramatic destabilization of the cellular transcripts as determined by mRNA half-life analysis. Third, we found that the reduced amounts of free HuR during a SinV infection results in the increased targeting of mRNAs by miRNAs. Together, these data indicate that in the process of commandeering the cellular HuR protein for its own use, alphaviruses are also effectively destabilizing numerous cellular mRNAs. Interestingly, many of the cellular mRNAs affected by alphaviruses play key roles in inflammation, innate immune responses and other fundamental cellular processes. Finally, we observed a novel effect of SinV infection on alternative polyadenylation of cellular transcripts. This is likely a direct result of sequestration of the HuR protein in the cytoplasm by the virus, preventing the protein from influencing nuclear polyadenylation site choice. Intriguingly, SinV infection influences the poly(A) site choice of the HuR pre-mRNA, favoring a more translatable isoform to promote the overexpression of this viral host factor. Therefore, the alphaviral-induced alterations in cellular mRNA stability and polyadenylation identified in this thesis may play a very important but underappreciated role in pathogenesis.

ACKNOWLEDGEMENTS

First off, I would like to send many thanks to Drs. Jeff and Carol Wilusz because I know if it wasn't for their generosity to allow me into the lab, I would have never accomplished so much in such a short amount of time. Both of them taught me how to walk and talk like a scientist and to question any data that seems ambiguous. I cannot thank you enough for the other important scientific skills I learned such as experimental procedures, how to present data, and how to write scientifically. Jeff constantly motivated me to explore his crazy ideas and I did without hesitation because he was always there for me when I needed advice, help with an experiment, or writing edits despite his busy schedule. Furthermore, I could not have made it without Jeff's hilarious jokes. Carol definitely influenced me to learn every little detail about every experiment I performed and to be confident in myself. Finally, I would like to thank my third committee member Dr. Paul Laybourn for teaching me the ins and outs of ethical scientific research.

Secondly, I would like to thank Stephanie Moon because if it weren't for her excellent experimental expertise I would not have made it a month in the lab. Stephanie was always patient with me and inspired me to become a better scientist. Also, I would like to thank John Anderson for giving me experimental advice and for the thorough explanations of every question I posed. Furthermore, I want to extend my thanks to every member of the Wilusz lab for providing me with experimental advice, laughter, and the occasional awkwardness.

Finally, I would like to thank my loving wife, Ashley Barnhart, for her never-ending love, kindness, understanding and support. I would also like to thank my parents, Dennis and Louise Barnhart for their love and support through this journey. Last but definitely not least, I

would like to thank all my family and friends for their support and words of encouragement along the way, especially Hunter Kent who was always there to lend an ear no matter the subject of topic.

All-in-all, everyone listed here has played a critical role in my success over the past couple years and I couldn't have done it without them. Thank you.

TABLE OF CONTENTS

LIST OF TABLES

LIST OF FIGURES

INTRODUCTION

Alphavirus species have long been studied due to their significant impact on both human and veterinary health. Alphaviruses are generally transmitted to mammals via mosquito vectors. Recent epidemic outbreaks of alphaviral infections are largely due to the introduction of alphaviruses into naïve mosquito populations. Studies have shown that some of the largest arbovirus outbreaks have been due to alphavirus species (Calisher, 1994; Ligon, 2006). Alphaviral pathology of infection, the molecular biology of their life cycles, the epidemiology of the diseases they cause, and their method of transmission have all well been studied since their discovery; however, there are currently no effective anti-alphavirals available. An understudied area of pathogenesis is the alphaviral-induced alterations of host cellular post-transcriptional regulation of mRNAs. Therefore, since it was previously shown that the binding of the cellular HuR protein to alphaviruses is necessary for the virus to grow to high titers (Garneau et al., 2008; Sokoloski et al., 2010), the goal of this thesis was to explore what effects this has on the host cell, particularly mRNA stability and polyadenylation, and to determine the viral mechanism of HuR commandeering. These effects may play a very important but underappreciated role in viral pathogenesis. The identification of these novel pathways of pathogenesis will hopefully breathe new life into the development of effective anti-alphavirals.

I. Alphavirus Biology

a. Overview. The genus *Alphavirus* belongs to the family *Togaviridae* and comprises a diverse group of positive sense single-stranded RNA viral species separated by serogroup and geographical location. Geographically, alphaviruses are classified as either Old World

(emerging from the Eastern hemisphere) or New World (emerging from the Western hemisphere) (Luers et al., 2005; Powers et al., 2001). Although not all alphaviruses are arthropod-borne viruses (i.e. arboviruses), a majority of them are transmitted via mosquito vectors. Alphaviruses cause a variety of diseases of humans, including rash, arthritis, and encephalitis. The recent emergence of Chikungunya virus resulting in large scale epidemics in Africa and Southeast Asia illustrate the public health importance of the alphavirus group (Thiboutit et al, 2010). Sindbis virus, an Old World alphavirus, serves as the laboratory model for the group. This thesis focuses primarily on an analysis of Sindbis virus-host cell interactions; however, aspects of Chikungunya and Ross River viruses were also analyzed to measure our ability to generalize aspects of our analyses to other members of the group.

b. Molecular Biology of Alphaviruses. In order for a cell to become infected with an alphavirus, the pathogen must first be endocytosed by the target cell. Cell receptors involved in this process include liver and lymph node-SIGN (L-SIGN; also known as CLEC4M), heparin sulphate, laminin, integrins, and the ICAM3-grabbing non-integrin 1 (DC-SIGN; also known as CD209; which is dendritic cell-specific) (Schwartz and Albert, 2010). Although these receptors have been identified as virus-interacting moieties, their relative importance to alphavirus infection has not yet been fully uncovered (Wang et al., 1992; Strauss et al., 1994). As the endosome forms, the increasingly acidic environment results in a conformational change of the glycoproteins of the viral envelope which exposes the fusion domain of the viral E1 protein. The viral E1 protein can then fuse with the endosome membrane and the nucleocapsid core and viral genome are deposited into the cytoplasm of the target cell. Once deposited, the viral RNA undergoes translation by the host translation machinery. This is possible because the positive-sense alphavirus ~9-11kb genomic RNA contains a 5' 7-methyl guanosine cap and a 3' poly(A)

tail which makes it look very similar to endogenous cellular mRNA (Strauss and Strauss, 1994). Translation of the viral genomic RNA results in a polyprotein which then undergoes proteolytic processing to form the four nonstructural proteins (nsPs).

The synthesis of the viral RNA negative strand is mediated by non-structural protein 1 (nsP1), which also has RNA capping activity (Wang et al., 1991; Ahola et al., 1997) and appears to play a role as an antagonist of BST2/tetherin to enable virus release from cells (Jones et al., 2013). Non-structural protein 2 (nsP2) has RNA helicase, RNA triphosphatase, and proteinase activity (Strauss et al., 1992; Hardy and Strauss, 1989), and in Old World alphaviruses it is known to shut-off host transcription (Gorchakov et al., 2005; Gorchakov et al., 2004; Frolov et al., 1999; Garmashova et al., 2006). It also appears to have a direct or indirect role in packaging of the viral genomic RNA (Kim et al., 2013) and may play a role in the induction of protective immune responses (Bao et al., 2013). Until recently, the function of nsP3 was unknown; however, now it has been shown to interact with Ras-GAP SH3 domain-binding protein (G3BP) and by doing so it inhibits stress granule assembly (Fros et al, 2012). The fourth nonstructural protein, nsP4, results from read through of an opal termination codon to form the nsP1234 polyprotein. It is the RNA-dependent RNA polymerase (RdRP) (Sawicki et al., 1990; Barton et al., 1988; Lemm et al., 1998) and has also been show to exhibit poly(A) polymerase-like activities (Tomar et al., 2006). Just recently, it was also shown to suppress eIF2α phosphorylation (Rathore et al., 2013). Together, these proteins form the viral replication complex.

The viral replication complex synthesizes an intermediate full length viral RNA negative strand. From this RNA template, both genomic (49S) and subgenomic (26S) RNAs can be synthesized. The structural C-pE2-6K-E1 polyprotein is translated from the subgenomic RNA

and is inserted into the endoplasmic reticulum. Following autoproteolytic serine protease processing of the polyprotein, the capsid (C) is released while pE2 and E1 glycoproteins undergo further processing by associating with the Golgi apparatus and are then transported to the plasma membrane. pE2 is then cleaved into E2 and E3. The viral nucleocapsid binds to the viral genomic RNA and promotes viral assembly by recruiting the membrane-associated envelope glycoproteins. Once properly assembled, the mature virion buds off the host cell membrane. Refer to Figure 1 for a pictorial representation of the life cycle of alphaviruses (adapted from Schwartz and Albert, 2010).

While much attention has been paid to elucidating the function of the coding regions of the alphavirus genome, the role of the non-coding regions in virus-host interactions is still relatively unexplored. The 5' end of the genome contains a set of four predicted stem loop structures that are thought to play a role in determining negative strand replication efficiency (Nickens and Hardy 2008). A similar role is envisioned for the 3'UTR in plus-strand synthesis, although the precise roles of individual RNA elements have not been well-described. Therefore, the focus of our study was to elucidate novel roles and relationships for the 3'UTR of alphaviruses in host-viral interactions.

c. Alphavirus 3'UTR Organization. As shown in Figure 2, the majority of alphavirus 3'UTRs consist of three main elements. The set of repeat sequence elements (RSEs) are located towards the 5' end of the 3'UTR and widely differ between alphavirus species in composition and number (Ou et al., 1982; Khan et al., 2002; Saleh et al., 2003). The secondary structures formed by these RSEs are thought to recruit RNA binding proteins (George and Raju, 2000).

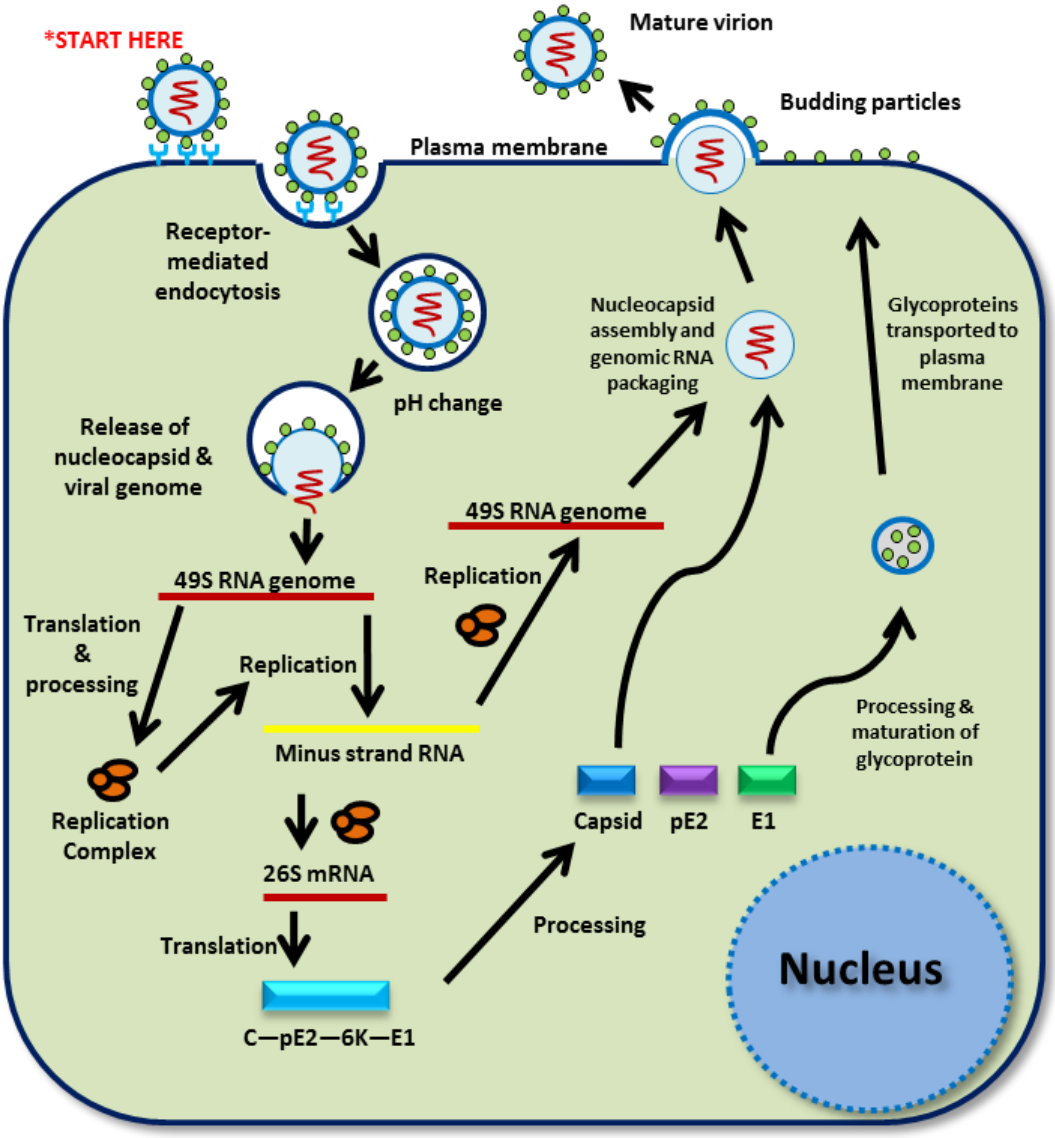

Figure 1. The Life Cycle of an Alphavirus. Beginning at the indicated "*START HERE," the virus particle binds to receptors presented on the plasma membrane and undergoes receptor-mediated endocytosis. The endosome containing the virus experiences a change in pH, resulting in the conformational change of the viral capsid proteins so the viral genome can be deposited in the host cell's cytoplasm. The viral genome is then translated by host translation machinery, resulting in the formation of the viral replication complex. The viral replication complex transcribes the viral minus strand RNA followed by the 26S mRNA. Translation of the 26S mRNA produces the viral polyprotein which is then cleaved and processed into structural components of the virion. The glycoproteins are processed and transported to the plasma membrane while the nucleocapsid and the viral genomic RNA are packaged and exocytosed, resulting in the formation of mature virions. Adapted from Schwartz and Albert, *Nature Reviews Microbiology*, 2010.

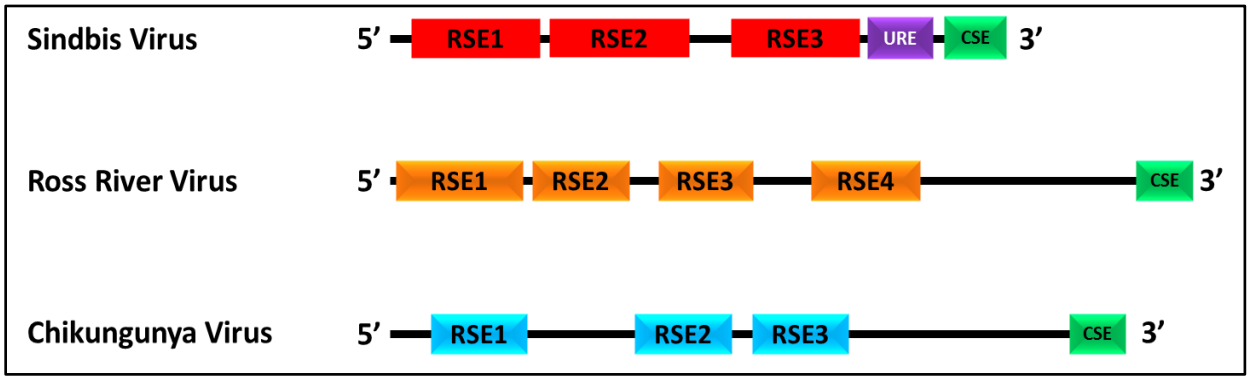

Figure 2. Alphavirus 3'UTR Organization. The Sindbis virus 3'UTR, like the majority of alphavirus species, contains repeat sequence elements (RSEs), a U-rich element (URE) and a conserved sequence element (CSE). However, some alphaviruses including Ross River and Chikungunya viruses lack the "typical" URE in their 3'UTR.

Located just upstream from the poly(A) tail of the 3'UTR is the conserved sequence element (CSE). The CSE is a 19 nucleotide conserved element between all alphavirus species and aids in the replication of the genomic viral RNA (Strauss and Strauss, 1994; Hardy and Rice, 2005; Hardy, 2006). Upstream of the CSE is the U-rich element (URE). The URE is a 40 nucleotide element and has been shown to bind the cellular HuR protein to stabilize and protect the viral RNA from host RNA decay machinery (Sokoloski et al., 2010). Although a majority of alphavirus species (such as Sindbis Virus, Semliki Forest Virus, and Eastern Equine Encephalitis Virus) contain the "typical" URE, some species do not, such as Chikungunya (ChikV) and Ross River (RRV) viruses (Fig. 2).

d. Alphavirus Interactions with Host Proteins. Alphavirus have been shown to interact with several host cellular proteins. For example, Sindbis viral RNA translation is enhanced by binding of host hnRNP A1 to the 5'UTR of Sindbis virus (Lin et al., 2009). Conversely, the binding of ZAP (zinc-finger antiviral protein) severely inhibits viral growth (Bick et al., 2003). Furthermore, a recent study has shown that the binding of several cellular proteins by the Chikungunya late replicase complex assembly is necessary for progeny RNA synthesis (Sreejith et al., 2012). However, the protein of interest in this study is the cellular HuR protein.

The cellular HuR protein has been shown to bind with high affinity to both the URE and the CSE within the Sindbis virus 3'UTR (Garneau et al., 2008; Sokoloski et al., 2010). The binding of this cellular factor results in the repression of host RNA decay machinery; thereby, allowing the virus to efficiently infect the host and grow to high viral titers (Garneau et al., 2008; Sokoloski et al., 2010). In normal resting mammalian cells, the cellular HuR protein mainly resides in the nucleus (Fan and Steitz, 1998a). However, multiple alphaviruses have been shown to cause a cytoplasmic accumulation of HuR during an infection (Sokoloski et al., 2010; Dickson

et al., 2012). Therefore, the relationship between alphaviruses and the cellular HuR protein plays an important yet understudied role in viral pathogenesis. This thesis explores this relationship and the impacts it has on the host cell, such as the dysregulation of host posttranscriptional gene expression.

II. Cellular mRNA Decay Pathways and Regulation

As revealed above, alphavirus RNAs are capable of avoiding host decay machinery by binding the cellular factor HuR. There are two main categories of cytoplasmic cellular mRNA decay pathways: typical RNA decay which begins with deadenylation or specialized RNA decay which is triggered by endonucleolytic cleavage or exosome recruitment.

a. Typical Cellular mRNA Decay. In order to remove undesired or abnormal RNAs, the cell must degrade them, as shown in Figure 3. The deadenylation of RNA is typically the first and rate limiting step in this decay pathway (Chen and Shyu, 2011). CCR4, CAF1, PARN, and PAN2/3 have been identified as deadenylase enzymes (Fabian et al., 2011; Collart et al., 2012). Upon deadenylation, the body of the RNA is subjected to exonucleolytic decay from either the 5'-to-3' and/or 3'-to-5' direction. The association of the LSm1-7 complex and PAT1 with the 3' end of the deadenylated RNA signals factors to remove the m^7Gppp cap from the 5' end, which is indicative of the initiation of 5'-to-3' exonucleolytic decay pathway (Chowdhury et al., 2012). DCP2 and Nutd16 were the only identified decapping enzymes (Liu et al., 2008) until recently when Nudt2, Nudt3, Nudt12, Nudt15, Nudt17 and Nudt19 were identified to have decapping activity (Song et al, 2013). Next, the highly processive 5'-to-3' exoribonuclease XRN1 binds to

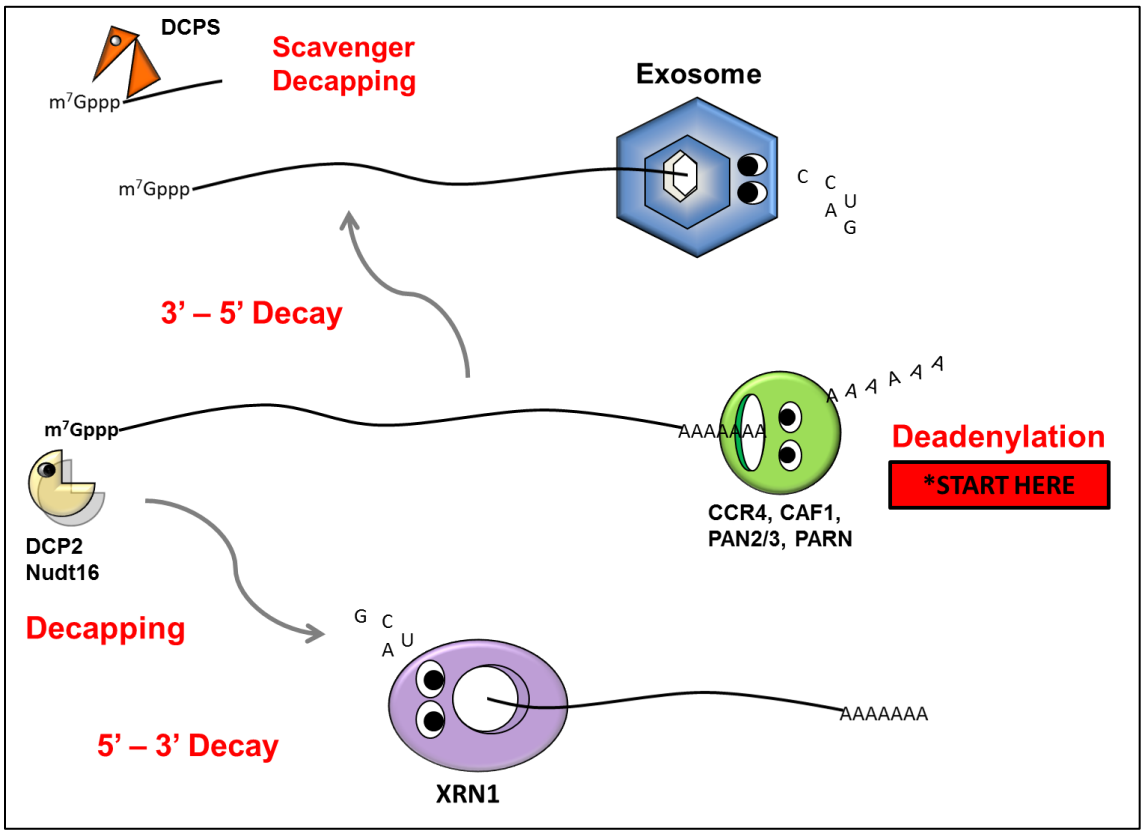

Figure 3. Typical mRNA Decay Pathways. Once RNA becomes deadenylated, it can either undergo 3'-to-5' decay by the exosome or 5'-to-3' decay by XRN1. Scavenger decapping occurs in the 3'-to-5' decay pathway, once the RNA has been almost fully degraded by the exosome. Decapping in the 5'-to-3' decay pathway must occur first to create the substrate for XRN1 to bind.

the 5’ monophosphate substrate created by the decapping enzyme (Chang et al., 2011), resulting in the degradation of the transcript into single nucleotides.

The 3’-to-5’ exonucleolytic decay pathway is initiated by the binding of the cytoplasmic exosome to the 3’ end of the deadenylated RNA. This exosome contains a PIN domain-mediated endonucleolytic activity and an RNase II-like hydrolytic exonuclease in the DIS3 subunit (Lykke-Andersen et al., 2011). Scavenger decapping activity (DCPS) removes and recycles the 5’ cap once the exosome degrades the majority of the RNA (Liu et al., 2008).

b. Specialized Cellular mRNA Decay. Endonucleases such as PMR1, IRE1, G3BP, SMG6, APE1 and Zc3h12a/MCPIP can trigger specialized decay via the endonucleolytic cleavage of RNAs (Schoenberg, 2011). During a viral infection, another endonuclease, RNase L, has been shown to be up-regulated (Chakrabarti et al., 2011). Furthermore, endonucleolytic cleavage of mRNAs can be mediated by the argonaute protein associated with the RNA-induced silencing complex (RISC; Davidson and McCray, 2011). UPF1-3 and SMG proteins are involved in nonsense mediated decay (NMD) resulting in endonucleolytic cleavage (Yepiskoposyan et al., 2011). Additionally, no-go decay is triggered when ribosomes become stalled on an mRNA, resulting in the mediation of decay of the mRNA and the dysfunctional 18S rRNA by the DOM34-Hbs1 (Becker et al., 2011). The SKI complex mediates the decay of mRNAs that lack a termination codon, also known as nonstop mRNA decay (Schaeffer and van Hoof, 2011). Lastly, short poly(A) or poly(U) sequences can be attached to structured RNAs by a non-canonical poly(A/U) polymerase thereby providing a landing pad for the exosome and initiating decay (Ibrahim et al., 2006). These pathways are illustrated in Figure 4.

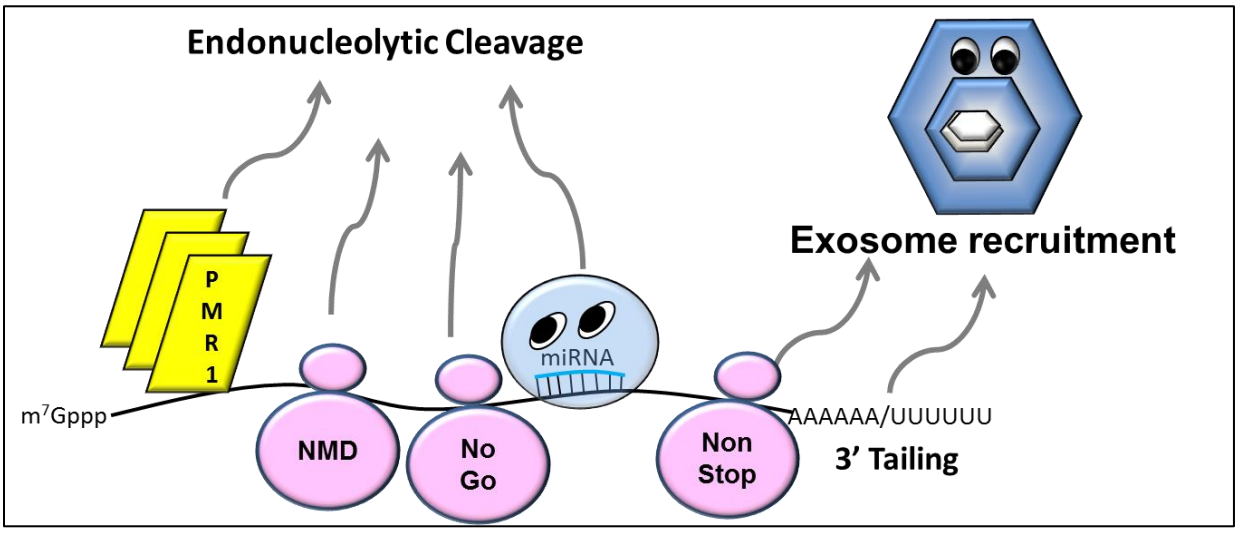

Figure 4. Specialized mRNA Decay Pathways. Endonucleases (in yellow) or ribosome associated proteins involved in nonsense mediated decay (NMD), no-go decay, or miRNA decay result in the endonucleolytic cleavage of RNAs. Proteins involved in nonstop decay or 3' tailing result in exosome recruitment.

c. 3'UTR Regulatory Elements. mRNA decay is highly regulated by 3'UTR elements. These regulatory elements include AU-rich elements, GU-rich elements, UGUA elements and miRNA binding sites. Several mRNA binding proteins have been identified to influence the stability of their target mRNAs. For example, HuR and PCBP2 have been shown to stabilize their target mRNAs (Mukherjee, et al., 2011; Xin et al., 2011), while tristetraprolin (TTP), AUF1, and KSRP have been shown to destabilize the mRNAs they associate with (Kratochvill et al., 2011; Gratacós and Brewer, 2010; Gherzi et al., 2010). The stability or lack thereof, of the targeted mRNAs possibly results from the combinatorial association of these factors, the translation machinery and the mRNA's subcellular localization (Moon et al., 2012).

III. Cellular Alternative Polyadenylation

Although there are multiple post-transcriptional processing steps for every mRNA produced, such as capping and splicing, one focus of this thesis is on alternative polyadenylation during a Sindbis virus infection. Nascent mRNAs become mature mRNAs once they are cleaved and polyadenylated. When the final sequences of the mRNA are transcribed, the 3' end formation machinery, including the Cleavage/Polyadenylation Specificity Factor (CPSF) and the Cleavage Stimulation Factor (CStF), assembles and cleaves the newly transcribed message (Mandel et al., 2006). CPSF binds the core (AAUAAA) upstream element, while CStF binds the U-rich downstream element located on the 3' end of the newly synthesized message which results in the cleavage between these two elements by CPSF (Mandel et al., 2006). Once cleavage occurs, a poly(A) tail is created by the addition of adenosine residues on the 3' end of the mRNA by a poly(A) polymerase (Sheets and Wickens, 1989). Polyadenylation is necessary

as it protects the mRNA from decay enzymes and promotes its translation. To modulate gene expression, cells can influence the polyadenylation of genes which results in the production of multiple transcripts from one gene. By changing the 3'UTR sequence of an mRNA, its stability, localization and translation may be affected. It is estimated that approximately 50% of mRNAs can be alternatively polyadenylated (Tian et al., 2005; Wang et al., 2013).

IV. The Role of HuR in Cellular Processes.

As discussed above, the cellular HuR protein plays an important role in alphavirus pathogenesis, given that it binds to alphavirus RNAs and protects them from degradation. However, this RNA binding protein is involved in several cellular processes. Human antigen R (HuR or HuA) or embryonic lethal abnormal vision (ELAV)-like protein 1 is encoded by the *ELAVL1* gene and is expressed in a wide variety of cell types (Ma et al., 1996; Good, 1995). The architecture of the HuR protein, as shown in Figure 5, consists of three RNA Recognition Motifs (RRMs) and a Hinge region. RRM1 and RRM2 have been shown to bind AU-rich elements (AREs) on mRNAs (Chen et al., 2002), while RRM3 interacts with poly(A) sequences (Ma et al., 1997). The HuR nucleocytoplasmic shuttling (HNS) sequence lies in the Hinge region (Fan and Steitz, 1998a).

a. *Regulation of mRNA Decay by the RNA Binding Protein HuR*. HuR interacts with approximately 15% of the cellular transcriptome (López de Silanes et al., 2004; Lebedeva et al., 2011) and it has been identified as a key regulator of post-transcriptional mRNA metabolism (Fan and Steitz, 1998b; Peng et al., 1998). When HuR binds target mRNAs, one of its roles is to stabilize and protect the mRNAs from degradation and increase its translation. However, HuR

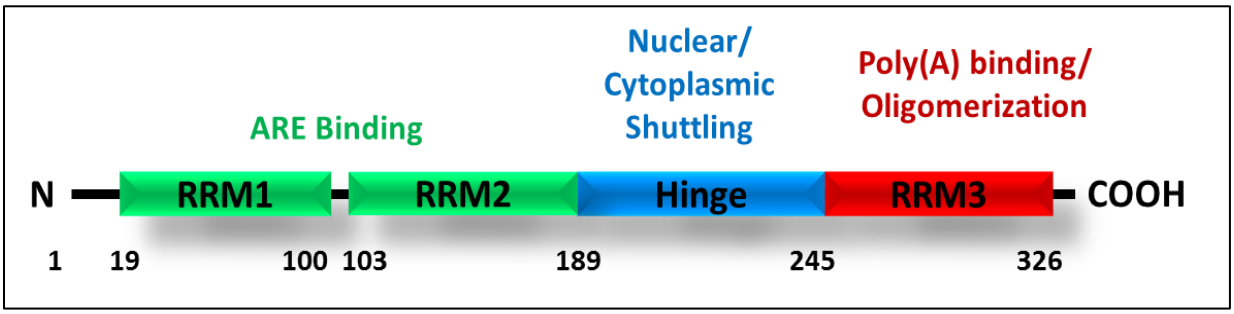

Figure 5. Mammalian HuR Protein Structure. The mammalian HuR protein contains three RNA Recognition Motifs (RRMs) and a Hinge region. RRM1/2 are involved in AU-rich element (ARE) binding. The hinge region is involved in nuclear/cytoplasmic shuttling, while RRM3 binds poly(A) plays a role in oligomerization. The numbers indicate the amino acid position of each element.

has recently been shown to destabilize mammalian long intergenic noncoding RNAs (lincRNAs) (Yoon et al., 2012). Although the exact mechanism of HuR mRNA stabilization is still unknown, three models have been proposed to explain it. One model suggests that the decay of mRNAs is prevented because HuR binding competes with miRNAs that may otherwise destabilize the transcript (Bhattacharyya et al., 2006). Another model shows that when HuR binds to target mRNAs it interacts with poly(A) binding proteins which aids in the stabilization of the mRNA (Nagaoka et al., 2006). The final model suggests that HuR competes with other RNA binding proteins (RBPs), such as tristetraprolin (TTP), that initiate decay of their target mRNA (Kratochvill et al., 2011). Furthermore, HuR binding has been shown to increase the translation of the target mRNA (Gantt et al., 2006; Kawai et al., 2006; Lu et al., 2009; Nguyen et al., 2009; Perlewitz et al., 2010). See Figure 6 for a pictorial representation of the role of HuR in a normal cell.

b. HuR Competes with miRNAs for RNA Binding. As discussed above, the cellular HuR protein is mainly localized to the nucleus (Fan and Steitz, 1998b). During cell proliferation and in response to environmental stressors, HuR is shuttled to the cytoplasm where it is thought to antagonize destabilizing factors thereby stabilizing normally labile mRNA targets (Fan and Steitz, 1998b; Bhattacharyya et al., 2006; Tominaga et al., 2011; Kim et al., 2009; van Kouwenhove et al., 2011; Epis et al., 2011; Abdelmohsen et al., 2008). See Figure 7 for a simplified pictorial explanation. Established mRNA targets include, but are not limited to, *C-MYC, C-FOS, HIF-1α, VEGF, COX-2* (Abdelmohsen et al., 2010). When HuR binds to these target mRNAs, the cooperative binding of multiple HuR molecules ensues (Levine et al., 1993;

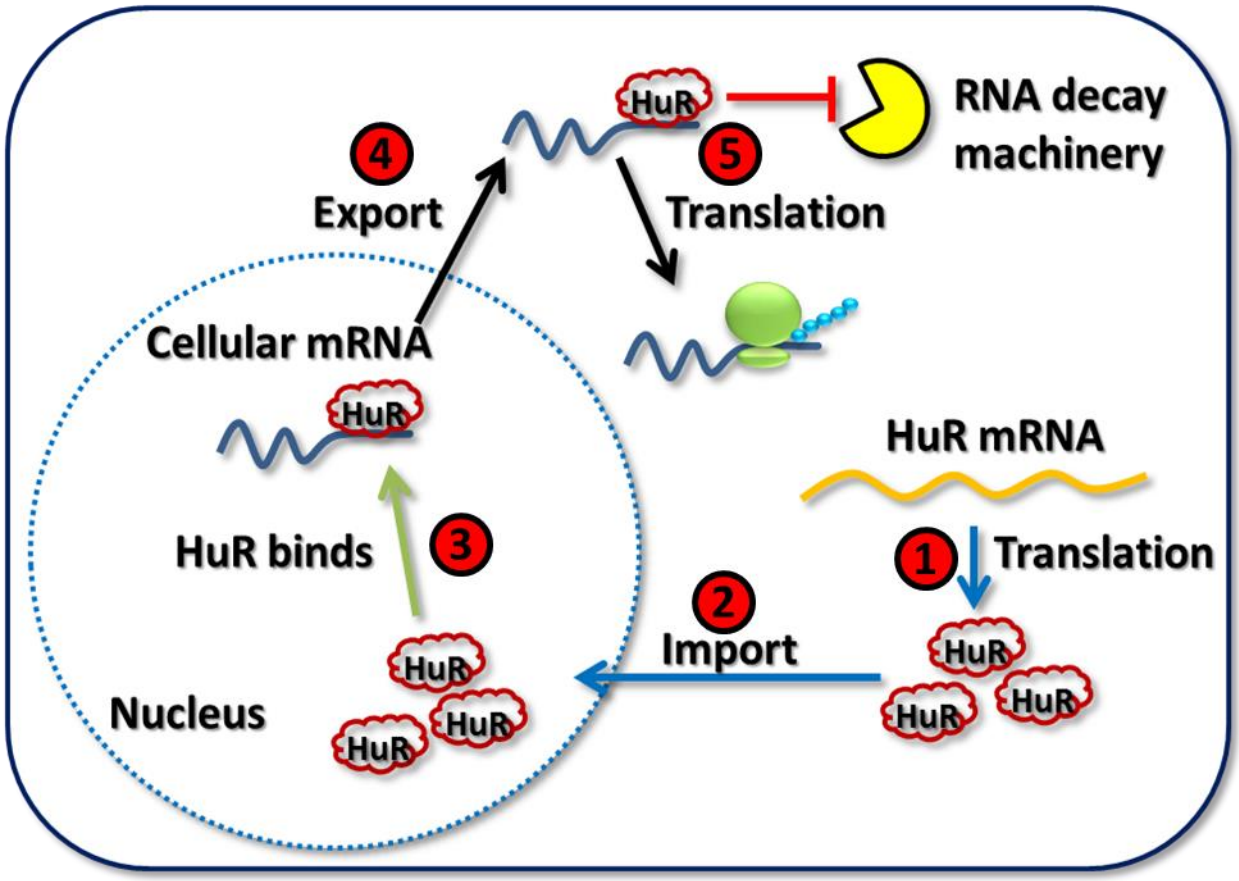

Figure 6. The Role of the Cellular HuR Protein in a Normal Cell. In a normal cell, (1) HuR protein is translated in the cytoplasm, (2) imported to the nucleus, (3) binds transcripts with an AU/GU-rich element (ARE/GRE). When these transcripts are (4) exported to the cytoplasm the bound HuR (5) protects them from RNA decay machinery and influences translation.

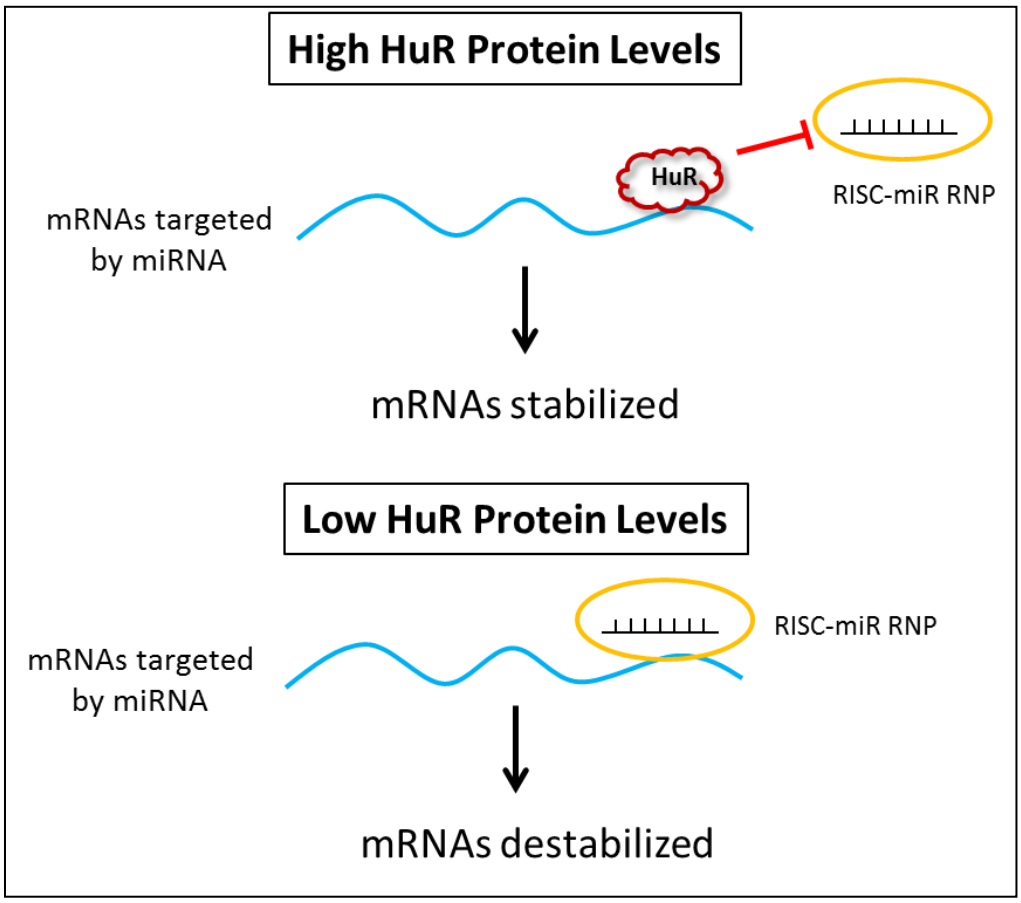

Figure 7. HuR Competes with the RISC-miR RNP. During high levels of free HuR protein, HuR is available to bind to targeted mRNAs resulting in the physical displacement or the steric hindrance of the RNA-induced silencing complex (RISC), thereby stabilizing the mRNAs. However, during low levels of free HuR protein, HuR is unavailable to bind to target mRNAs and compete with the RISC, resulting in the destabilization of the mRNAs.

Chung et al., 1996; Abe et al., 1996; Fan and Steitz, 1998b; Gao and Keene, 1996; Kasashima et al., 2002; Fialcowitz-White et al., 2007; Toba and White, 2008; Soller and White, 2005; Chung and Wooley, 1986; Devaux et al., 2006). This multimeric binding of HuR on target mRNAs is believed to result in the physical displacement or steric hindrance of the RNA-induced silencing complex (RISC) (Simone and Keene, 2013). HuR would then act as an antagonist against the RISC destabilization functions; therefore, the target mRNAs would be stabilized, as demonstrated (Mukherjee et al., 2011; Filipowicz et al., 2008; Bartel, 2004).

c. HuR Regulates Alternative Polyadenylation. Alternative polyadenylation variants have been identified in several different genes in which the shorter isoforms do not contain an ARE sequence while the longer isoforms do contain an ARE (Khabar et al., 2005; Moucadel et al., 2007), one of these genes being HuR (Al-Ahmadi et al., 2009; Dai et al., 2012). As mentioned above, the ARE sequence plays an important role in the stability of mRNAs. HuR protein autoregulates its own pre-mRNA; therefore, polyadenylation of HuR pre-mRNA is thought to be dependent on the nuclear HuR protein levels (Dai et al., 2012). As shown in Figure 8, low levels of nuclear HuR protein result in proximal polyadenylation, while high levels of nuclear HuR protein result in distal polyadenylation (Dai et al., 2012). The shorter HuR mRNA isoform is more stable when exported to the cytoplasm, allowing more translation of HuR protein which will then reestablish the higher levels of nuclear HuR (Dai et al., 2012). The longer isoform of HuR contains an ARE sequence. It is thought that HuR can bind this sequence and stabilize the longer HuR mRNA isoform. However, tristetraprolin (TTP), a potent decay promoter, competes with HuR to bind to the ARE (Al-Ahmadi et al., 2009; Dai et al., 2012). During a Sindbis virus infection, HuR accumulates in the cytoplasm resulting in reduced levels

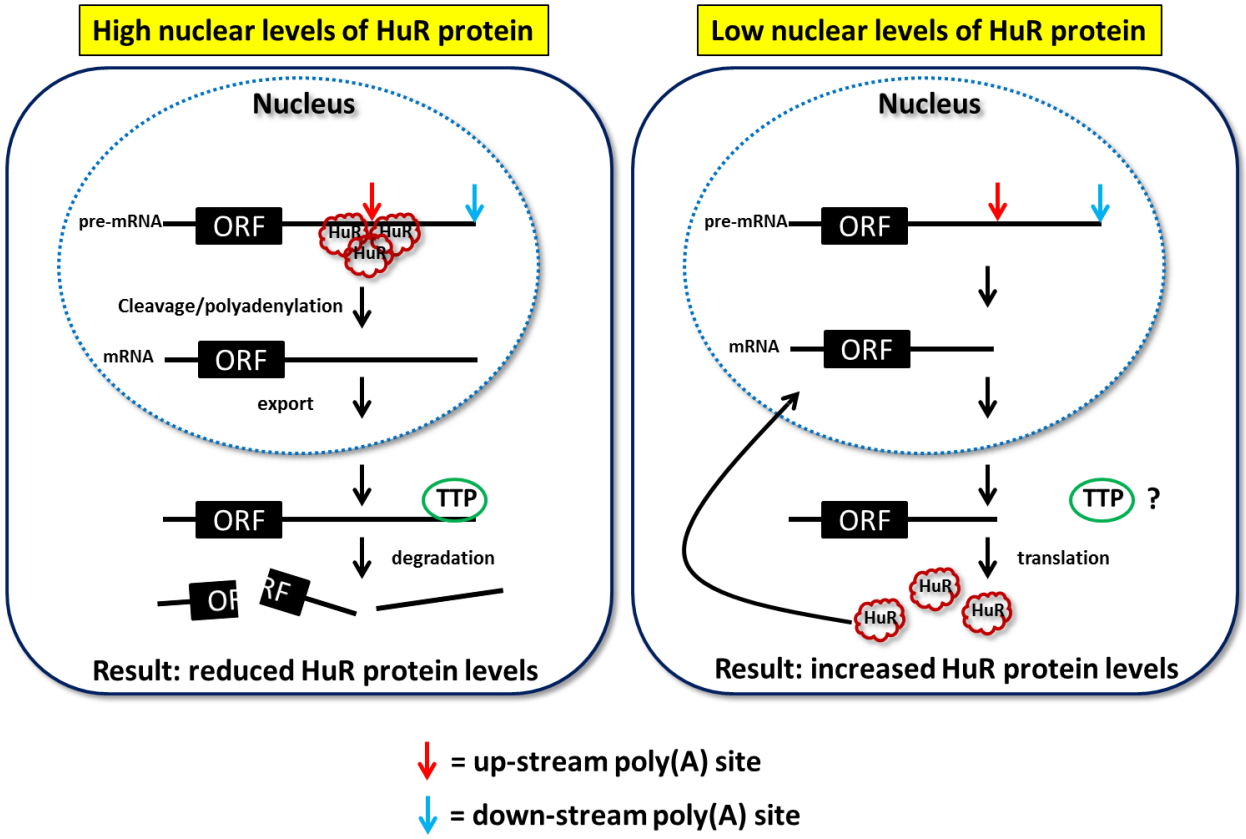

Figure 8. Alternative Polyadenylation of the HuR pre-mRNA is Autoregulated by the HuR Protein. During high nuclear levels of HuR protein, the HuR protein binds and covers the upstream poly(A) site on the HuR pre-mRNA, resulting in polyadenylation at a downstream signal and production of longer isoform of the HuR mRNA. This long isoform contains sequences in its 3'UTR that attract the destabilizing protein TTP, resulting in an unstable mRNA and reduced translation of new HuR protein. When HuR protein is a low levels in the nucleus, the upstream poly(A) site on the HuR pre-mRNA is not bound by the protein and available to the polyadenylation machinery. This results in the production of an isoform of the HuR mRNA with a shorter 3'UTR that lacks the destabilizing elements found in the longer isoform. Thus this isoform of the HuR mRNA is more stable and more translatable, thus increasing the production of new HuR proteins that can be imported to the nucleus.

of nuclear HuR (Sokoloski et al., 2010; Dickson et al., 2012). Therefore, we hypothesize that during a Sindbis virus infection, the low levels of nuclear HuR will trigger the proximal polyadenylation of HuR pre-mRNA. This will result in a more stable HuR mRNA and thus more HuR protein which can then bind and stabilize Sindbis virus RNAs.

RATIONALE

The experimental goals of this thesis were designed to answer three interrelated questions. First, the cellular HuR protein has been shown previously to interact with several alphaviral RNAs that contain a "typical" URE sequence in their 3'UTR and this interaction protects the viral RNA from host decay machinery. However, not all alphaviruses contain this "typical" URE sequence. To determine if this HuR interaction is species-specific or a general property of alphaviruses, this study therefore set out to examine if and where HuR interacts with these alphavirus species that do not possess an identifiable URE in their 3'UTRs. Second, many, if not all, alphavirus infections result in the unexpected accumulation of the cellular HuR protein in the cytoplasm. Thus, the next goal of this project was to identify the mechanism for this virus-specific HuR relocalization phenomenon. Finally, the impact SinV RNA interaction and cytoplasmic accumulation of HuR has on cellular mRNAs has yet to be studied. Therefore, the last part of this thesis project examined the influence of SinV commandeering of HuR protein on two important aspects of post-transcriptional RNA regulation – polyadenylation and mRNA stability. The long term goal of this study was to identify novel alphaviral pathways of virus-host interaction and pathogenicity in hopes it would shed some light for the development of effective anti-alphavirals.

MATERIALS AND METHODS

I. Cell Lines

a. 293T (ATCC CRL-11268) cells were grown in 5% CO_2 at 37ºC and maintained in Dulbecco's Modified Eagle's Medium (DMEM) containing 10% fetal bovine serum (FBS), streptomycin (10,000µg/mL), and penicillin (10,000units/mL). Stock cells were grown in a T-175 flask and split every three days. Cells were split by rinsing with 1x phosphate buffered saline (PBS) then incubated with 1.5mL of 0.25% trypsin until the cells became detached from the flask. Once detached, cells were diluted in complete culture medium and split at a 1:10 ratio.

b. BHK-21 (Baby Hamster Kidney, ATCC CCL-10) cells were maintained in Minimum Essential Medium (MEM) containing 10% fetal bovine serum (FBS), streptomycin (10,000µg/mL), and penicillin (10,000units/mL) at 37ºC in 5% CO_2. Stock cells were grown in a T-175 flask and split every three days. Cells were split by rinsing with 1x PBS then incubated with 1.5mL of 0.25% trypsin until the cells became detached from the flask. Once detached, cells were diluted in complete culture medium and split at a 1:10 ratio.

II. Virus Production

a. MRE16. The Sindbis virus strain MRE16 cDNA clone was kindly provided by Aaron Philips from the Arthropod-borne Infectious Disease Laboratory (AIDL), Colorado State University. The plasmid was linearized with AscI and used to transcribe infectious Sindbis virus RNA using Sp6 RNA polymerase.

b. Viral Stocks. Sindbis viral stocks were created by the electroporation of the infectious viral RNA (transcribed from pMRE16) into BHK-21 cells. $1x10^7$ BHK-21 cells suspended in 400μL of 1x PBS were placed in a 4mm electrode gap Gene Pulser® Cuvette (Bio-Rad). The cuvette containing the cells and the infectious viral RNA was placed into the BTX EMC 630 apparatus and electroporated with either 1 pulse at 400LV, 800Ω, and 75μF or 2 pulses at 400LV, 800Ω, and 50μF. The cells were then plated in a T-75 flask and incubated at 37ºC in 5% CO_2. 48 hours later, cytopathic effects (CPE) were observed, indicating virus growth. The virus was amplified by taking the medium off the infected cells and placing it on an 80% confluent T-75 flask of BHK-21 cells. 48 hours later, the virus (passage 1) was collected by scraping the cells off the flask and centrifuging the cells at 500xg for 5 minutes at 4ºC. The supernatant was removed and centrifuged at 1000xg for 10 minutes at 4ºC to remove any particulates. Aliquots of 0.5mL were stored at -80ºC. Viral titers were determined via BHK-21 plaque assays.

c. Plaque Assay. Confluent BHK-21 cells grown in 12 well plates were infected with 500μL of ten-fold serial dilutions of virus in complete MEM. The virus was allowed to absorb for one hour at 37ºC in 5% CO_2. Following absorption, infected cells were overlaid with 2% methylcellulose in complete MEM and incubated for 5 days at 37ºC in 5% CO_2. Following incubation, the virus was inactivated by adding 7% formaldehyde (v/v in 1x PBS) to each well for 30 minutes. Next, the liquid was removed and the monolayers were gently rinsed with water several times. Crystal violet was then used to stain the monolayers for 10 minutes; then de-stained by gentle rinsing with water. The monolayers were dried overnight at room temperature. The next day, only the wells containing more than 20 countable plaques were used to calculate

the viral titer. Multiplying the number of plaques by the viral serial dilution factor determined the viral titer of the stock virus.

(number of plaques)*(2)*(serial dilution factor) = plaques forming units (PFU)/mL

III. Generation of Transcription Templates and Plasmids for Transfections

Specific DNA fragments were created and either cloned into the EcoR1 and BamH1 sites of pGEM-4 (Promega) to determine the binding regions of HuR to the Chikungunya or Ross River virus 3' UTRs, or cloned into the BsrG1 and Not1 sites of pEFGP-N1 (Clontech) to use for transfections. Either the PCR amplification or the oligonucleotide annealing methods were used to generate the DNA fragments. PCR amplified products were digested with EcoR1 & BamH1 or BsrG1 & Not1, and gel purified via 1% agarose gel electrophoresis followed by electroelution in dialysis tubing. The DNA was then PCI (25 volumes equilibrated phenol / 24 volumes chloroform / 1 volume iso-amyl alcohol) extracted and precipitated 2.5 volumes of 100% ethanol and 0.3M sodium acetate. The purified DNA pellets were resuspended in 10µL of dH_2O and ligated into pGEM-4 by combining 1µL of the DNA fragment, 1µg of digested plasmid, 1µL 1x T4 DNA Ligase Buffer (50mM Tris-HCl pH 7.5 / 10mM $MgCl_2$ / 1mM ATP / 10mM DTT), 6µL of dH_2O, and 1µL of T4 DNA Ligase (Thermo Scientific), and incubated at room temperature for one hour. Next, DH5α competent cells were transformed with the ligated plasmids by adding 5µL of the ligation reaction to 200µL of cells, incubated on ice for 30 minutes, heat shocked for exactly 1.5 minutes and quenched on ice for three minutes. The transformed bacteria were then plated on Luria Broth (LB)-ampicillin plates. Colonies were then screened for the insert by Taq PCR using primers specific to the Sp6 and T7 promoters that flank the cloning site. One positive

colony was chosen and grown overnight, in at least 250mL of Luria Broth (LB) with ampicillin. Next, the bacteria were harvested and the plasmids were isolated via Maxi-prep (Invitrogen). The purified plasmids were sequenced to verify the integrity of the insert.

DNA fragments less than 80 nucleotides long were created by combining the complementary oligonucleotides (sense and anti-sense) in 1x NEB Buffer #2 (10mM Tris-HCl / 50mM $NaCl_2$ / 10mM $MgCl_2$ / 1mM DTT) and heating the mixture at 90ºC for five minutes, followed by slow cooling to room temperature so the oligonucleotides can anneal. The resulting dsDNA was phosphorylated in 1x T4 DNA Ligase Buffer (50mM Tis-HCl pH 7.5 / 10mM $MgCl_2$ / 1mM ATP / 10mM DTT) with T4 Polynucelotide Kinase (New England Biolabs) for 30 minutes at 37ºC followed by an inactivation at 60ºC for 20 minutes. The dsDNA fragments were PCI (25 volumes equilibrated phenol / 24 volumes chloroform / 1 volume iso-amyl alcohol) extracted and precipitated with 2.5 volumes of 100% ethanol and 0.3M sodium acetate. Next, the purified 5' phosphorylated dsDNA was ligated into the appropriate digested plasmid, transformed in DH5α competent cells, screened, Maxi-prep'ed (Invitrogen), and sequenced (as described above). The plasmids used for transfections underwent endotoxin removal (Mirus Endotoxin Removal Kit). All plasmids were stored at a stock concentration of 1μg/μL at -20ºC. The oligonucleotides used in this thesis can be found in Table 1.

Table 1. Oligonucleotides Used in this Thesis for Cloning.

Sequence Cloned	Nucleotide Sequence (5'-to-3')	Primer Name	Plasmid Name
ChikV1	CATGAATTCTGAATACCATAATTGGCAAACG CATGGATCCAACATCTCCTACGTCCCTGTGGG	ChikV F1.1 (EcoR1) ChikV R2.1 (BamH1)	ChikV1
ChikV3	AATTCTAGTTTAAAGGGCTATAAAACCCCTGAATAG TAACAAAACATAAAGTTAATAAAAATCAAAG GATCCTTTGATTTTTATTAACTTTATGTTTTGTTACTA TTCAGGGGTTTTATAGCCCTTTAAACTAG	ChikV 3 Sense ChikV 3 Antisense	ChikV3
ChikV4	AATTCTGAATACCATAATTGGCAAACGGAAGAGAT GTAGGTACTTAAGCTTCCTAAAAGCAGCCGAACTCA CTG GATCCAGTGAGTTCGGCTGCTTTTAGGAAGCTTAAG TACCTACATCTCTTCCGTTTGCCAATTATGGTATTCA G	ChikV4 Sense ChikV4 Antisense	ChikV4
ChikV5	AATTCTTGAGAAGTAGGCATAGCATACCGAACTCTT CCACGATTCTCCGAACCCACAGGGACGTAGGAGAT GTTG GATCCAACATCTCCTACGTCCCTGTGGGTTCGGAGA ATCGTGGAAGAGTTCGGTATGCTATGCCTACTTCTC AAG	ChikV5 Sense ChikV5 Antisense	ChikV5
ChikV6	AATTCTAGTTTAAAGGGCTATAAAACCCCTGAATAG GATCCTATTCAGGGGTTTTATAGCCCTTTAAACTAG	ChikV6 Sense ChikV6 Antisense	ChikV6
ChikV7	AATTCGTAACAAAACATAAAGTTAATAAAAATCAA AG GATCCTTTGATTTTTATTAACTTTATGTTTTGTTACG	ChikV7 Sense ChikV7 Antisense	ChikV7
RRV1	CATGAATTCTATGTAGTTAAGTACTAACCAAC CATGGATCCTAGACGCCTACGTCCCCGGTG	RRV F1.3 (EcoR1) RRV R2.1 (BamH1)	RRV1
RRV2	CATGAATTCTATGTAGTTAAGTACTAACCAAC CATGGATCCTAGACGCCTACGTCCCCGGTG	RRV F1.3 (EcoR1) RRV R2.1 (BamH1)	RRV2
RRV4	AATTCTATGTAGTTAAGTATTATAAGATGTGG GATCCCACATCTTATAATACTTAACTACATAG	RRV4 Sense RRV4 Antisense	RRV4
RRV5	AATTCTATGTAGTTAAGTACTAACCAACAAGTAGAC AAATAGATGCTAACCATATATG GATCCATATATGGTTAGCATCTATTTGTCTACTTGTT GGTTAGTACTTAACTACATAG	RRV5 Sense RRV5 Antisense	RRV5

RRV6	AATTCATAACCAGCTATAGTATACTATATTTAGCTAAGCAGTTGCAGTAGTAAGAATGG GATCCCATTCTTACTACTGCAACTGCTTAGCTAAATATAGTATACTATAGCTGGTTATG	RRV6 Sense RRV6 Antisense	RRV6
RRV8	AATTCTACTAATAAAAATTTAAAAATCACTAGAAATCCAATCATTAAATTATTAATTG GATCCAATTAATAATTTAATGATTGGATTTCTAGTGATTTTTAAATTTTTATTAGTAG	RRV8 Sense RRV8 Antisense	RRV8
RRV9	AATTCTACTAATAAAAATTTAAAAATCACTAGAAATCCAATCATTAAATTATTAATTGGCTAGCCGAACTCTAAGGAGATG GATCCATCTCCTTAGAGTTCGGCTAGCCAATTAATAATTTAATGATTGGATTTCTAGTGATTTTTAAATTTTTATTAGTAG	RRV9 Sense RRV9 Antisense	RRV9
RRV10	AATTCGTAGGCGTCCGAACTCTGCGGAGATGTAGGACTAAATTCTGCCGAACCCCATAACACCGGGGACGTAGGCGTCTAG GATCCTAGACGCCTACGTCCCCGGTGTTATGGGGTTCGGCAGAATTTAGTCCTACATCTCCGCAGAGTTCGGACGCCTACG	RRV10 Sense RRV10 Antisense	RRV10
SinV 3’UTR	CATTGTACAATGACCGCTACGCCCCAATG CATGCGGCCGCATGTTAAAAACAAAATTTTG	SinV 3'UTR Fwd (BsrGI) SinV 3'UTR Rev (NotI)	SinV 3’UTR
SinV 3’UTR RSEs	CATTGTACAATGACCGCTACGCCCCAATG GCGGCCGCGCATTATGCACCACGCTTCCTC	SinV 3'UTR Fwd (BsrGI) SinV RSEs Rev (Not1)	RSEs
SinV 3’UTR CSE/URE	TGTACACACGCAGCGTCTGCATAACTTTT CATGCGGCCGCATGTTAAAAACAAAATTTTG	SinV URE/CSE Fwd(BsrG1) SinV 3'UTR Rev (NotI)	CSE/URE
SinV 3’UTR ΔURE	CATTGTACAATGACCGCTACGCCCCAATG GAATTCGTTATGCAGACGCTGCGTGGC GAATTCATTTTGTTTTTAACATGCGGCCGC	SinV 3'UTR Fwd (BsrGI) SinV pre-URE Rev (EcoR1) SinV CSE (EcoR1 & Not1)	ΔURE
TNFα ARE	TGTACAATTATTTATTATTTATTTATTATTTATTTATTTA CGGCCGCTAAATAAATAAATAATAAATAAATAATAAATAAT	TNFa ARE sense (BsrG1) TNFa ARE anti-sense (Not1)	TNFα ARE

IV. *In Vitro* Transcription

a. Radiolabeled RNA. RNA transcribed for Electrophoretic Mobility Shift Assays (EMSAs) were 5' capped and internally radiolabeled. The reaction mixture consisted of the following: 1µg of linearized DNA template, 1mM ATP, 1mM CTP, 0.05mM GTP, 0.05mM UTP, 0.5mM 7^{me}GpppG cap analog (NEB), 45µCi α^{32}P UTP (800Ci/mmol, PerkinElmer), 20U RNAse Inhibitor (Fermentas), 10U of Sp6 RNA Polymerase (Fermentas) and 1x Transcription Buffer (10mM NaCl / 6mM $MgCl_2$ / 40mM Tris-HCl pH 7.6 / 2mM spermidine / 10mM DTT). Transcription reactions were incubated at 37ºC for two hours. Following incubation, dH_2O was added to at least 100µL followed by the addition of an equal volume of PCI. After PCI extraction, 1µL of glycogen (Thermo Scientific), ammonium acetate (2M final concentration), and 2.5 volumes of 100% ethanol were added to precipitate the RNA. RNA was precipitated at -80ºC for a minimum of 10 minutes and then centrifuged at max speed (>16,000xg on microfuge) for a minimum of 10 minutes. The RNA pellet was washed with 150µL of 70% ethanol for 2.5 minutes at max speed. The RNA pellet was dried for 3-5 minutes at room temperature. The pellet was thoroughly resuspended in 10µL of RNA loading buffer (7M urea / 20mM EDTA / 100mM Tris-HCl pH 7.5 / 0.25% w/v bromophenol blue and 0.25% w/v xylene cyanol) and heated at 95ºC for 30 seconds then quenched on ice. Next, the RNA was resolved on a 5% denaturing polyacrylamide gel containing 7M urea. When the RNA was sufficiently resolved, autoradiography was employed to determine the location of the RNA. The RNA was excised from the gel and placed in 400µL of High Salt Column Buffer (HSCB: 400mM NaCl / 25mM Tris-HCl pH 7.6 / 0.1% sodium dodecyl sulfate (SDS)) overnight at room temperature to elute the RNA from the gel. The purified RNA was extracted with 400µL of PCI and precipitated with 500µL of 100% ethanol followed by a 70% ethanol wash. The RNA pellet was resuspended

in at least 16µL of dH_2O. The amount of radiolabeled UTP that was incorporated into the RNA was determined by adding 1µL of the sample to 4mL of ScintiSafe Econo scintillation fluid and analyzed on the liquid scintillation counter (LSC). The RNA sample was then diluted to a stock concentration of 20,000 Counts Per Minute (CPM) per µL.

b. RNA for Transfections. Capped and polyadenylated RNAs for the RNA transfections were transcribed using the following protocol. The reaction mixture consisted of 5µg of either GEMA60 (Control) or MREA60 (SinV 3'UTR) linearized template (kindly provided by Jason Christianson), 10µL 5x Transcription Buffer (10mM NaCl / 6mM $MgCl_2$ / 40mM Tris-HCl pH 7.6 / 2mM spermidine / 10mM DTT), 10µL of rNTPs (25mM ATP, CTP, UTP, GTP), 20µL of 5mM 7^{me}GpppG cap analog (NEB), 50U RNase Inhibitor (Fermentas), 50U of SP6 RNA Polymerase (Fermentas). The reaction mixture was then incubated at 37ºC for 2 hours. Following incubation, dH_2O was added to at least 100µL followed by the addition of an equal volume of PCI. After PCI extraction, 1µL of glycogen (Thermo Scientific), ammonium acetate (2M final concentration), and 2.5 volumes of 100% ethanol were added to precipitate the RNA. RNA was precipitated at -80ºC for a minimum of 10 minutes and then centrifuged at max speed (>16,000xg on microfuge) for a minimum of 10 minutes. The RNA pellet was washed with 150µL of 70% ethanol for 2.5 minutes at max speed. The RNA pellet was then dried for 3-5 minutes at room temperature. The pellet was resuspended in at least 16µL of dH_2O and 1µL was used to determine the concentration by measuring the optical density (OD) at 260nM.

V. Electrophoretic Mobility Shift Assays (EMSA)

The following protocol was used to determine the binding affinity of HuR to RNA. 20,000 CPM of RNA, 2.5µL of Gel Shift Buffer (70mM HEPES pH 7.9 / 450mM KCl / 10mM $MgCl_2$ / 30% v/v glycerol), 1.25µL of 1.5mM spermidine, 10U RNase inhibitor, 3.55µL dH_2O, and 4µL of HuR protein (kindly provided by Dr. Jerome Lee) or lysis buffer to a total volume of 12.8µL. RNA concentrations remained the same in every experiment while the concentration of the protein varied. The reaction mixture was incubated at 30ºC for 5 minutes, after which 3µg of heparin sulfate was added, and the samples were then incubated on ice for 5 minutes. Following incubation, 6x EMSA Loading Dye (10mM Tris-HCl pH 7.6 / 60mM EDTA / 0.03% w/v bromophenol blue / 0.03% w/v xylene cyanol / 60% v/v glycerol) was added to the samples to a final concentration of 1x. The samples were quickly spun down and loaded onto a native 5% polyacrylamide gel and resolved by electrophoresis for several hours (the time was dependent on the length of the RNA). The gel was then dried on a Savant Slab Gel Drier until completely dry and exposed to a Molecular Dynamics phosphorimager screen. The screen was scanned on the Typhoon Trio Variable Mode Imager and analyzed using ImageQuant software. The data was then plotted on a Scatchard plot and the slope of the line was used to determine the dissociation constant (K_d). The dissociation constants were determined from at least three separate experiments.

VI. Immunofluorescence Assays

The following protocol was used to visually identify the location of HuR or SinV in cells. 293T cells were plated in 10cm tissue culture dishes containing glass coverslips, making sure the

coverslips were pressed firmly against the bottom. The cells were grown to 70% confluency and either infected with SinV at an MOI of 10 or transfected with the indicated vectors for either 24 hours (for SinV) or 72 hours (for transfections). When ready, the coverslips were gently rinsed with 1x PBS. Next, the PBS was removed and 5mL of 4% Paraformaldehyde (PFA; v/v in 1xPBS) was added and the coverslips were rocked at room temperature for 15 minutes. PFA was removed and 5mL of methanol was added and the coverslips were rocked at room temperature for 15 minutes. Next, the methanol was removed and 5mL of 70% ethanol was added for 15 minutes at room temperature, rocking. Ethanol was removed and the coverslips were washed with 5mL of 1x PBS for 10 minutes at room temperature with rocking. Then, PBS was removed and coverslips were removed from the 10cm dishes and placed in 12 well tissue culture plates. 1mL of 6% Bovine Serum Albumin (BSA; w/v in 1x PBS) was added to each well containing a coverslip and rocked for 1 hour at room temperature. The coverslips were rinsed three times with 1x PBS for 10 minutes, rocking at room temperature. Next, 500µL of the primary antibody (HuR (Santa Cruz Biotechnology 3A2): 1:500 or SinV (ATCC VR-1248AF): 1:500 in 0.6% BSA in 1x PBS) was added to each well containing a coverslip and rocked at room temperature for at least one hour. The coverslips were then rinsed three times with 1x PBS for 10 minutes, rocking at room temperature. Next, 500µL of the secondary antibody (anti-mouse Cy2 (for SinV) 1:1000 or anti-mouse Alexa Fluor® 594 (for HuR) 1:1000 in 0.6% BSA in 1x PBS) was added to each well containing a coverslip and rocked at room temperature for exactly one hour – protecting from light. The coverslips were rinsed three times with 1x PBS for 10 minutes, rocking at room temperature – protecting from light. Coverslips were then dried thoroughly on a Kimwipe and mounted on a slide using 8µL of Prolong® Gold with DAPI and tacked to the slide with four drops of clear nail polish. Slides were allowed to cure overnight at

room temperature in the dark. The next day, samples were analyzed via fluorescence microscopy using an Olympus IX71 inverted microscope which is fully equipped with a Q imaging retiga 2000R digital camera (courtesy of Dr. Alan Schenkel).

VII. Cell Transfections

The following procedure was used to transfect DNA or RNA in to 293T cells. Cells were grown as described in the immunofluorescence or biochemical fractionation sections. Next, DNA or RNA was diluted in Opti-MEM® I Reduced Serum Medium without serum and gently mixed. Then, the Lipofectamine® 2000 Transfection Reagent was diluted in Opti-MEM® I Reduced Serum Medium without serum as well. Volume of medium and transfection reagent was dependent on the size of the culture vessel (see Life Technologies Lipofectamine® 2000 Transfection Reagent protocol for required volumes). Both mixtures were allowed to incubate for 5 minutes at room temperature. Following the incubation, the Lipofectamine® and DNA/RNA mixtures were mixed together and incubated at room temperature for 20 minutes. The entire volume of the reaction mixture was then added to the medium of the culture vessels. Subsequently, the cells were incubated at 37ºC in 5% CO_2 for 6 hours (RNA) or 72 hours (DNA) at which time they were collected for either immunofluorescence or biochemical fractionation.

VIII. RNA Co-Immunoprecipitation Assays

The protocol described here was used to visualize the HuR:RNA interactions in living cells. 293T cells were grown to confluence in 15cm tissue culture dishes and either mock

infected or SinV infected at an MOI of ten. Cells were gently washed three times with cold 1x PBS, 24 hours post infection. Next, the protein:RNA interactions were cross-linked by adding 7.5mL of 1% formaldehyde (v/v) in 1x PBS for 15 minutes at room temperature, rocking. Following cross-linking, the reaction was quenched by the addition of 2.25mL of 1M glycine (0.25M final concentration) and incubated at room temperature for five minutes. Cells were then washed with cold 1x PBS three times. 500µL of RIPA Buffer (50mM Tris pH 7.5 / 1% v/v NP40 / 0.5% w/v sodium deoxycholate / 0.05% w/v sodium dodecyl sulfate (SDS) / 1mM EDTA / 150mM sodium chloride) was then added to the cells along with 1U of RNase inhibitor (Fermentas). Cells were lifted from the plate by scraping and pipetting. The resulting lysate was sonicated on ice using three 10 second bursts with a minute break between each. The insoluble particles were then pelleted out by centrifuging at max speed (>16,000xg on microfuge) for 10 minutes a 4ºC. 20µL of lysate was saved for the 10% input sample at -80ºC. 300µL of 1x PBS plus 200µL of lysate was incubated with 5µL of anti-HuR (Santa Cruz Biotechnology 3A2) or 5µL of normal mouse IgG (Santa Cruz Biotechnology sc-2025) and 1U of RNase inhibitor was rotated at 4ºC for once hour. After incubation, 50µL of 50% Protein G Sepharose beads (GE Healthcare) were added to the lysates for 15 minutes at 4ºC, rotating. Next, the lysates were centrifuged for 20 seconds at 8,000xg at 4ºC to pellet the beads. Supernatant was saved as the unbound fraction and the pellets were resuspended in 500µL of RIPA containing 1M urea and vortexed. Pellets were washed five times by resupending the pellets in 500µL of the RIPA-urea solution and centrifuged at 8,000xg at 4ºC for 20 seconds. The final pellet was resuspended in 200µL of TEDS Buffer (50mM Tris pH 7.0 / 5mM EDTA / 1% v/v SDS). Cross-links were reversed in all samples (including the input) by shaking the samples at 800 rpm for 45 minutes at 70ºC in an Eppendorf Thermomixer R. Samples were then centrifuged at max speed for 20

seconds at 4ºC. Supernatant was removed and spun down again to remove all insoluble particles. Finally, 1mL of TRIzol® (Life Technologies) was added to each sample; RNA was extracted and analyzed via standard PCR.

IX. RNA TRIzol Extractions

To extract RNA from samples suspended in TRIzol® the following protocol was followed. 20% v/v of chloroform was added to TRIzol® samples and vortexed and centrifuged at max speed (>16,000xg on microfuge) for 10 minutes at 4ºC. The aqueous layer was transferred to a new tube where 1µL of glycogen (Thermo Scientific) and 500µL of isopropanol was added and rotated 10 times to mix and incubated for 10 minutes at room temperature. Following incubation, samples were centrifuged at max speed for 10 minutes at 4ºC. The resulting pellet was washed with 150µL of 70% ethanol and centrifuged at max speed for 2.5 minutes at 4ºC. The pellet was then air dried for 3-5 minutes at room temperature. Next, pellets were resuspended in 160µL of dH_2O and 20µL of DNase buffer (Thermo Scientific) and 20µL of RNase-free DNase (Thermo Scientific) was added and the sample was incubated at 37ºC for 20 minutes. Following incubation, samples were PCI extracted and ethanol precipitated (as described above). The extracted RNA was resuspended in 16µL of dH_2O and 1µL was used to measure concentration (OD260). Concentration was typically diluted to 1µg/µL and samples stored at -80ºC.

X. Biochemical Subcellular Fractionation Assays

To analyze the cellular location of HuR; 293T cells were grown to confluence in a 10cm tissue culture dish. Cells were either infected with SinV at an MOI of ten or transfected with the indicated vectors and collected either 24 hours later (for SinV) or 72 hours later (for transfections). The cells were rinsed one time with 1x PBS and then scraped and resuspended in 5mL of 1x PBS. Cells were centrifuged for 5 minutes at 500xg at 4ºC in a microfuge. The cell pellets were rinsed one more time with 5mL of 1x PBS and re-pelleted. The PBS was then removed and the pellet was resuspended in 500µL of EBKL Buffer (25mM HEPES pH7.6 / 5mM $MgCl_2$ / 1.5mM KCl / 2mM DTT / 0.1% v/v NP-40) and swollen on ice for 15 minutes. The cells were then transferred to a dounce homogenizer and lysed by 30 swift draws of the pestle. The nuclei were pelleted out of the lysate via centrifugation for 2.5 minutes at 900xg at 4ºC in a microfuge. The cytoplasmic supernatant was removed and placed in a new tube and centrifuged at max speed for ten minutes to remove any contaminating nuclei. The nuclear pellet was washed with EMBK Buffer (25mM HEPES pH 7.6 / 5mM $MgCl_2$ / 1.5mM KCl / 75mM NaCl / 175mM sucrose / 2mM DTT) twice to remove any remaining cytoplasmic fractions. The nuclei were then resuspended in 100µL of 0.5% NP-40 (in dH_2O). To make the nuclear fraction easier to work with, the genomic DNA was sheared via brief sonication. 4µL of the nuclear fraction plus 16µL of dH_2O and 20µL of the cytoplasmic fraction was used for western blot analysis.

XI. Western Blotting Assays

For Western Blots, 1/6 volume of 6x SDS Protein Dye (50mM Tris-HCl pH 6.8 / 2% SDS / 10% glycerol / 1% β-mercaptoethanol / 12.5mM EDTA / 0.02% bromophenol blue) was added to cell lysate samples prior to boiling. Samples were resolved using SDS-Polyacrylamide Gel Electrophoresis (PAGE) for approximately two hours at 80 volts. Following electrophoresis, the gel was soaked in Transfer Buffer (10mM Tris / 100mM glycine / 10% v/v methanol) for a few minutes along with the nitrocellulose membrane (cut to gel size). The proteins were transferred to the nitrocellulose membrane by running the Trans-Blot Semi-Dry Transfer Cell (Bio-Rad) at 18 volts for 20 minutes. Following transfer, the membrane was blocked with 5% (w/v) dehydrated milk in TBST (100mM Tris-HCl pH 7.5 / 0.9% w/v NaCl / 0.1% v/v Tween 20) for at least an hour at room temperature with constant rotation. Next, the primary antibody (1:1000 Tubulin (Sigma T9026); 1:1000 XRN2 (NB 100-57541); 1:500 HuR (Santa Cruz Biotechnologies 3A2) was diluted in 5% (w/v) dehydrated milk in TBST and added to the membrane for one hour at room temperature or overnight at 4ºC with rocking. After incubation, the solution was removed and the membrane was washed at least three times for 10 minutes with TBST. Subsequently, the appropriate secondary antibody conjugate to horse radish peroxidase (HRP), was diluted 1:20,000 in 5% (w/v) dehydrated milk in TBST and incubated with the membrane for exactly one hour at room temperature. Following incubation, the solution was removed and the membrane was washed at least three times for 10 minutes with TBST. To identify the protein bands, 1.5mL (750µL each of the Luminol/ Enhancer Solution and the Peroxide Solution) of SuperSignal® West Pico Chemiluminescent Substrate (Thermo Scientific) was added to the blot and imaged via VersaDoc (Bio-Rad) and analyzed using Image Lab software (Bio-Rad).

XII. Half-life Analysis

a. mRNA half-lives. Actinomycin-D (ActD) was used to shut off transcription in cells to measure the half-lives of transcripts. 293T cells were grown to confluence in 10cm tissue culture dishes and either mock infected or infected with SinV at a MOI of 10. 24 hours post infection, 25μL of ActD (5mg/mL stock in DMSO) was added to 25mL of complete DMEM. ActD is sensitive to light, so it was protected from light during thawing. Next, the media on the plates was removed and replaced with 2.5mL of the ActD containing medium. After adding the ActD, the cells were incubated at 37ºC in 5% CO_2. 30 minutes later the first sample (time 0) was collected by completely removing the ActD media and resuspending the cells in 500μL of TRIzol® via scraping and pipetting. Additional samples were collected 45, 90, and 180 minutes later. The RNA from these samples were extracted (as described above) and analyzed via real time qRT-PCR (as described below).

b. Protein half-lives. Cycloheximide (CHX) was used to shut off translation in cells to measure the half-life of HuR protien. 293T cells were grown to confluence in 10cm tissue culture dishes. When ready, 10μL of CHX (100mg/mL stock in DMSO) was added to 10mL of complete DMEM for a final concentration of 100μg/mL of CHX. Next, the media on the plates was removed and replaced with 10mL of the CHX containing medium. The cells were incubated at 37ºC in 5% CO_2. 30 minutes after the CHX addition, the time 0 sample was collected by scraping the cells and pelleting them by centrifugation at 500xg in megafuge for five minutes at 4ºC. The media was then removed and the pellet was washed in 1xPBS and resuspended in 300μL of RIPA Buffer. The other samples were collected at 1, 2, 3, 4, and 5 hours later. Next, the samples were briefly sonicated twice for 10 seconds with a minute rest between each, to shear genomic DNA. Insoluble particles were pelleted via centrifugation of samples at max

speed (>16,000xg in microfuge) for 10 minutes at 4ºC. Lysate samples were stored at -80ºC. The protein concentration of each sample was then measured by the following Bio-Rad Protein Assay. First, the Dye Reagent Concentrate (Bio-Rad) was diluted 1:4 in dH_2O. 2µL of the lysate (or RIPA for the blank) was mixed with 18µL of dH_2O. Next, 1mL of the diluted Dye Reagent was added to the sample mixture and vortexed. The mixture was incubated at room temperature for five minutes before absorbance was measured at 595nm. The BSA standard curve (y=0.0529x + 0.1593) was used to calculate the concentration of each sample. Finally, equal concentrations of protein from each sample were analyzed via western blot to determine the half-life of HuR.

XIII. Real Time qRT-PCR

To determine the abundance of specific RNAs in a sample, real time quantitative reverse transcription PCR (qRT-PCR) was employed. First, cDNA had to be made from the RNA. 2µg of RNA, 1µL of random hexamers (IDT), and dH_2O to 5µL was incubated at 70ºC for five minutes then quenched on ice. Next, 4µL of 5x Reverse Transcriptase Buffer (Promega), 5.6µL of dH_2O, 1µL dNTPs (10mM dATP, dCTP, dTTP, dGTP), 2.4µL $MgCl_2$ (25mM), 1U of RNase inhibitor, and 1µL of Reverse Transcriptase (Promega). Reaction mixture was incubated at 25ºC for five minutes, 42ºC for one hour, and 70ºC for five minutes to make cDNA. Next, 2.64µL of cDNA, 5µL of SYBR® Green Supermix (Bio-Rad), 0.4µL of forward primer (2.5µM), 0.4 of reverse primer (2.5µM), and 3.4µL of dH_2O were added to each well of the 96 well qPCR plates. Samples were always run in triplicate. The 96 well plates were loaded into the CFX96 Real-Time System (Bio-Rad) and incubated at 95ºC for three minutes, [95ºC for 10 seconds, 55ºC for

30 seconds, followed by a plate read], bracketed steps were repeated 39 times then, 95ºC for 10 seconds, followed by a melt curve plate read from 60ºC to 95ºC in increments of 0.5ºC for five seconds. The RNA abundances were analyzed using the Bio-Rad CFX Manager software. PCR efficiencies were calculated by plotting Ct values from five 10-fold dilutions of cDNA. Nucleotide sequences used for detection of genes or virus in this protocol are listed in Table 2.

XIV. Standard PCR

Standard PCR was used to detect the presence of RNAs in the Immunoprecipitation (IPPT) assays. cDNA from the IPPT samples was made as described above. 1µg of cDNA, 1µL each of the forward and reverse primers at 10µM, 1µL of dNTPs (10mM ATP, TTP, GTP, CTP), 3µL $MgCl_2$ (25mM), 10µL 5x GoTaq® Flexi Buffer (Promega), 32.5µL dH_2O, and 0.5µL of GoTaq® Flexi DNA polymerase (Promega) were mix thoroughly. The reaction mixture was then incubated at 94ºC for five minutes, [94ºC for 30 seconds, 55ºC for 30 seconds, 72ºC for one minute], repeated bracketed cycle 20-34 times depending on the abundance of the cDNA amplifying, with a final step at 72ºC for five minutes. Resulting DNA was resolved on a 1% agarose gel with ethidium bromide. The primers used in this protocol are listed in Table 2.

Table 2. Oligonucleotides Used in this Thesis for Standard PCR and qPCR.

cDNA Amplified	Nucleotide Sequence (5'-to-3')	Efficiencies
SinV Genomic RNA	Forward: AGCGCAATGTCCTGGAAAGA Reverse: CTTTTGTTGGCTTCGGTGGG	N/A
RIG-I	Forward: GCATGACCACCGAGCAGCGA Reverse: CCTCCCTAAACCAGGGGGCCA	90.2%
TUT1	Forward: TGCTCACTGTGACCCCGCTCC Reverse: GACTGTATTAATAAACTAGCA	98.6%
RNASE L	Forward: CACGTGCACAGCGGGAAGTCT Reverse: ACAAGTGGCCCCTGTGGCTCT	99.9%
IL-6	Forward: TCGAGCCCACCGGGAACGAA Reverse: GCAACTGGACCGAAGGCGCT	101%
GAPDH	Forward: TCTTTTGCGTCGCCAGCCGA Reverse: ACCAGGCGCCCAATACGACC	94.9%
MYC	Forward: TGTCAAGAGGCGAACACACA Reverse: ACCTTGGGGGCCTTTTCATT	90%
COX-2	Forward: GGCGCTCAGCCATACAG Reverse: CCGGGTACAATCGCACTTAT	95%
FOS	Forward: GTGGGAATGAAGTTGGCACT Reverse: CTACCACTCACCCGCAGACT	95.8%
HIF1A	Forward: GCGCGAACGACAAGAAA Reverse: GAAGTGGCAACTGATGAGCA	109.7%
VEGF-A	Forward: AGGAGGAGGGCAGAATCATCA Reverse: ATGTCCACCAGGGTCTCGATT	94%
HuR CDS	Forward: CAGAGGTGATCAAAGACGCCA Reverse: ATGATCCGCCCAAACCGAG	93.2%
HuR 6kb Isoform	Forward: TGGCGTGTAATGATGGCAGT Reverse: AGCCATTAGAGGTCAGGGGA	95.7%

XV. Preparation of Samples for Global Analysis

Mock infections or SinV infections at an MOI of 10 were performed in triplicate. Twenty four hours post infection, Actinomycin-D was used to shut-off transcription and samples were collected at 0, 45, 90, and 180 minutes post shut-off. Next, RNAs were extracted and quality controlled by determining the half-life of *TUT1* for each sample. 5μg of RNA from each individual sample were sent to Dr. Bin Tian at UMDNJ-New Jersey Medical School where they were analyzed via deep-sequencing.

RESULTS

I. HuR Binds to the 3'UTR of Many if Not All Alphaviruses

The Wilusz lab has previously shown that the cellular HuR protein binds to the U-rich element (URE) and the conserved sequence element (CSE) of the 3' untranslated region (UTR) of Sindbis virus (SinV) genomic RNA (Garneau et al, 2008; Sokoloski et al., 2010). This binding of the HuR protein has been shown to stabilize and protect SinV RNA from the host mRNA decay machinery (Garneau et al., 2008; Sokoloski et al., 2010). Furthermore, the binding of HuR to this conserved region of the 3'UTR can be seen in several alphavirus species such as Venezuelan Equine Encephalitis virus (VEE), Eastern Equine Encephalitis virus (EEE), Western Equine Encephalitis virus (WEE) and Semliki Forest Virus (SFV) (Sokoloski et al., 2010). Although a majority of alphaviral 3'UTRs contain a URE, several lack an obvious homologous region. Chikungunya virus (ChikV) and Ross River virus (RRV), for example, contain only repeat sequence elements (RSEs) and a CSE in their 3'UTR. Therefore, we set out to determine whether the cellular HuR protein binds to the 3'UTRs of ChikV and RRV with high affinities and, if so, identify the sequence region it binds.

Radioactively labeled RNAs containing the entire ChikV or RRV 3'UTR, as well as a set of deletion-derivatives, were prepared by *in vitro* transcription of linearized plasmid DNA templates. RNA substrates were analyzed for HuR interactions using a purified recombinant HuR protein and Electrophoretic Mobility Shift Assays (EMSA). As shown in Fig. 9A, the 3'UTR sequence of ChikV contains only RSEs and a CSE. It lacks an obvious URE which is located just upstream of the CSE near the 3' end of the UTR. As shown in Fig. 9B, HuR bound to the 3'UTR of ChikV with high affinity (mean dissociation constant of 3.4 +/-0.4 nM).

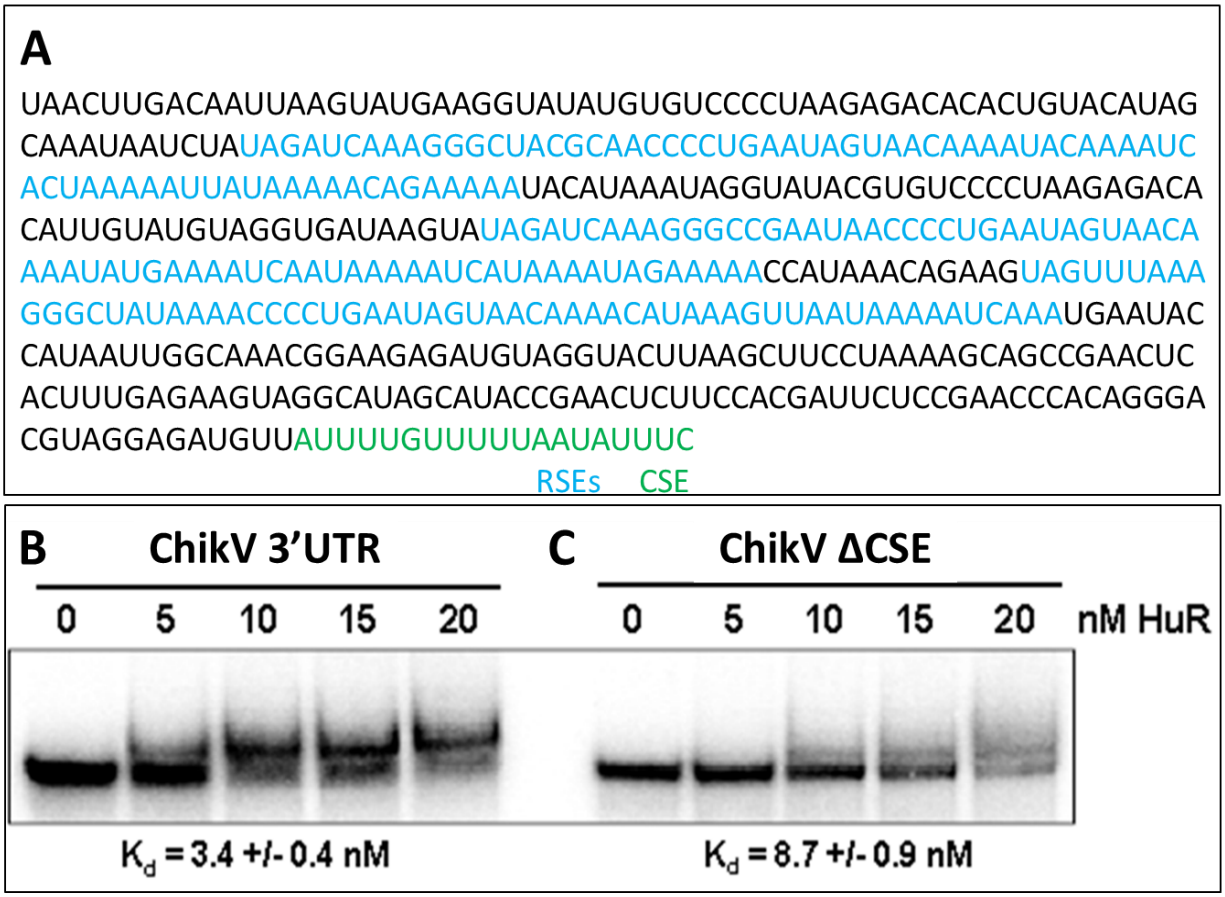

Figure 9. HuR Binding to the Chikungunya 3'UTR is Not CSE Dependent. (A) The nucleotide sequence of the ChikV 3'UTR; the repeat sequence elements (RSEs) are highlighted in blue while the conserved sequence element (CSE) is highlighted in green. RNAs containing the entire 3'UTR (B) with or (C) without the CSE (ΔCSE) of ChikV were incubated with the indicated nM amounts of a recombinant HuR protein. The RNA:HuR complexes were resolved on a 5% non-denaturing gel and visualized by phosphorimaging. The mean dissociation constant (K_d) for each RNA:HuR interaction from three independent experiments +/- the standard deviation is indicated below the gel images.

However, when the CSE was deleted from the 3'UTR to create ChikVΔCSE, HuR binding still occurred, albeit with ~2-3 fold less affinity (based on a comparison of K_d with that obtained from the full length 3'UTR construct, Fig. 9C). These results indicate that like the 3'UTR of SinV and other alphaviruses that contain a URE, HuR can interact with regions of the ChikV 3'UTR other than the CSE.

To begin to identify where HuR is binding upstream of the CSE in the ChikV 3'UTR, we first took a bioinformatics approach and scanned for possible HuR binding sites in the ChikV 3'UTR using RBPDB, a database of RNA-binding protein specificities (http://rbpdb.ccbr.utoronto.ca). Based on previous work that implicated AU/GU-rich sequences as HuR binding sites (Abe et al., 1996; López de Silanes et al., 2004; Meisner et al., 2004), we were able to identify possible binding regions and used this information to rationally prepare a set of ChikV 3'UTR deletion derivatives (shown in Fig. 10A). RNAs from each deletion derivative were analyzed for HuR binding by EMSA (Fig. 10B) and binding was quantitatively assessed by comparing dissociation constants (K_d) (see Fig. 10A). From these data, we concluded that HuR is interacting either with the most 3' RSE element (RSE3) (construct ChikV3; K_d 217.4 nM) and/or with the region between the CSE and RSE3 (construct ChikV1; K_d 401.6 nM). Additional deletion variants ChikV4 and ChikV5 that were designed to further delineate the weaker HuR binding site in the CSE-RSE3 intervening region. However, both RNAs failed to interact with HuR. Thus, HuR may be capable of a relatively weak interaction at the interface between the 3' border of ChikV4 and the 5' end of ChikV5. Since the ChikV3 RNA fragment had the highest affinity for HuR, we opted to further pursue the analysis of this binding site. As shown in Fig. 11A, HuR interacted with the isolated RSE3 element with relatively high affinity (mean dissociation constant of 217.4 +/- 22.7 nM).

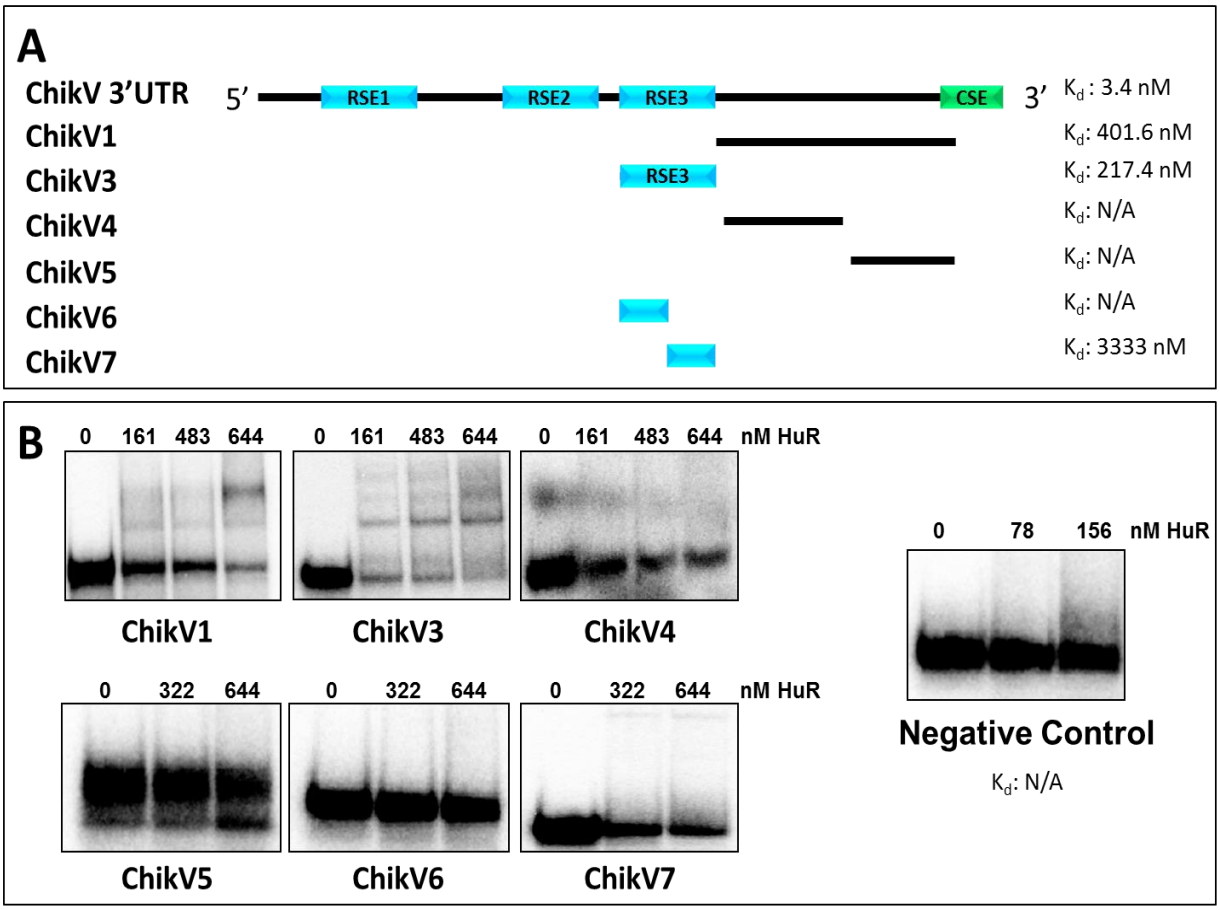

Figure 10. Constructs Created to Determine the Specific Binding Region of HuR on the 3'UTR of ChikV. (A) The regions on the ChikV 3'UTR isolated and investigated for RNA:HuR interactions. K_d values for each construct as determined by EMSA are listed on the right side of the panel. (B) Each of the constructs listed in panel A was incubated with the indicated amount of a recombinant HuR protein. The RNA:HuR complexes were resolved on a 5% non-denaturing gel and visualized by phosphorimaging. The constructs without K_d (N/A) values failed to interact with HuR. The negative control was transcribed from the multiple cloning region of pGEM-4 and the K_d value listed below the gel picture.

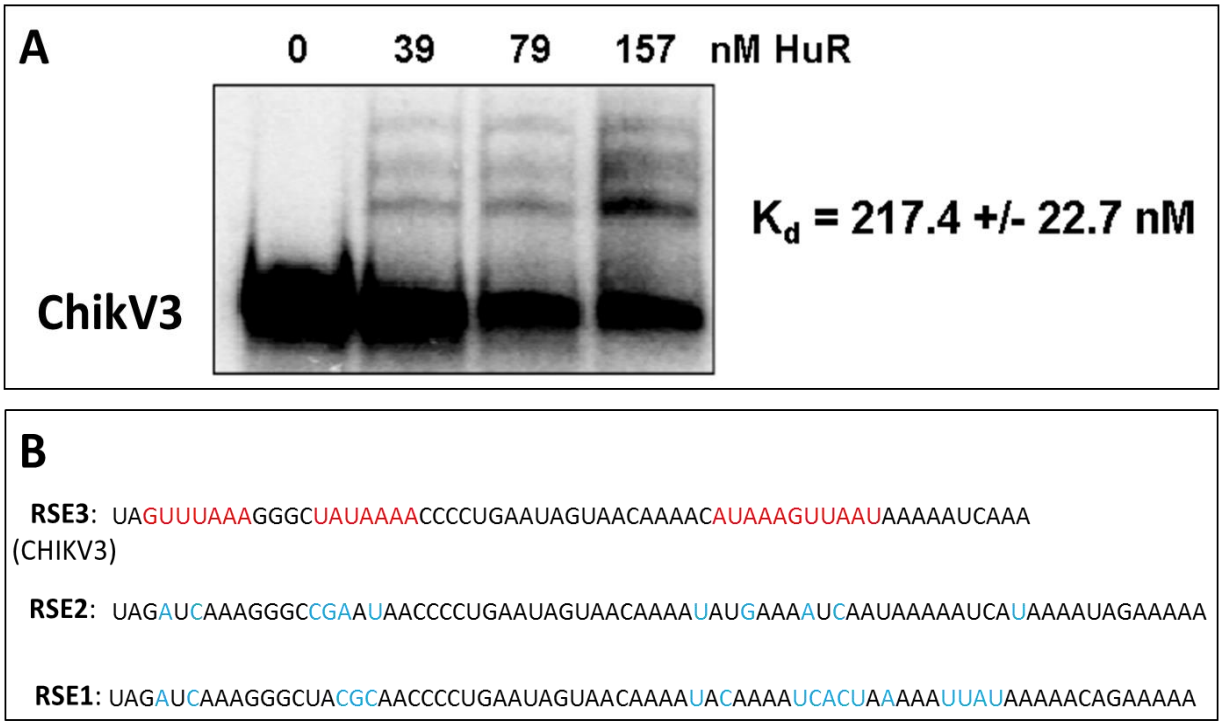

Figure 11. HuR Interacts with RSE3 on the ChikV 3'UTR. (A) ChikV3 was incubated with the indicated amount of recombinant HuR protein. Complexes were resolved on a 5% non-denaturing gel and visualized by phosphorimaging. The mean dissociation constant (K_d) +/- the standard deviation was determined by three separate experiments and is listed on the right side of panel A. (B) The sequences of the three repeat sequence elements (RSEs) of the 3'UTR of ChikV. Highlighted in red along RSE3 are the possible binding sites of HuR. The nucleotides highlighted in blue on RSE2 and RSE1 indicate differences in nucleotides when compared to RSE3.

Attempts to narrow down the HuR binding region on RSE3 were not successful as RNAs representing the 5' half (ChikV6) or the 3' half (ChikV7) of RSE3 failed to interact with HuR protein (see Fig. 10). As shown in Fig. 11B, RSE3 is rather unique from the other RSE elements in ChikV in that it contains three AU-rich tracts that are not seen in RSE1 or RSE2. These AU-rich tracts may represent the binding platform for HuR on RSE3.

Similar to ChikV, the RRV 3'UTR also lacks an obvious URE but contains RSEs and a CSE consistent with the standard organization of the alphavirus 3'UTR (Fig. 12A). As shown in Fig. 12B, the 3'UTR of RRV binds HuR with a mean dissociation constant of 1.3 nM, indicating that it is capable of a high affinity interaction with the cellular protein similar to other alphaviruses analyzed to date. Deletion of the CSE the RRV 3'UTR only diminishes HuR binding affinity by ~4X (Fig. 12C). These data suggest that HuR can interact with regions upstream of the CSE in the 3'UTR of RRV.

To locate this novel HuR binding region on the 3'UTR of RRV, possible binding regions were identified using RBPDB and used to design the eight constructs shown in Fig. 13A. As seen in Fig. 13B, a high affinity (K_d ~23 nM) HuR binding site was localized to the region between the CSE and the 3' most RSE. Further analysis of deletion derivatives narrowed down the binding site to a 75 base region downstream of RSE4 that interacted with reasonably high affinity with HuR protein (RRV9; K_d 79.4 +/- 18.3 nM; see Figs. 13 and 14). Analysis of the sequence of this 75 base region revealed three AU-rich tracts that may represent HuR binding sites (Fig. 14B).

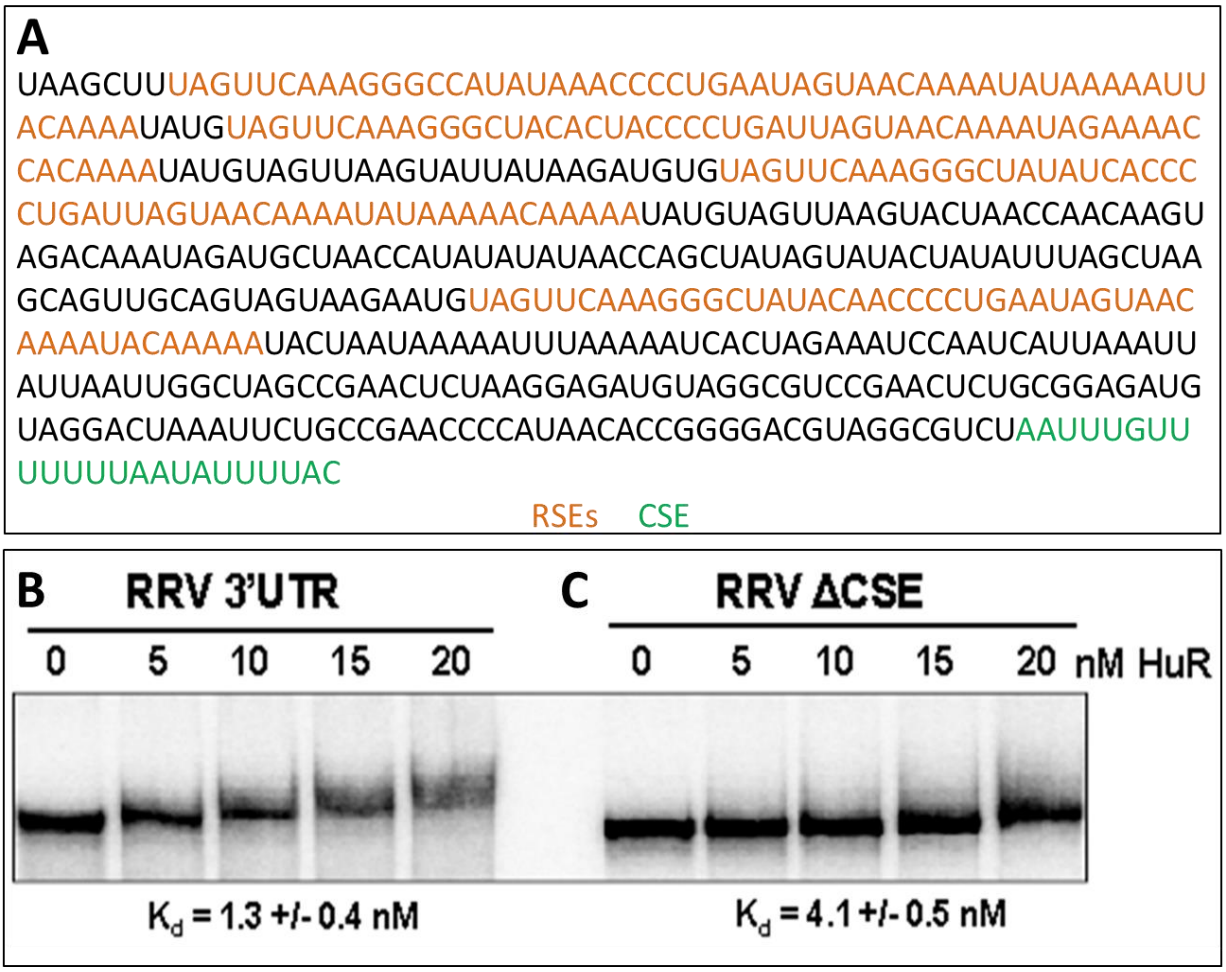

Figure 12. HuR Binding to the Ross River 3'UTR is Not CSE Dependent. (A) The nucleotide sequence of the RRV 3'UTR; the repeat sequence elements (RSEs) are highlighted in orange while the conserved sequence element (CSE) is highlighted in green. (B and C) RNAs containing the entire 3'UTR with or without the CSE (ΔCSE) of RRV were incubated with the indicated amounts of a recombinant HuR protein. The RNA:HuR complexes were resolved on a 5% non-denaturing gel and visualized by phosphorimaging. The mean dissociation constant (K_d) for each RNA:HuR interaction from three independent experiments +/- the standard deviation is indicated below the gel images.

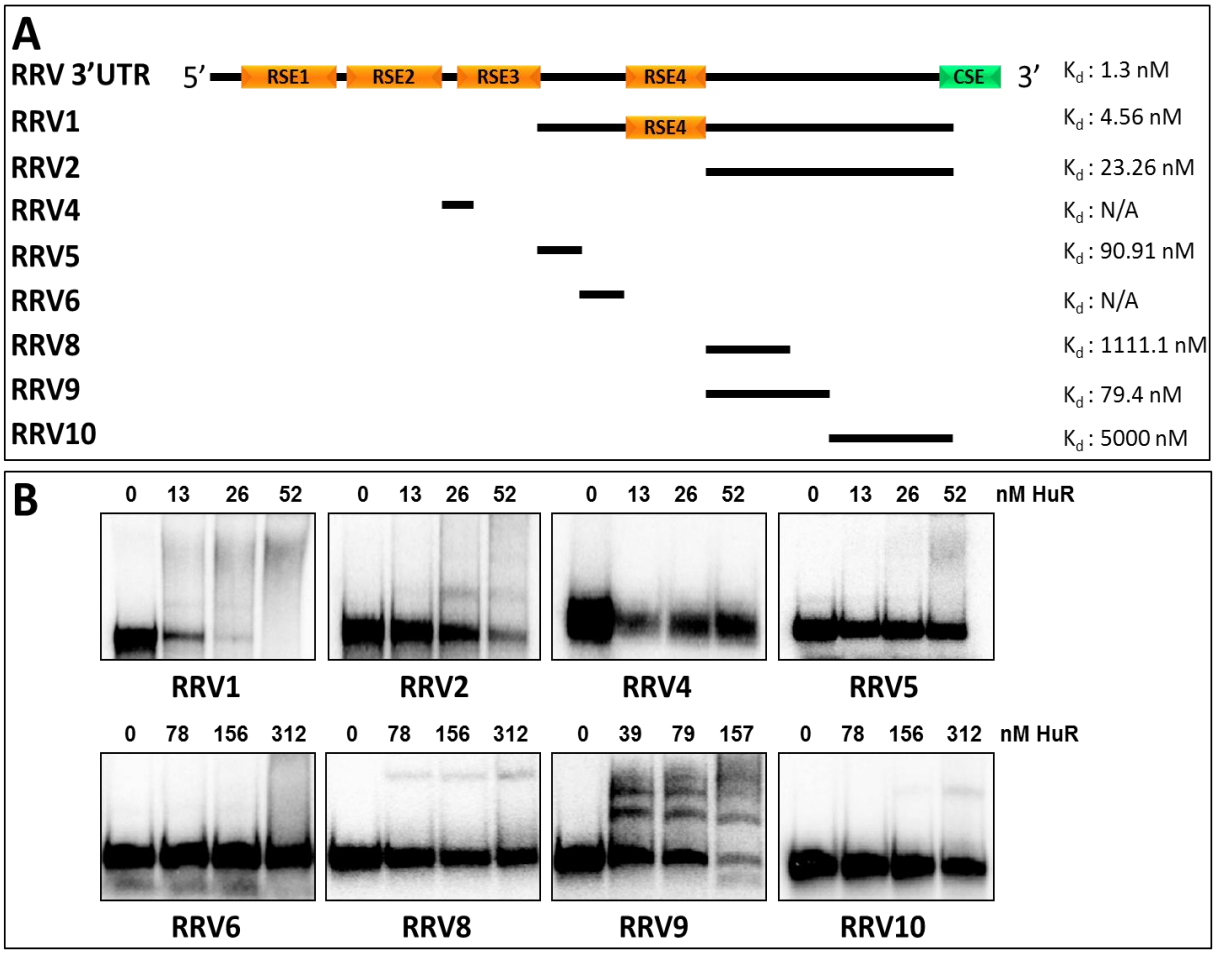

Figure 13. Constructs Created to Determine the Specific Binding Region of HuR on the 3'UTR of RRV. (A) Diagrammatic representation of the regions on the RRV 3'UTR that were investigated for RNA:HuR interactions. K_d values obtained for each RNA-HuR protein interaction are listed on the right side of the panel. (B) Each of the constructs listed in panel A was incubated with the indicated amount of a recombinant HuR protein. RNA:HuR complexes were resolved on a 5% non-denaturing gel and visualized by phosphorimaging.

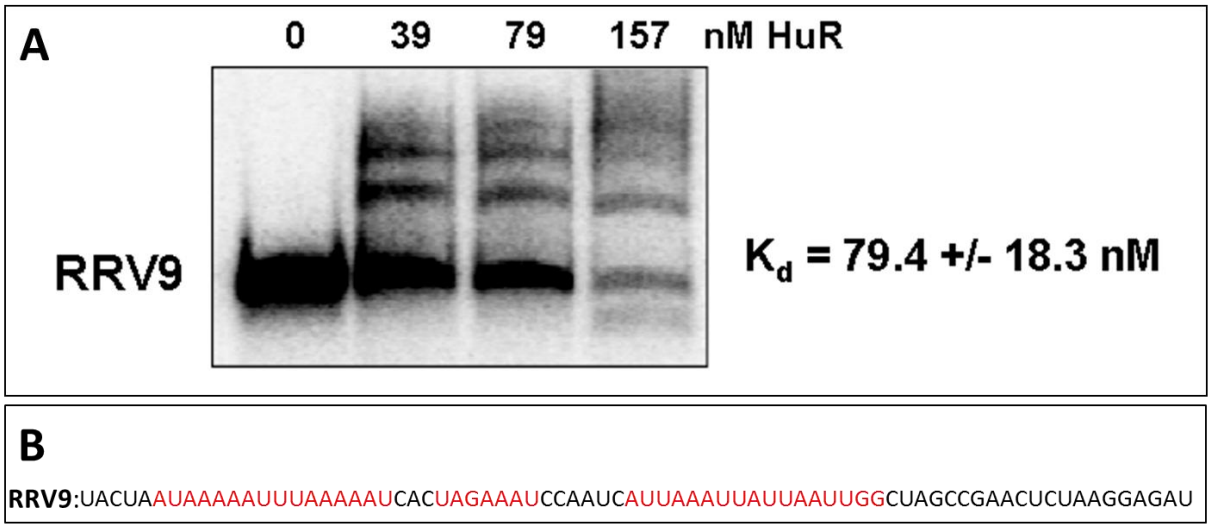

Figure 14. HuR Interacts with a 75 Nucleotide Region Just Downstream of RSE4 on the RRV 3'UTR. (A) RRV9 RNA was incubated with the indicated amount of recombinant HuR protein. RNA-protein complexes were resolved on a 5% non-denaturing gel and visualized by phosphorimaging. The mean dissociation constant (K_d) +/- the standard deviation was determined by three separate experiments and is listed on the right side of panel A. (B) The sequences of the 75 base RRV9 RNA fragment. A-rich and AU-rich sequences that may represent HuR binding sites are highlighted in red.

Based on these data, we conclude that even though ChikV and RRV do not contain a URE adjacent to the CSE in their 3'UTR as found in many alphaviruses, they have evolved similar high affinity HuR protein binding sites at other locations upstream of the CSE. This supports and strengthens the hypothesis that HuR protein may interact with the 3'UTR of all alphaviruses and be universally required for alphavirus RNA stability and replication efficiency.

II. Towards a Mechanism of Sindbis Virus-Induced Accumulation of HuR in the Cytoplasm

The Wilusz lab has previously shown that Sindbis virus and other alphaviruses such as Ross River virus, Chikungunya virus and Western Equine Encephalitis virus cause a cytoplasmic accumulation of the cellular HuR protein during an infection (Sokoloski et al., 2010; Dickson et al., 2012). Fig. 15 shows the relocalization of HuR protein from the nucleus to the cytoplasm in a Sindbis virus infection. It is currently unknown how the cytoplasmic accumulation of HuR occurs during an alphavirus infection. Previous work has shown that during a stress event HuR becomes phosphorylated at several different residues resulting in the relocalization of the protein from the nucleus to the cytoplasm (Kim et al., 2008a; Doller et al., 2010; Yu et al., 2011; Doller et al., 2011; Kim et al., 2010; von Roretz et al., 2010; Liu et al., 2009; Kim et al., 2008b; Kim et al., 2008c). Interestingly, during a Sindbis virus infection HuR becomes dephosphorylated (Dickson et al., 2012), suggesting that the virus is inducing the cytoplasmic accumulation by a mechanism that is different than what is observed in a stress response.

Previous work in the lab using SinV mutants in nonstructural proteins did not affect the relocalization of HuR during infection (Sokoloski et al., unpublished observations). Therefore,

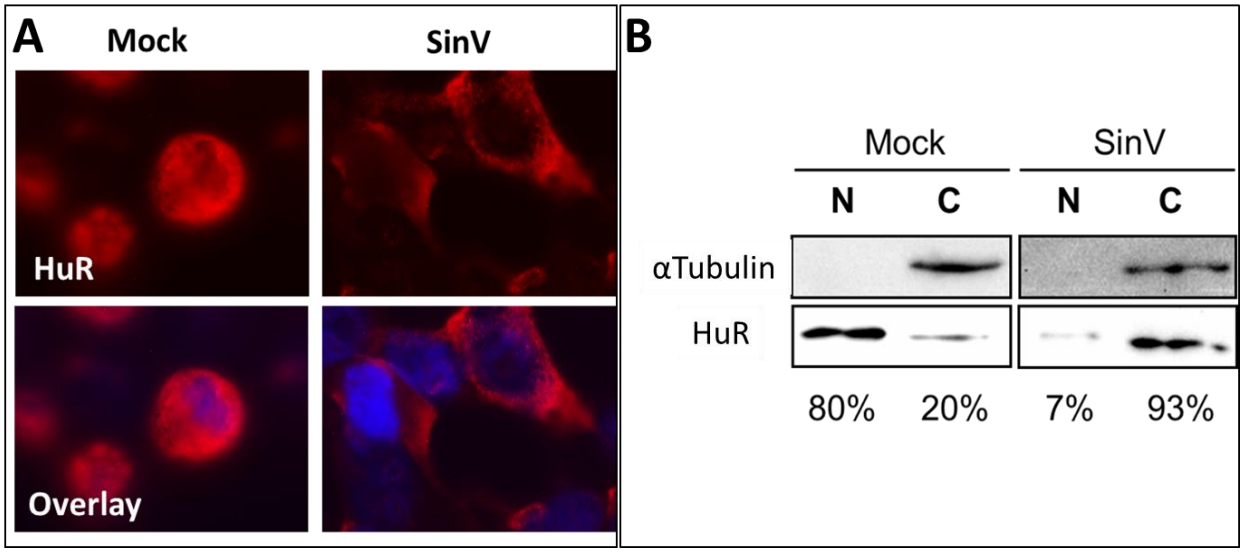

Figure 15. HuR Accumulates in the Cytoplasm During a Sindbis Virus Infection. 293T cells were mock infected or infected with SinV at an MOI of 10pfu/cell. At 24 hours post infection, cells were either fixed and stained with DAPI and HuR specific antibodies and analyzed by fluorescence microscopy (panel A) or biochemically fractionated into the nuclear (N) and cytoplasmic (C) fractions and analyzed via Western Blot (panel B). The relative percentage of HuR in each subcellular fraction is shown beneath the gel lanes.

we hypothesized that perhaps the high affinity binding sites present on the 3'UTR of the large amount of SinV RNAs in the cytoplasm were playing a key role in the relocalization of HuR during infection. To test this hypothesis, the SinV 3'UTR was inserted downstream of the GFP open reading frame of pEGFP-N1 to generate a source of an RNA containing the SinV high affinity HuR binding site in the absence of infection. Plasmids were transfected into 293T cells and HuR localization was analyzed by immunofluorescence or biochemical fractionations 72 hours post transfection. As shown in Fig. 16, constructs expressing an mRNA containing the 3'UTR of SinV in the absence of other components of the viral infection resulted in the cytoplasmic accumulation of HuR protein. These data indicate that the 3'UTR of SinV by itself appears to be the primary cause of the cytoplasmic accumulation of HuR.

We next used this GFP-SinV 3'UTR transfection assay to identify what specific region(s) of the SinV 3'UTR were required for the cytoplasmic accumulation of HuR. A series of GFP ORF-fusion constructs containing defined regions of the SinV 3'UTR, as well as a cellular AU-rich element (ARE) from TNFα that was shown previously to be capable of binding HuR protein (Dean et al., 2001; Ford et al., 1999; Katsanou et al., 2005) were prepared (Fig. 17). Plasmids were transfected into 293T cells and analyzed 72 hours later by immunofluorescence and western blotting of subcellular fractions. As shown in Fig. 18, only the construct expressing the URE/CSE of the SinV 3' UTR caused a significant accumulation of HuR in the cytoplasm. Furthermore, the ΔURE construct which contained SinV 3'UTR without the previously defined high affinity HuR binding site located upstream of the CSE resulted in only slight accumulation of HuR in cytoplasm. Interestingly, constructs containing the HuR-binding ARE element from the cellular TNFα mRNA failed to induce cytoplasmic relocalization of HuR protein.

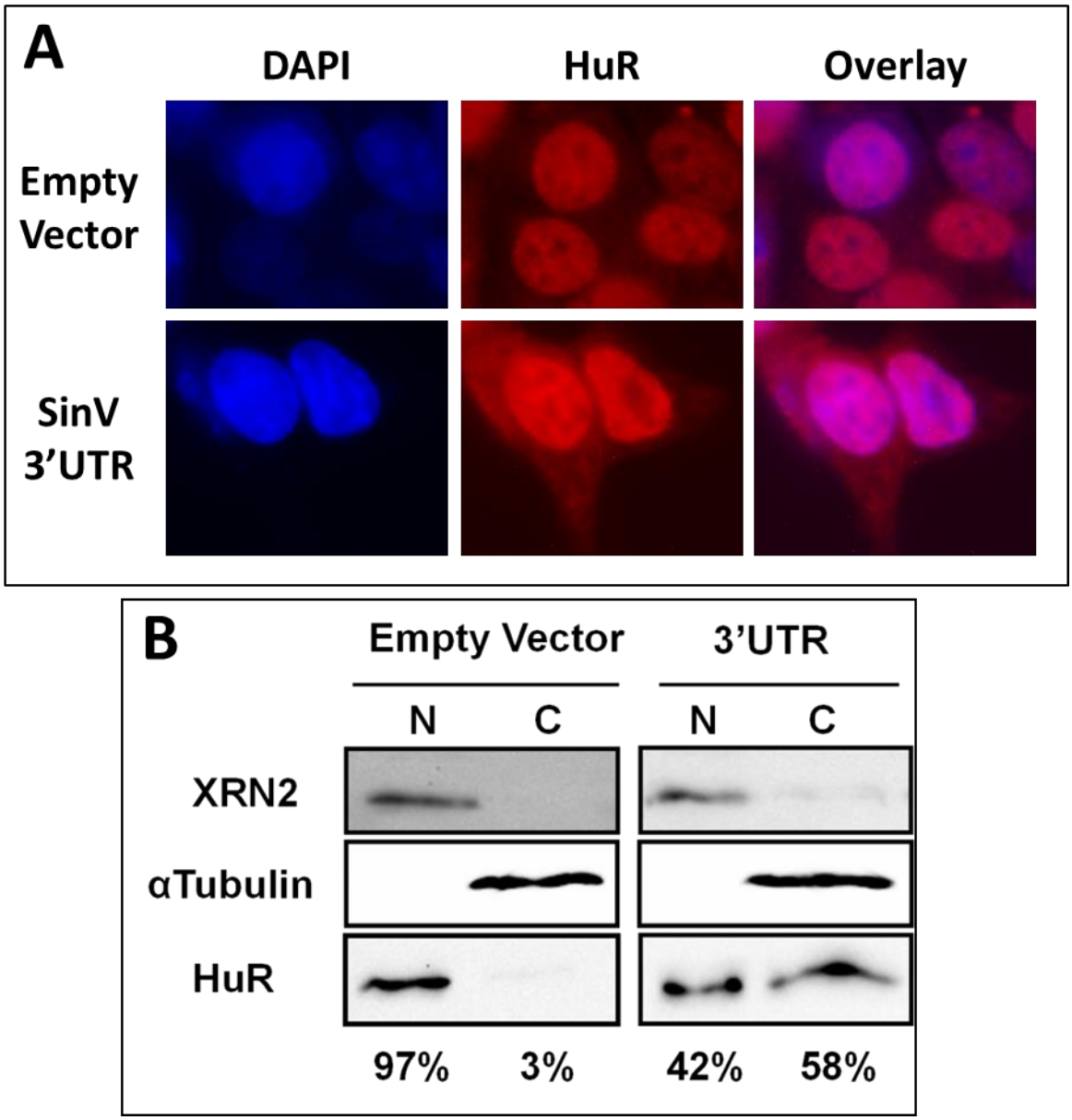

Figure 16. A Plasmid Expressing an mRNA that Contains the 3'UTR of Sindbis Virus Causes the Cytoplasmic Accumulation of HuR. 293T cells were transfected with pEGFP-N1 vectors expressing just GFP (Empty Vector panels) or expressing GFP mRNA containing the 3'UTR of SinV (3'UTR panels). At 72 hours post transfection, cells were either fixed and stained with DAPI and HuR specific antibodies and analyzed by fluorescence microscopy (Panel A) or biochemically fractionated into the nuclear (N) and cytoplasmic (C) fractions and analyzed via western blot (Panel B). Fractions were probed for XRN2 and αTubulin to assess the quality of the subcellular fractionation. The numbers below the lanes refer to the relative amount of HuR protein present in each fraction.

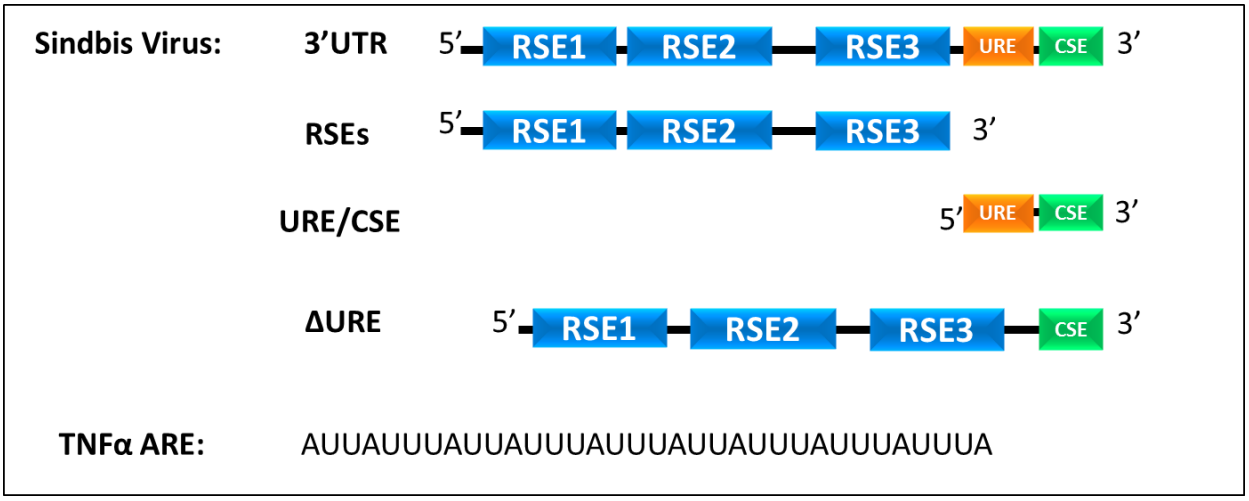

Figure 17. Diagrammatic Representation of the 3'UTR Regions of SinV Fused to the GFP ORF to Analyze the Sequence Requirements for HuR Cytoplasmic Accumulation. These regions were cloned downstream of the GFP in pEGFP-N1. The TNFα ARE was also inserted into pEGFP-N1 to assess whether the HuR relocalization was specific for SinV sequences or could be induced by any HuR binding moiety.

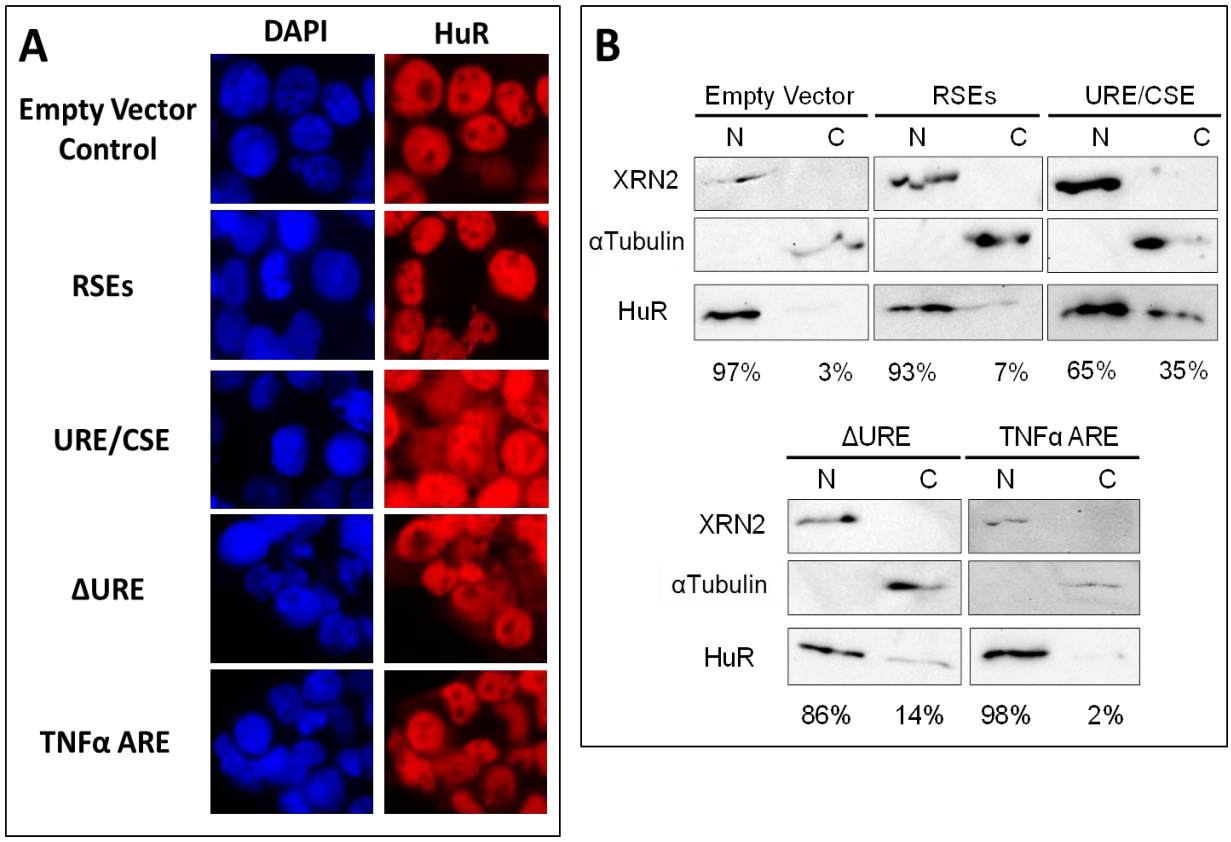

Figure 18. The Ability to Induce the Cytoplasmic Accumulation of HuR Maps Specifically to the URE/CSE Sequence of the SinV 3'UTR and is Not a General Property of Any HuR Binding Site. 293T cells were transfected with a pEGFP-N1 vector expressing only GFP (empty vector) or expressing GFP with the indicated SinV 3'UTR or TNFα ARE region (diagrammed Fig. 9). At 72 hours post transfection, cells were either fixed and stained with DAPI and HuR specific antibodies and analyzed by fluorescence microscopy (Panel A) or biochemically fractionated into the nuclear and cytoplasmic fractions and analyzed via western blot (Panel B). Fractions were probed for XRN2 and αTubulin to assess the efficiency of the subcellular fractionation. The numbers below the lanes refer to the relative amount of HuR protein present in each fraction.

Collectively, these data indicate that the high affinity URE or URE/CSE HuR binding sites in the SinV 3'UTR have the specific ability to induce the cytoplasmic accumulation of HuR.

While the data obtained above using plasmid-derived mRNAs to induce cytoplasmic HuR accumulation are encouraging, there is a feature of the experimental design that differs from a standard SinV infection. SinV gene expression occurs exclusively in the cytoplasm of infected cells. Since transfected plasmids are transcribed in the nucleus and the resulting mRNAs are then transported to the cytoplasm, HuR protein could have been binding the mRNA containing the SinV 3'UTR in the nucleus and being moved with the transcript into the cytoplasm. Such a scenario could not occur in a *bona fide* SinV infection. To assess an 'RNA-only' mechanism of HuR cytoplasmic accumulation under more SinV infection-like conditions, an RNA containing the SinV 3'UTR was transcribed (along with a similarly sized control transcript derived from pGEM-4 plasmid sequences), purified and transfected directly into 293T cells. The subcellular localization was then assessed six hours later by immunofluorescence. As shown in Fig. 19, the transfection of the SinV 3'UTR RNA alone caused the cytoplasmic accumulation of HuR. Transfection of the control RNA had no effect on HuR protein subcellular localization. Collectively, these data suggest that the 3'UTR of SinV RNA and its high affinity HuR binding sites alone plays a key role in the cytoplasmic accumulation of HuR during a SinV infection.

Our hypothesis is that the SinV 3'UTR acts like a HuR 'sponge,' sequestering the HuR protein in the cytoplasm immediately after translation or trapping it when it is naturally shuttled out of the nucleus during infection. If this hypothesis is correct, then the population of HuR in the nucleus must be either transported to the cytoplasm or degraded. In order to assess the contribution of HuR protein turnover to the observed re-localization of HuR to the cytoplasm

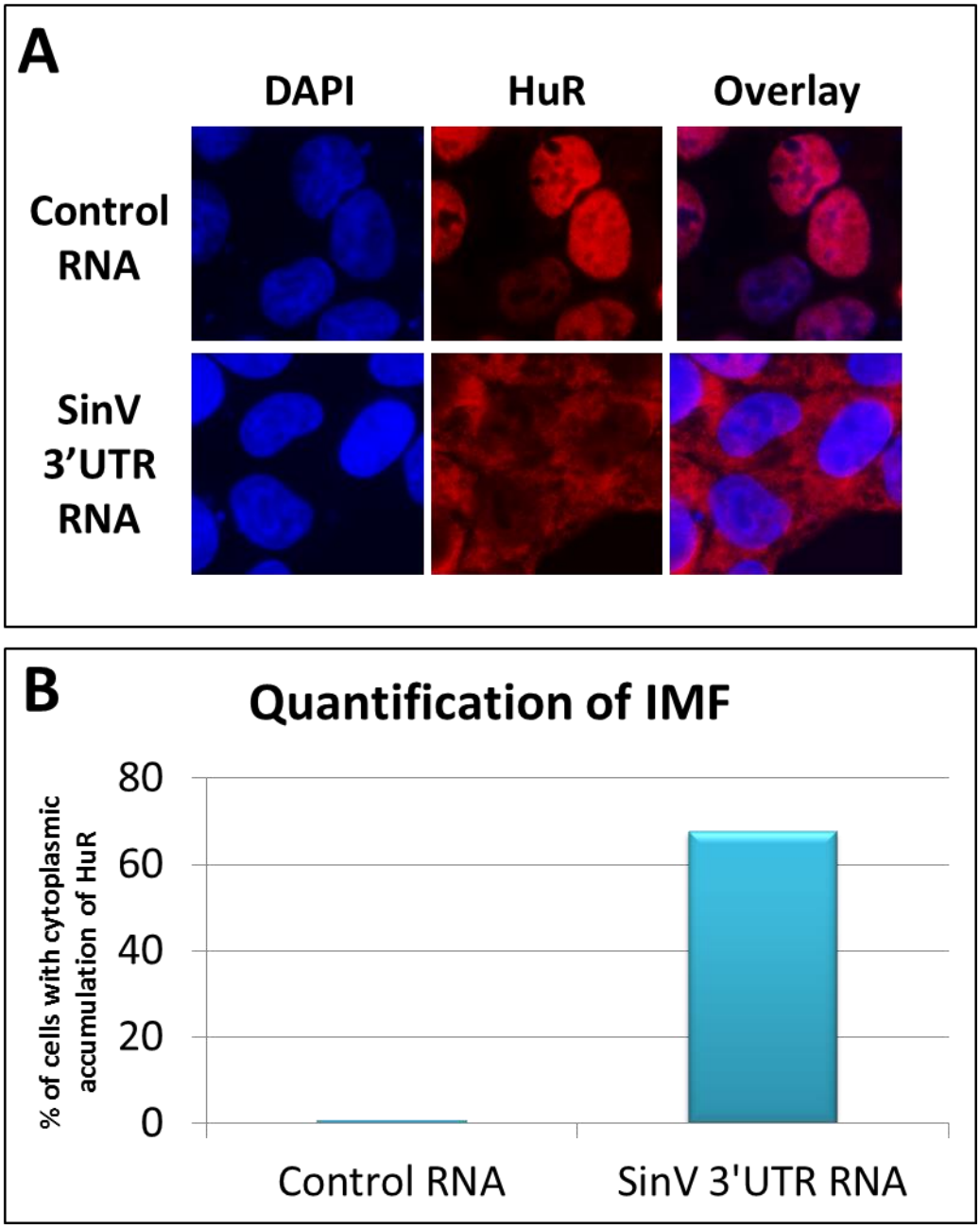

Figure 19. The Transfection of an RNA Containing the SinV 3'UTR Results in the Cytoplasmic Accumulation of HuR. The 3'UTR of SinV or a non-specific control RNA were transcribed *in vitro* (capped and polyadenylated) and transfected into 293T cells. 6 hours post transfection, cells were fixed and stained with DAPI and HuR specific antibodies and analyzed by immunofluorescence microscopy (A). Quantification of immunofluorescence was performed by counting 300 cells (B).

during SinV infection, we determined the half-life of the HuR protein via cycloheximide (CHX) translation shut-off. 293T cells were treated with 100µg/mL of CHX and samples were collected every hour for three hours post drug treatment. The level of HuR protein at each time point was analyzed by western blots. As shown in Fig. 20, the half-life of HuR protein is slightly over two hours in this assay, making it a relatively short lived protein. These data suggest that the natural turnover of HuR protein in the nucleus could contribute to its apparent re-distribution to the cytoplasm during virus infection. In summary, these findings have identified a novel 'RNA sponge' mechanism of virus-induced accumulation of HuR in the cytoplasm used by Sindbis virus and possibly all alphaviruses in order to commandeer the cellular protein for its own use (Fig. 21).

III. The Effects of the SinV:HuR Interaction on Host Cell mRNA Stability

As shown above, the cellular HuR protein accumulates in the cytoplasm during a SinV infection likely by binding to viral transcripts. This probably results in low levels of HuR protein available to interact with cellular mRNAs. Since HuR has been shown to interact with approximately 15% of the cellular transcriptome (López de Silanes et al., 2004) and is a potent stability factor (Fan and Steitz, 1998b; Peng et al., 1998; Levy et al., 1998; Antric and Keene, 1999), we hypothesized that low levels of available HuR protein in the cell may result in the destabilization of many of the mRNAs that typically bind HuR.

To determine the effect of SinV infection on the half-lives of cellular mRNAs, 293T cells were either mock infected or SinV infected for 24 hours. Cells were treated with Actinomycin-D (ActD) to shut off transcription, thereby preventing further mRNA synthesis. Total RNA was

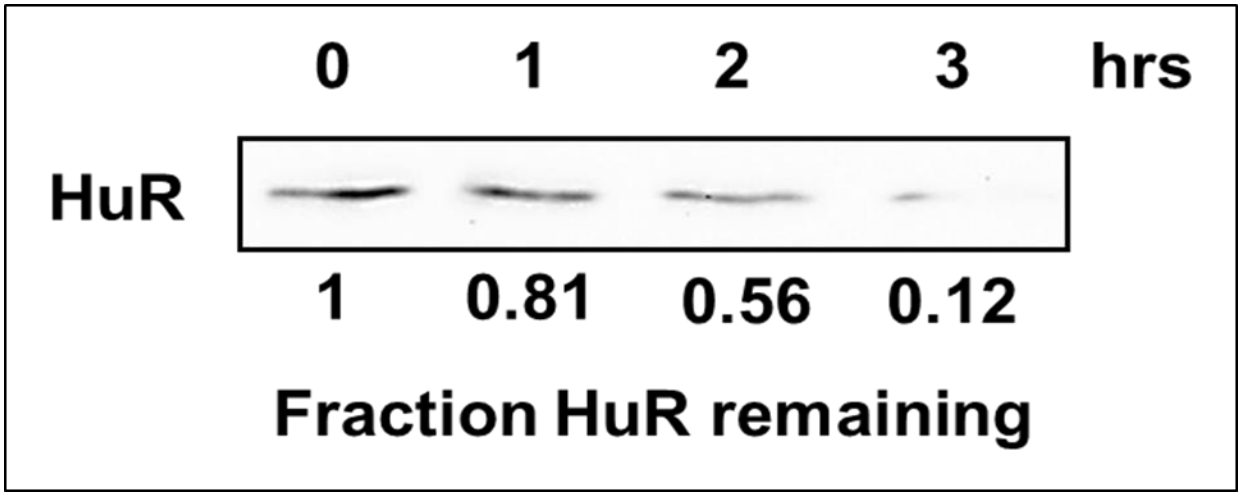

Figure 20. The Half-Life of the Cellular HuR Protein. 293T cells were treated with cycloheximide at Time 0 to shut off translation. Samples were collected at the indicated time points post drug treatment and analyzed via western blotting using HuR-specific antibodies. The numbers beneath the gel lanes indicate that relative amount of HuR remaining at that time point.

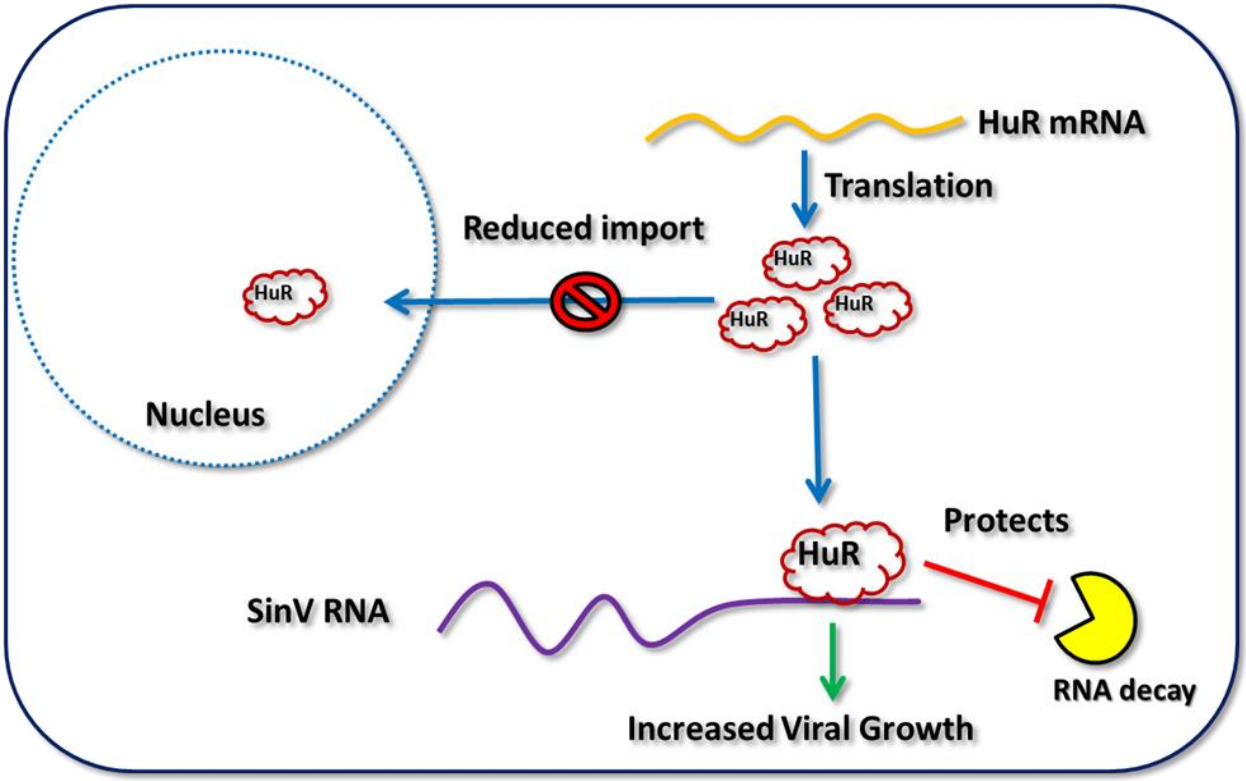

Figure 21. Working Model: Sindbis Virus Commandeers the Cellular HuR Protein During an Infection. During a SinV infection, HuR is commandeered by the high affinity HuR binding site on abundant viral RNAs, resulting in the cytoplasmic accumulation HuR. This sequestration could be occurring by trapping shuttled HuR proteins in the cytoplasm or immediately following the translation of HuR in the cytoplasm thus. The end result is a significant reduction in the amount of HuR that is being imported into the nucleus.

isolated from cells at 0, 0.75, 1.5, and 3 hours post ActD treatment. The levels of individual mRNAs in each of the samples were then analyzed by RT-qPCR to determine mRNA half-lives.

As shown in Fig. 22, *TUT1* and *RIG-I* mRNAs were significantly destabilized in the SinV infected cells when compared to mock infected samples. However, not all cellular mRNAs were destabilized during an infection. As seen in Fig. 23, *IL-6* showed little variation in their mRNA stability while one mRNA (*RNASE L*) appeared to be stabilized. Therefore, we concluded that SinV is having selective effects on the stability of mRNAs during infection.

We hypothesized that the cellular mRNAs that were destabilized during a SinV infection may be those that rely on HuR protein for their stability and were now being degraded more quickly due to the sequestration of HuR by SinV RNAs. To investigate this hypothesis, cells were either mock infected or SinV infected for 24 hours, incubated with formaldehyde to stabilize protein-RNA interactions in living cells, lysed and RNA-protein complexes immunoprecipitated using control or HuR-specific antibodies under stringent conditions. Co-immunoprecipitating mRNAs were analyzed by RT-PCR. As seen in Fig. 24, the mRNAs that were destabilized during a SinV infection (Fig. 22) did indeed bind HuR in mock infected cells but interacted very poorly with HuR in SinV-infected cells. Furthermore, the two transcripts analyzed that were not destabilized during a SinV infection (*RNASE L* and *IL-6*; Fig. 23) did not bind HuR in either the mock infected cells or the SinV infected cells. Together, these data indicate that because SinV RNAs sequester a large proportion of HuR protein, cellular transcripts no longer interact efficiently with the RNA stability factor. Thus, these cellular mRNAs are now susceptible to degradation by the cellular mRNA decay machinery. As presented in more detail in the Discussion, viral-induced dysregulation of cellular mRNA stability could be a very important but heretofore largely overlooked mechanism of pathogenesis during infection.

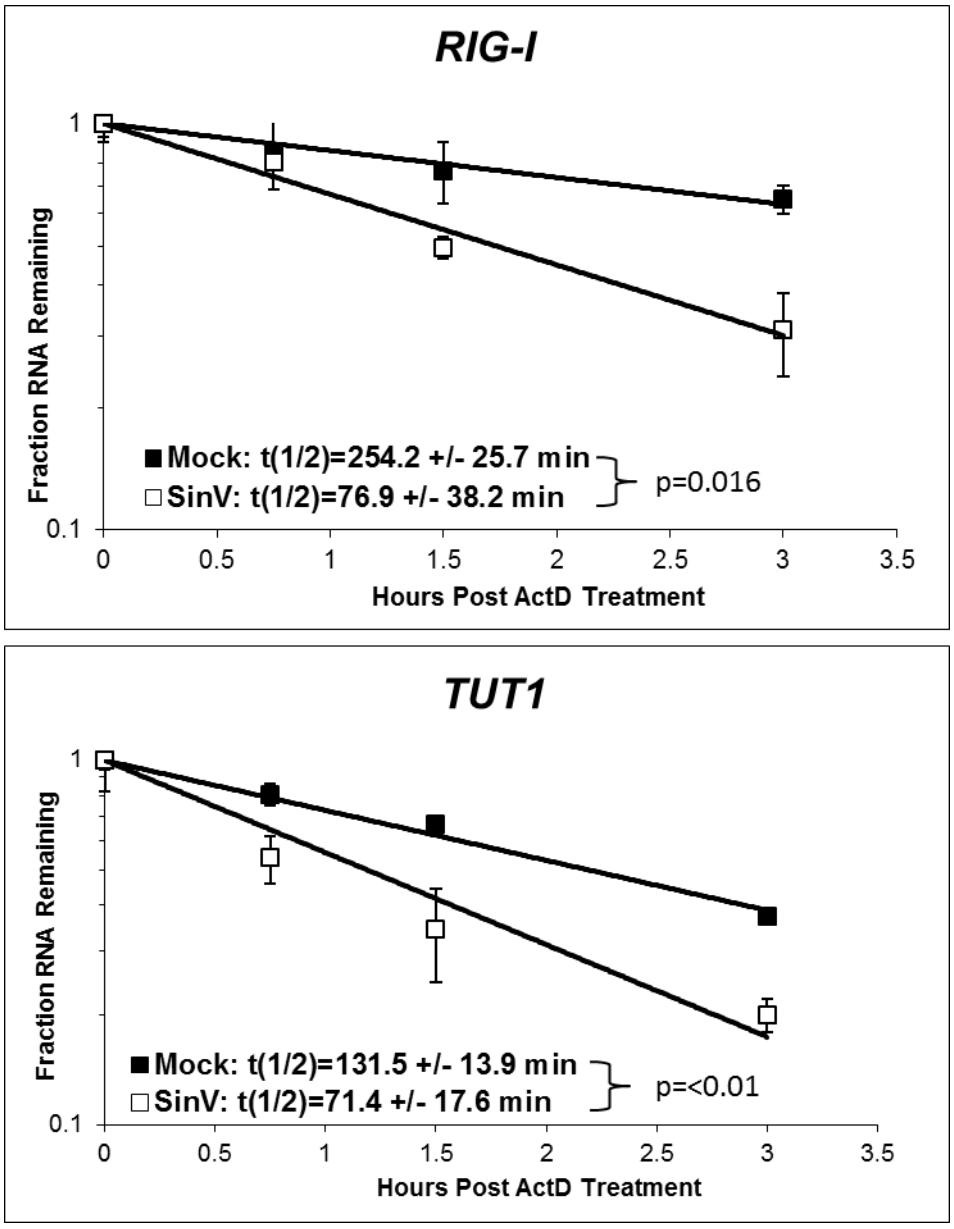

Figure 22. Specific mRNAs are Destabilized During a SinV. 293T cells were mock infected or SinV infected. 24 hours post infection cells were treated with Actinomycin-D to shut off transcription and total RNA was collected at the indicated time points. Half-lives were determined using RT-qPCR. Average mRNA half-lives from at least two independent infections are reported +/- the standard deviation.

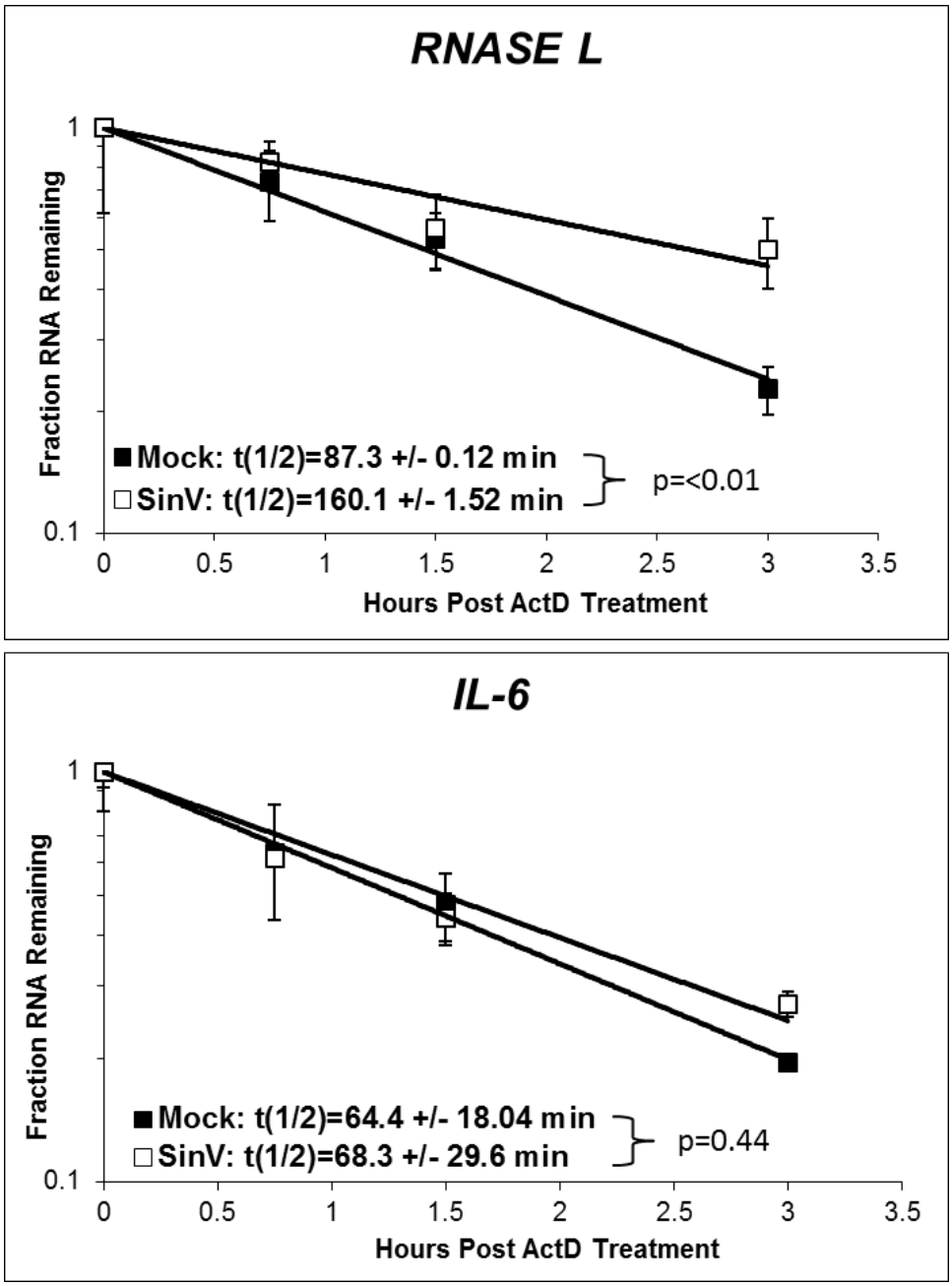

Figure 23. Not All mRNAs are Destabilized During a SinV Infection. 293T cells were mock infected or SinV infected. 24 hours post infection cells were treated with Actinomycin-D to shut off transcription and total RNA was collected at the indicated time points. mRNA half-lives were analyzed using RT-qPCR. Average mRNA half-lives from at least two independent infections are reported +/- the standard deviation.

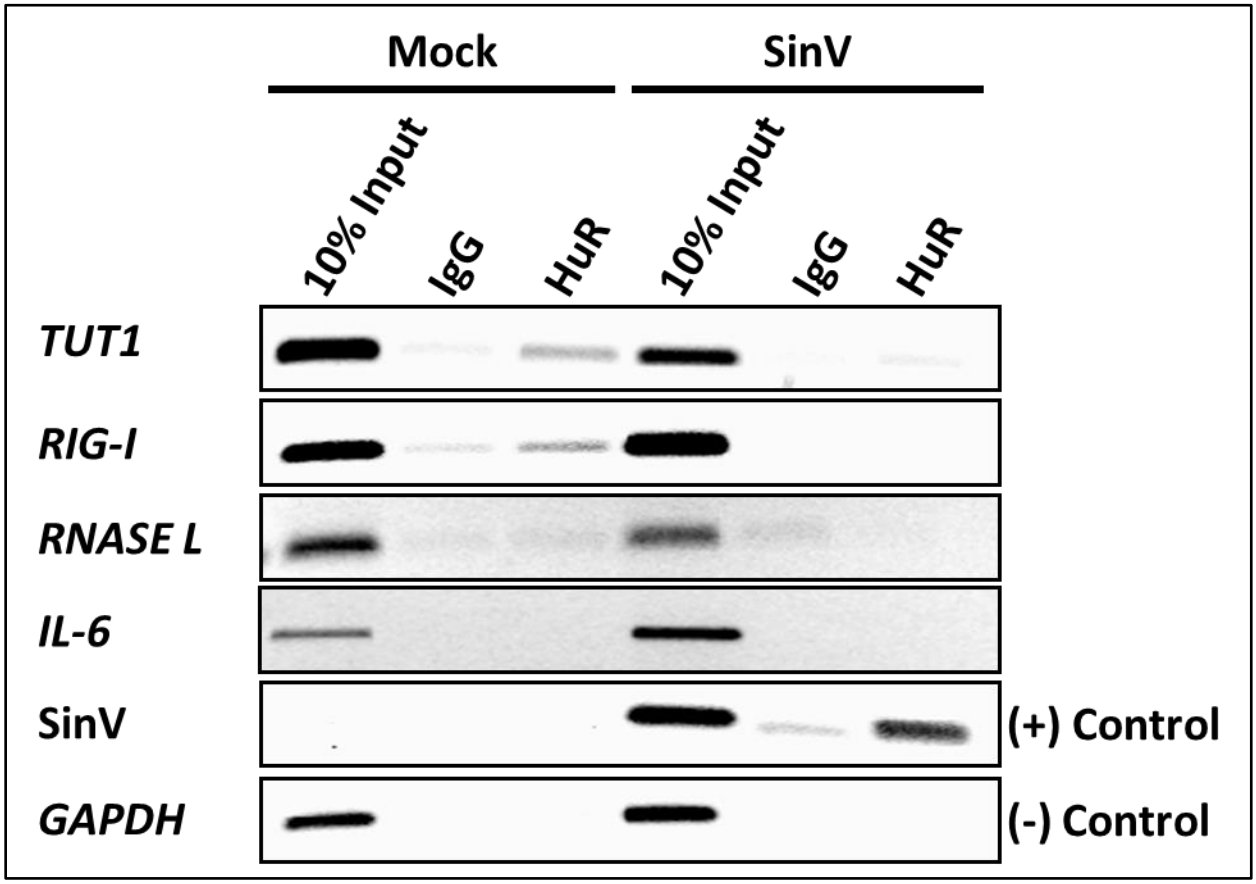

Figure 24. mRNAs that are Destabilized During SinV Infection Bind HuR to a Lesser Extent in SinV Infected Cells. 293T cells were mock infected (Mock lanes) or SinV infected (SinV lanes). 24 hours post infection cells were formaldehyde cross-linked and RNA was co-immunoprecipitated using a control antibody (IgG lanes) or a HuR specific antibody (HuR lanes). Co-immunoprecipitated mRNAs were then analyzed via RT-PCR. GAPDH and SinV RNAs were assayed to serve as controls to establish specificity of the HuR immunoprecipitation. The data in the 10% input lanes were generated by RT-PCR analysis of the indicated ratio of starting extracted to the amount used in the immunoprecipitated lanes.

One suggested mechanism for how HuR stabilizes mRNAs lies in its ability to compete with miRNAs for binding to targeted mRNAs (Simone and Keene, 2013), as discussed in the introduction (Fig. 7). When HuR protein levels or availability is high in cells, HuR binds to mRNAs and sterically blocks the binding site of miRNAs or it can refold the mRNA to reduce miRNA access, thus preventing the RISC complex from initiating mRNA decay. Since the data above suggest that HuR protein is largely unavailable to bind to cellular mRNAs during a SinV infection, we investigated the effect of SinV infection on the abundances of five mRNAs that have been previously shown to the regulated by the interplay between HuR and miRNA binding (Abdelmohsen and Gorospe, 2010). 293T cells were either mock infected or infected with SinV. At 36 and 72 hours post infection, total RNA samples were obtained and analyzed via qRT-PCR. As seen in Fig. 25, all five mRNAs that are normally coordinately regulated by HuR-miRNA competitions (*MYC, COX-2, FOS, HIFIA,* and *VEGF-A*) were greatly decreased in expression during SinV infection (to ~40% or less of values obtained in mock infected cells). These results are consistent with our model that HuR is unavailable to promote the stability of cellular transcripts during a SinV infection.

Finally, we wished to extend these observations to a global analysis of cellular mRNA half-lives during SinV infection. Total RNA samples were obtained from time points post ActD treatment of cells either mock infected or infected with SinV for 24 hours. All infections/mock-treatments were performed in triplicate to ensure reproducibility. Samples were quality controlled by assessing the effect of SinV infection on the half-life of TUT1 mRNA (Fig. 22), and were subjected to RNA-seq analysis by Dr. Tian at UMDNJ-New Jersey Medical School. Recently, we received the preliminary results of this experiment and are working with Dr. Liu (UMDNJ-NJMS) to further analyze the data using bioinformatics.

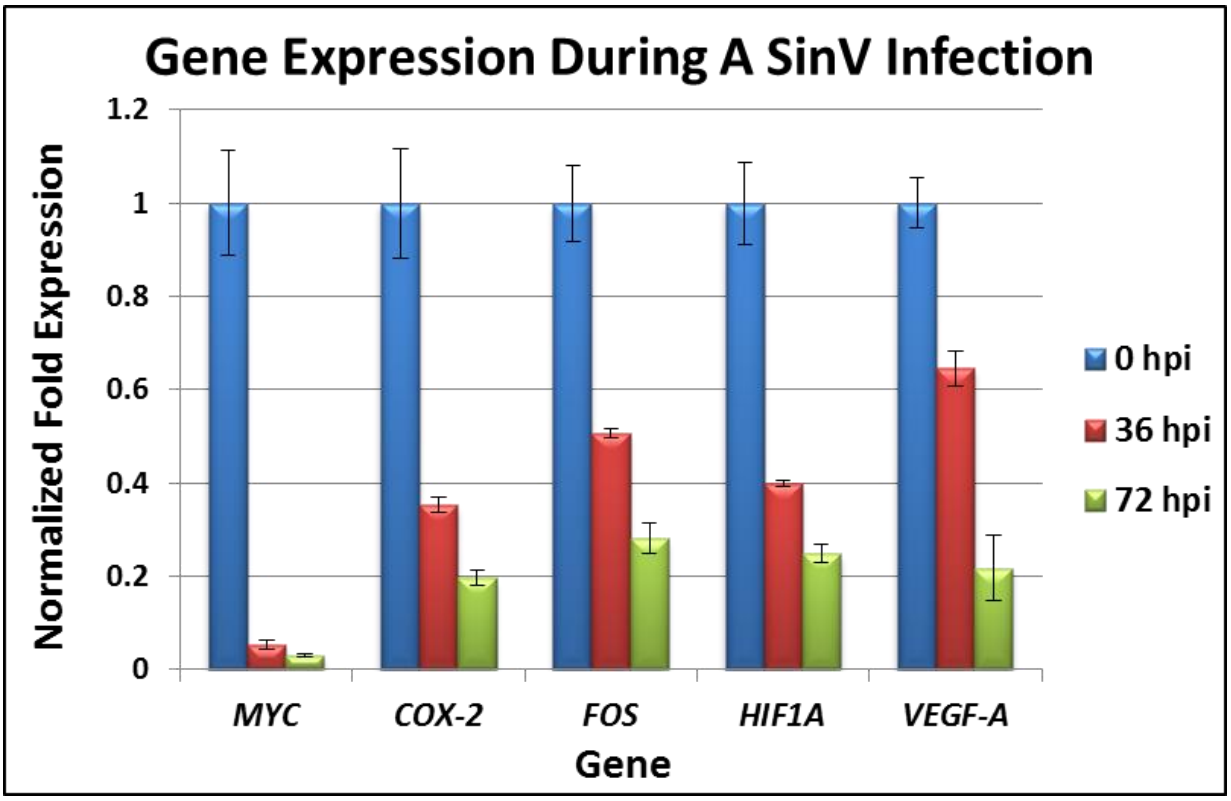

Figure 25. mRNAs that are Naturally Coordinately Regulated by HuR and miRNA Competitive Binding are Dysregulated in SinV Infection. 293T cells were mock infected or infected with SinV. Total RNA was collected at 0, 36 and 72 hours post infection (hpi) and levels of the indicated mRNA were analyzed via RT-qPCR. Gene expression was normalized to *GAPDH* were levels remained relatively unchanged throughout the infections.

IV. Sindbis Virus Infection Causes Dysregulation of Nuclear mRNA Processing: Effects on Alternate Polyadenylation of pre-mRNAs

In addition to its well-described role as an RNA stability factor, HuR protein has also been shown to regulate pre-mRNA processing events in the nucleus (Glisovic et al., 2008; Sanchez-Diaz and Penalva, 2006). Alternative polyadenylation of the HuR pre-mRNA, for example, is autoregulated by the HuR protein (Dai et al., 2012; Al-Ahmadi et al., 2009). As shown above in Fig. 8, the relative level of HuR protein in the nucleus influences poly(A) site choice. During periods of high levels of HuR protein in the nucleus, HuR binds to the proximal polyadenylation site and prevents the polyadenylation machinery from gaining access to this site. Thus, 3' end cleavage and polyadenylation occurs instead at a downstream site, resulting in the production of an isoform of the HuR mRNA with a longer 3'UTR that contains destabilizing elements that cause it to have a short half-life and thus possibly less translatable. Alternatively, when there are low nuclear HuR levels, the upstream poly(A) site is readily used by the polyadenylation machinery and a shorter, more stable and possibly more translatable isoform of HuR mRNA is produced (Dai et al., 2012).

Since levels of HuR levels in the nucleus are dramatically reduced during a SinV infection (Sokoloski et al., 2010; Dickson et al., 2012; see Fig. 15), we hypothesized that alternative polyadenylation of HuR pre-mRNA would likely be dysregulated. To test this, 293T cells were infected with SinV and total RNA was collected at 24, 36, 48, and 72 hours post infection. The samples were then analyzed by RT-qPCR with HuR mRNA isoform-specific primers to assess and relative differences in isoform abundance. As seen in Fig. 26, the shorter HuR mRNA isoforms (which are produced when HuR does not bind and insulate the upstream

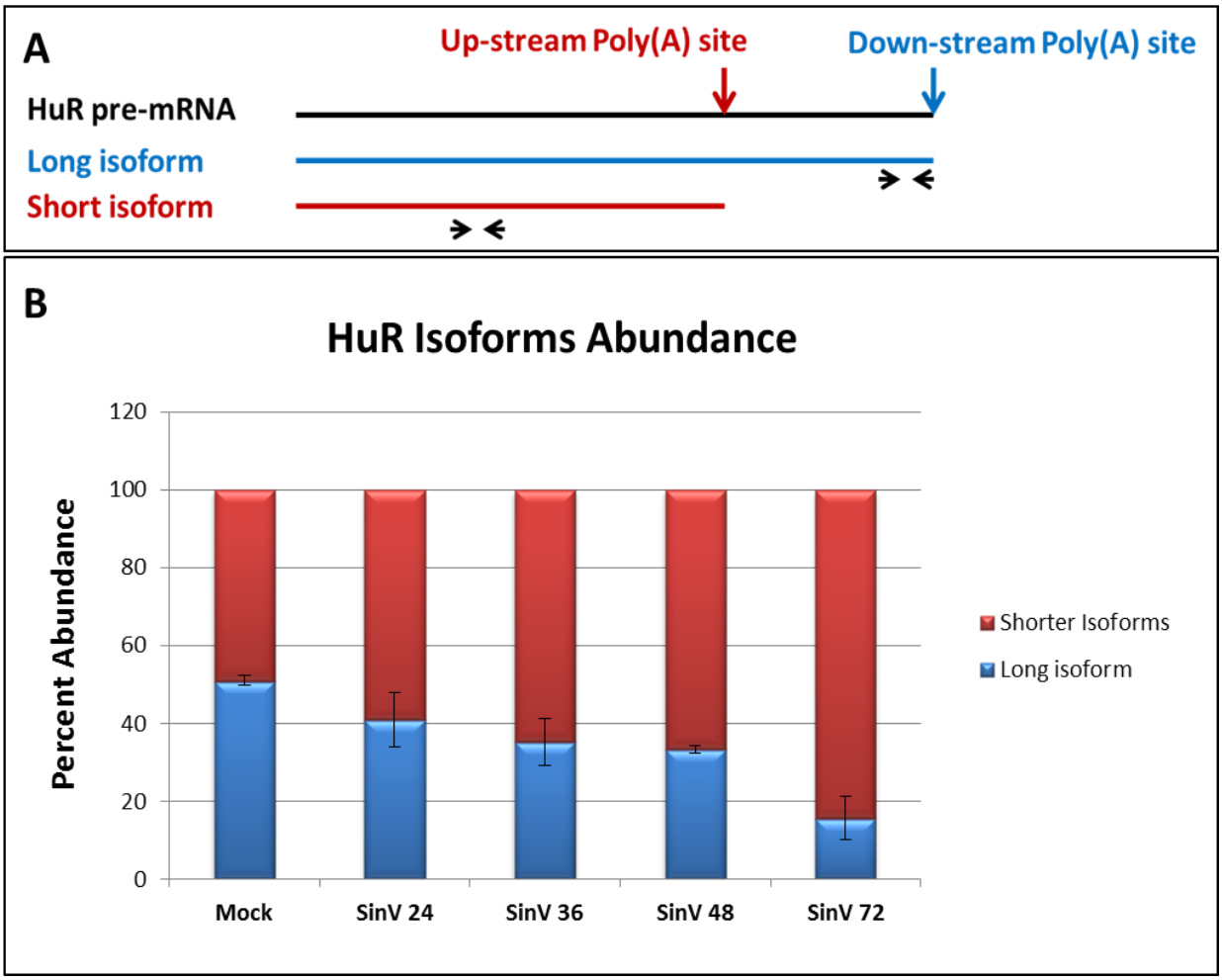

Figure 26. The Regulation of Alternative Polyadenylation of HuR Pre-mRNA is Altered During SinV Infection. (A) HuR isoform schematic; the arrows indicate the region of primer amplification. (B) 293T cells were mock infected or SinV infected and total RNA was collected at the indicated time points. Samples from two separate infections were analyzed by RT-qPCR.

poly(A) site from the 3' end processing machinery) comprised approximately 50% of the HuR mRNAs in an uninfected cell. However, this ratio decreased throughout the time course of SinV infection. By 72 hours post infection, the shorter HuR isoforms now comprise approximately 85% of the HuR mRNA population. These data suggest that SinV infection influences alternative polyadenylation of HuR pre-mRNA, most likely through its sequestration of HuR protein to the cytoplasm of infected cells. Interestingly, by promoting the production of the shorter, more translatable form of HuR mRNA, SinV likely encourages the production of more HuR protein to be used to promote viral RNA stability and efficient replication. To our knowledge, this is the first time that a cytoplasmic RNA virus has been shown to influence the regulation of alternative polyadenylation in the nucleus.

DISCUSSION

Previous work in our lab has shown that several alphaviral species interact with the cellular HuR protein with high affinity to a URE sequence contained in their 3'UTR and that this binding is necessary in order for the virus to grow to high titers (Garneau et al., 2008; Sokoloski et al., 2010). However, not all alphaviruses contain a typical URE. The work described in this thesis has shown that the cellular HuR protein binds with high affinity to alphaviral species that do not contain a typical URE sequence. This observation has led us to hypothesize that the HuR:alphaviral RNA interaction is a characteristic of several, if not all alphaviruses.

Furthermore, the examination of the mechanism of how SinV commandeers the cellular HuR protein to bind to its viral RNA has led us to hypothesize that the high affinity binding site of HuR on the viral 3'UTR acts as a sponge – soaking up the HuR protein immediately after translation or trapping it when it is naturally shuttled out of the nucleus during infection. Thus, the result is the cytoplasmic accumulation of the HuR protein during an alphavirus infection.

Finally, this thesis set out to investigate what effects the cytoplasmic accumulation of the cellular HuR protein caused by an alphavirus infection has on the host cell. We found that the lack of free HuR protein during a SinV infection results in at least two major cellular dysfunctions: 1) mRNAs that normally rely on the cellular HuR protein for stability are destabilized and 2) SinV influences the alternative polyadenylation of pre-mRNAs.

I. Many Alphaviruses Bind the Cellular HuR Protein

Previous work in our lab has shown that when the binding site for the HuR protein has been removed from the SinV RNA, the virus is unable to replicate efficiently (Sokoloski et al., 2010). Therefore, since HuR has been shown to bind several alphaviruses that contain a URE (Garneau et al., 2008; Sokoloski et al., 2010) and alphaviruses that do not contain a typical URE in their 3'UTR (as shown in this thesis), it is quite possible that the cellular HuR protein is universally required by all alphaviruses for efficient replication throughout the course of an infection.

In addition to ChikV and RRV, the alphavirus O'nyong-nyong virus (ONNV) lacks a typical URE sequence in its 3'UTR. HuR has been shown to bind to AU/GU rich tracts along RNAs (Abe et al., 1996; López de Silanes et al., 2004). Therefore, if HuR does in fact bind to all alphaviruses, then the 3'UTR sequence of ONNV should have similar HuR binding sites as those described above for ChikV and RRV. As shown in Figure 27, the 3'UTR sequence of ONNV has several potential binding sites for HuR based on the identified binding sites for HuR in other transcripts. Future studies could clone the 3'UTR of ONNV to determine if and where HuR protein binds.

Knowing that HuR is required by at least one alphavirus, SinV, to grow to higher titers (Sokoloski et al., 2010) and the discovery that the binding of HuR is characteristic of alphaviruses is paramount because it provides us a target for development of an anti-alphaviral drug. If we could block HuR binding to alphavirus RNAs, we could cripple virus replication and give the cell time to respond and eradicate the infection. Currently, our lab is in the process of screening compounds that would inhibit HuR binding to the 3'UTR of SinV, resulting in the

Figure 27. The O'nyong-nyong 3'UTR Sequence. Highlighted in green is the typical CSE, found in every alphavirus, while the red highlights are AU/GU rich sequences where the cellular HuR protein may bind.

deadenylation of the viral RNA, which would ultimately result in the degradation of the viral RNA.

The work described to determine the binding sites of HuR to ChikV and RRV was all performed *in vitro* using a recombinant HuR protein. To investigate the binding of HuR to these two viruses further, one could incubate the viral 3'UTRs in whole cell lysate, cross-link the proteins to the RNAs then perform a pull-down using a HuR specific antibody and sequence the regions bound by HuR. This assay could also be performed in infected cells to confirm the viral RNA:HuR interactions are occurring during an infection. One could also perform a RNA footprinting assay (Pearson et al., 1994). Both of these assays would supplement the HuR binding results described in this thesis and narrow down the exact regions that HuR is interacting on these viral 3'UTRs.

Our lab has shown that ChikV and RRV infection results in the cytoplasmic accumulation of HuR suggesting that HuR is needed for viral replication (Dickson et al., 2012). To determine if the binding of HuR to ChikV and RRV plays a role in stabilizing the virus so it can grow to higher titers, one could delete the above identified HuR binding regions and measure the efficiency in which the virus grows. If viral growth is hindered due to these deletions, it would further substantiate our hypothesis that the binding of HuR to alphaviral RNAs plays a critical role in the efficient replication of all alphaviruses.

The ELAV/Hu family contains three other family members: HuB, HuC and HuD. Interestingly, only HuR is localized to the nucleus and is expressed in every human cell while the other family members are only expressed in neuronal cells and are predominately cytoplasmic (Antic and Keene, 1997; Keene, 1999; Brennan and Steitz, 2001; Hinman and Lou, 2008). All

of these family members share the same RNA recognition motifs (Antic and Keene, 1997) and have been shown to bind to AU/GU rich tracts on mRNAs (Gao et al., 1994; Levine et al., 1993; Chung et al., 1996) and stabilize them (Jain et al., 1995; Jain et al., 1997; Fan and Steitz, 1998b; Peng et al., 1998; Levy et al., 1998; Antic et al., 1999). Therefore, it is quite possible that these host factors could also bind alphavirus RNAs. To test this idea, one could incubate alphaviral 3'UTRs in whole cell lysate from neuronal cells and determine if there are any viral RNA:Hu(B,C,D) interactions. If these interactions do occur, then it would be interesting to look at virus replication in neuronal cells versus other cells. It is plausible that an alphaviral infection in neuronal cells would be established faster because the Hu proteins are already available in the cytoplasm to bind the viral RNA and would not have to commandeer the protein from the nucleus as it does with HuR (as described in this thesis). However, if the virus did sequester these other Hu factors (like it does with HuR), then further research would have to be done to identify the effect(s), positive or negative, on virus replication.

II. The Underlying Mechanism of Alphaviral-Induced Cytoplasmic Accumulation of HuR

We have shown that several alphaviruses, containing a canonical URE sequence or not, cause the cytoplasmic accumulation of the cellular HuR protein. Yet, the mechanism of this accumulation was unknown until this study. At first, we believed that a phosphorylation event on the HuR protein was the culprit, resulting in the accumulation of HuR in the cytoplasm (Dickson et al., 2012). However, here we determined that the 3'UTR of SinV independent of other virus functions was responsible for the amassing amounts of HuR in the cytoplasm. To

confirm these findings, we transfected only the SinV 3'UTR RNA into cells and observed the cytoplasmic accumulation of HuR protein.

The regions identified on the SinV 3'UTR that were responsible for a significant accumulation of HuR in the cytoplasm were the URE and CSE. This finding suggests that the high affinity binding site of HuR to these two regions acts as a sponge in order to keep HuR in the cytoplasm as it is being translated or shuttled to the cytoplasm. However, to verify these results, one could transcribe the URE/CSE construct and transfect in only the 60 base RNA to see if the same accumulation of HuR occurs. Interestingly, we observed no change in the localization of HuR when the TNFα ARE was transfected into cells – despite the fact that the HuR protein has been shown to bind to this region (Dean et al., 2001). Perhaps the TNFα binding site is below the affinity and/or off-rate threshold for the HuR interaction that is required to cause the altered subcellular localization of the protein.

By determining the half-life of the HuR protein, we were able to support the HuR sponge hypothesis. Two events could be occurring during an alphaviral infection resulting in this cytoplasmic accumulation of HuR: 1) HuR is being relocalized from the nucleus to the cytoplasm or 2) the virus is keeping HuR in the cytoplasm as the protein is being translated or shuttled to the cytoplasm. Because we have shown that an atypical event regarding the phosphorylation of HuR was occurring during an infection (Dickson et al., 2012), we hypothesized that a combination of these two events could be happening. If the latter of the two was occurring, then the pre-existing population of HuR in the nucleus must be degraded or shuttled to the cytoplasm. The results in Fig. 20 indicate that because of the fairly short half-life of the protein, the pre-existing population in the nucleus could undergo degradation while the virus is soaking up the free HuR as it is being translated in the cytoplasm. However, a more in-

depth analysis of the de-phosphorylation event on the HuR protein during a SinV infection needs to be performed to reveal if a shuttling event is occurring.

As discussed above, we have shown that several alphavirus genomic RNA sequences bind HuR; therefore, it is quite possible that all these alphaviruses could be acting through the same mechanism to achieve a high cytoplasmic level of the HuR protein. To test this hypothesis, one could clone the high affinity binding sites of HuR identified above for ChikV and RRV, and through transfections of these constructs, investigate whether or not they cause an accumulation of HuR in the cytoplasm. If the high affinity binding sites alone resulted in the cytoplasmic accumulation of HuR, one could conclude that this is a mechanism in which many, if not all, alphaviruses commandeer the cellular HuR protein for its own benefit.

Several other positive sense (+) RNA viruses have been shown to sequester a variety of host RNA binding proteins (RBPs) to stabilize their RNAs during an infection (Zhenghe and Nagy, 2011). For example, Poliovirus has been shown to bind the cellular poly(rC)-binding protein (PCBP) to stabilize its genome (Murray et al., 2001). The La auto-antigen binds to the stem-loop structures and a large U-rich tract on the 3'UTR of Hepatitis C virus (HCV) which hinders the degradation of the HCV RNA (Spangberg et al., 2001). Furthermore, turnip yellow mosaic virus (TYMV) protects itself from RNase A digestion by binding eEF1A (a tRNA-binding protein) to its tRNA-like structure (Joshi et al., 1986). Knowing this, along with the mechanisms revealed in this study, one could speculate that the sponging of these other cellular proteins by these RNA viruses could result in severe cellular dysfunctions similar to the ones identified in this study.

Lastly, an accumulation of HuR in the cytoplasm has been directly linked to carcinogenesis due to the protein's ability to regulate the expression of several cell cycle mRNAs and proliferation-associated genes (Denkert et al., 2006; Erkinheimo et al., 2003; López de Silanes et al., 2003; Wang et al., 2000; Wang et al., 2002). Therefore, by developing transfection constructs containing the high affinity HuR binding sites uncovered in this thesis, one could potentially tie up all the free HuR in the cytoplasm. The hopes of this experiment would be to destabilize key HuR binding transcripts necessary for tumor growth. Moreover, this viral RNA sponge theory could be put to use during RNAi knockdown (KD) experiments. siRNAs or miRNAs target RNA sequences but do not always efficiently KD the protein. However, if one transfected in a construct containing high affinity binding sites for the protein of interest (to tie up any proteins still lingering around) and used it in conjunction with the siRNAs or miRNAs, more efficient KD could occur.

III. The Alphaviral-Induced Dysregulation of Cellular Transcripts

As mentioned above, the cellular HuR protein's normal function is to bind to approximately 15% of the cellular transcriptome (López de Silanes et al., 2004) and stabilize them. However, during several, if not all, alphaviral infections the HuR protein is bound by the viral RNAs, thus depleting the levels of free HuR. Consequently, we hypothesize that the transcripts that are customarily bound by HuR are no longer bound, resulting in their rapid degradation. This study has strengthened this hypothesis by showing, for the first time, that the commandeering of the cellular HuR protein by SinV results in a dysregulation of host cellular mRNAs.

One transcript identified in this study that was destabilized during a SinV infection is retinoic acid inducible gene I or *RIG-I*. This gene encodes a DExD/H box RNA helicase which is necessary for double-stranded RNA (dsRNA) recognition in the innate immune response (Yoneyama et al., 2004). During many viral infections, especially alphaviral infections, ds-viral-RNA intermediates are created throughout their life cycle. Therefore, by destabilizing *RIG-I*, it appears that SinV is able to reduce its detection by this host immune response. Another transcript that was found to be destabilized in a SinV infection was terminal uridylyl transferase 1 (*TUT1)*. *TUT1* encodes speckle targeted PIP5k1A-regulated poly(A) polymerase which has been shown to regulate the expression of select genes (Mellman et al., 2008). Therefore, by destabilizing this transcript, the virus would dysregulate normal gene expression. One could speculate that the result of this dysregulation would be to favor the viral replication and growth but further analysis is necessary for a deeper understanding. Further analysis of the RIG-I and TUT1 protein levels would strengthen this argument.

Together, the transcripts identified to be destabilized during an infection appear to be key transcripts that the virus would want to destabilize so it could establish an efficient infection and grow to higher titers. The preliminary investigations of our global analysis of transcripts destabilized during a SinV infection are beginning to strengthen these results as well. Although, *IL-6* and *RNASE L* both contain AREs and are thought to bind HuR (Hutin et al., 2013; Li et al., 2007), I did not see any binding to HuR in the RNA co-immunoprecipitations, suggesting there may be cell type specificities. Amazingly, the virus has evolved a binding site for this potent RNA stability factor (HuR) to stabilize its own RNA and it has also effectively destabilized crucial host mRNAs that may interfere with viral growth.

Not only does HuR play a role in inhibiting cellular decay machinery, it also covers microRNA (miRNA) binding sites preventing the binding of miRNAs on several mRNAs (Simone and Keene, 2013), thus stabilizing the transcripts. Knowing this, we hypothesized that due to the depletion of free HuR during a SinV infection, miRNAs must be binding to their target mRNAs more, resulting in the decreased abundance of these mRNAs. My initial investigation has shown a decrease in the abundance of these targeted mRNAs during an infection; however, much more research must be completed in order to strengthen this hypothesis. If miRNAs are targeting these mRNAs more during an infection, then the mRNAs should become more associated with the RNA-induced silencing complex (RISC). To determine if this occurring, one could perform RNA co-immunoprecipitations using antibodies specific for the Argonaute protein and using RT-PCR, determine if there is an increase of these miRNA targeted mRNAs bound to Argonaute during an alphavirus infection. Furthermore, one could design antigomirs against the specific miRNAs that target these mRNAs and transfect the antigomirs into the cells during an infection, then analyze the abundances on these RNAs (van Solingen et al., 2009). If the mRNA abundances are restored, the data would suggest that miRNA targeting is increased during an infection because HuR is unavailable to bind and cover the miRNA site on the mRNAs.

IV. The Alphaviral-Induced Regulation of Alternative Polyadenylation

Previous work has shown that the HuR protein autoregulates the alternative polyadenylation of the HuR pre-mRNA in the nucleus (Dai et al., 2012; Al-Ahmadi et al., 2009). According to these papers, the cell prefers high nuclear levels of the HuR protein. Therefore, when the cell experiences low nuclear levels of HuR protein, it wants to translate more of the

protein to return to the normal state. This is achieved through a negative feedback loop between the HuR protein and the HuR mRNA. During low nuclear levels of the HuR protein, the upstream poly(A) site on the HuR pre-mRNA – that is normally bound by the HuR protein – is uncovered which allows the shorter, more stable and possibly more translatable isoform of the HuR mRNA to be processed. Therefore, when this HuR mRNA is exported to the cytoplasm it is more efficiently translated, resulting in an increase of HuR protein that is imported back into the nucleus to reestablish the high nuclear levels of HuR protein. As previously described in our lab, HuR levels are increased in the cytoplasm during several alphavirus infections (Dickson et al., 2012). This led us to hypothesize that during an alphavirus infection there would be a shift in the HuR mRNA isoforms from long to short. The data we have described in this thesis suggests that there is in fact a shift in the HuR mRNA isoforms during a SinV infection, favoring the shorter more translatable form. This is the first time a cytoplasmic replicating virus has been shown to influence the polyadenylation of pre-mRNAs in the nucleus. This is very beneficial to the virus because it needs the HuR protein to grow to high titers and by influencing the processing of the shorter form of the HuR mRNA, more HuR will be available to bind the viral RNAs. This is a very interesting discovery and further investigation needs to be done in order to show whether or not a SinV infection influences the polyadenylation of any other transcripts, such as *CGRP* (Zhu et al., 2006).

Furthermore, HuR has been shown to bind and cover splicing sites during the processing of pre-mRNAs (Lebedeva et al., 2011). However, the low nuclear levels of HuR protein during an alphavirus infection could lead one to speculate that the virus could be influencing the alternative splicing of pre-mRNAs. By identifying mRNAs whose splicing is regulated by HuR one could design primers specific for detecting their different splicing variants. This would

determine if there is a change in splicing between uninfected and infected samples. If the virus infection results in alternative splicing, one can speculate that this regulation of splicing could favor the viral infection.

This is the first time that a cytoplasmic replicating virus has been shown to control alternative polyadenylation events in the nucleus. By regulating these cellular processes, the virus is able to induce a rapid infection and grow to higher titers more efficiently.

CONCLUSIONS

In conclusion, binding sites for the cellular HuR protein were identified on the 3'UTRs of both Chikungunya (ChikV) and Ross River (RRV) viruses. The HuR binding region on ChikV was identified as the distal (3') most RSE (RSE3). The HuR binding site in the 3'UTR of RRV was identified as a 75 base region just downstream of RSE4. Sequence analysis of both of these regions uncovered AU-rich tracts, a characteristic of many known HuR binding sites (Abe et al., 1996; López de Silanes et al., 2004; Meisner et al., 2004). These findings, as well as previous work on high-affinity HuR binding to U-rich elements in other alphaviruses, indicate that the commandeering of the HuR protein is likely a common trait among all alphavirus species.

Next, we uncovered the mechanism by which Sindbis virus (and likely other alphavirus) infection causes the cytoplasmic accumulation of the HuR protein that is predominantly nuclear in uninfected cells. The re-localization of HuR to the cytoplasm following transfection of an RNA containing the SinV 3'UTR in the absence of any other viral components suggested that the 3'UTR was the responsible moiety. Transfection studies using deletion derivatives of the SinV 3'UTR indicated that the 3' terminal 60 base URE/CSE region was necessary and sufficient to mediate HuR cytoplasmic accumulation. These data led us to hypothesize that the high affinity HuR binding sites in the SinV 3'UTR act like a sponge to sequester cytoplasmic HuR in order to cause its apparent re-localization. This process likely ensures that alphaviruses will have sufficient levels of available HuR to support a highly productive infection in the cytoplasm.

Finally, we report that the commandeering of HuR during a SinV infection led to a significant disruption in two aspects of cellular post-transcriptional regulation of gene

expression. First, cellular mRNAs that normally bind HuR and use the protein to regulate their stability can no longer efficiently interact with HuR during SinV infection thus leading to a significantly increased rate of degradation of this group of cellular transcripts. One factor in this observed destabilization may be that mRNAs that normally use the HuR protein to shield miRNA target sequences are now more prone to miRNA-mediated decay. Second, we demonstrated that Sindbis virus infection influences alternative polyadenylation in the nucleus. To our knowledge, this is the first time that a cytoplasmic RNA virus has been shown to influence regulated aspects of 3' end pre-mRNA processing.

In summary, this study has identified several novel molecular interactions between alphaviruses and host cells that may reflect unappreciated but fundamental mechanisms of viral pathogenesis and cytopathology.

REFERENCES

Abdelmohsen,K. and Gorospe,M. (2010). Posttranscriptional regulation of cancer traits by HuR. Wiley Interdiscip. Rev. RNA. *1*, 214-229.

Abdelmohsen,K., Srikantan,S., Kuwano,Y., and Gorospe,M.(2008). miR-519 reduces cell proliferation by lowering RNA-binding protein HuR levels. Proc. Natl. Acad. Sci. *105*, 20297-20302.

Abe,R., Sakashita,E., Yamamoto,K., and Sakamoto, H. (1996). Two different RNA binding activities for the AU-rich element and the poly(A) sequence of the mouse neuronal protein mHuC. Nucleic Acids Res. *24*, 4895-4901.

Ahola,T., Laakkonen,P., Vihinen,H., and Kaariainen,L. (1997). Critical residues of Semliki Forest virus RNA capping enzyme involved in methyltransferase and quanylyltransferase-like activites. J. Virol. *71*, 392-397.

Al-Ahmadi,W., Al-Ghamdi,M., Al-Haj,L., Al-Saif,M., and Khabar,K.S. (2009). Alternative polyadenylation variants of the RNA binding protein, HuR: abundance, role of AU-rich elements and auto-regulation. Nucleic Acids Res. *37*, 3612-3624.

Antic,D. and Keene,J.D. (1997). Embryonic lethal abnormal visual RNA- binding proteins involved in growth, differentiation, and posttranscriptional gene expression. Am. J. Hum. Genet. *67*, 273-278.

Antic,D., Lu,N., and Keene,J.D. (1999). ELAV tumor antigen, Hel-N1, by increases translation of neurofilament M mRNA and induces formation of neurites in human teratocarcinoma cells. Genes Dev. *13*, 449-461.

Bao,H., Ramamnathan,A.A., Kawalakar,O., Sundaram,S.G., Tingey,C., Bian,C.B., Muruganandam,N., Vijayachari,P., Sardesai,N.Y., Weiner,D.B., Ugen,K.E., and Muthumani,K. (2013). Nonstructural protein 2 (nsP2) of Chikungunya virus (CHIKV) enhances protective immunity mediated by a CHIKV envelope protein expressing DNA vaccine. Viral Immunol. *26*, 75-83.

Bartel, D.P. (2004). MicroRNAs: genomics, biogenesis, mechanism, and function. Cell. *116*, 281-297.

Barton,D.J., Sawicki,S.G., and Sawicki,D.L. (1988). Demonstration *in vitro* of temperature-sensitive elongation of RNA in Sindbis virus mutant ts6. J. Virol. *62*, 3597-3602.

Becker,T., Armache,J.P., Jarasch,A., Anger,A.M., Villa,E., Sieber,H., Motaal,B.A., Mielke,T., Berninghausen,O., and Beckmann,R. (2011). Structure of the no-go mRNA decay complex Dom34-Hbs1 bound to a stalled 80S ribosome. Nat. Struct. Mol. Biol. *18*, 715-720.

Bhattacharyya,S.N., Harbermacher,R., Martine,U., Closs,E.I., and Filipowicz,W. (2006). Relief of microRNA-mediated translational repression in human cells subjected to stress. Cell *125*, 1111-1124.

Bick,M.J., Carroll,J.W., Gao,G., Goff,S.P., Rice,C.M., and MacDonald,M.R. (2003). Expression of the zinc-finger antiviral protein inhibits alphavirus replication. J. Virol. *77*, 11555-11562.

Brennan,C.M. and Steitz,J.A. (2001). HuR and mRNA stability. Cell. Mol. Life Sci. *58*, 266-277.

Calisher,C.H. (1994). Medically important arboviruses of the United States and Canada. Clin. Microbiol. Rev. *7*, 89-116.

Chakrabarti,A., Jha,B.K., and Silverman,R.H. (2011). New insights into the role of RNase L in innate immunity. J. Interferon Cytokine Res. *31*, 49-57.

Chang,J.H., Xiang,S., Xiang,K., Manley,J.L., and Tong,L. (2011). Structural and biochemical studies of the 5'→3' exoribonuclease Xrn1. Nat. Struct. Mol. Biol. *18*, 270-276.

Chen,C.Y., Xu,N., and Shyu,A.B. (2002). Highly selective actions of HuR in antagonizing AU-rich element-mediated mRNA destabilization. Mol. Cell Biol. *22*, 7268-7278.

Chen,C.Y. and Shyu, A.B. (2011). Mechanisms of deadenylation-dependent decay. Wiley Interdiscip. Rev. RNA. *2*, 167-183.

Chowdhury,A., Raju,K.K., Kalurupalle,S., and Tharun,S. (2012). Both Sm-domain and C-terminal extension of Lsm1 are important for the RNA-binding activity of the Lsm1-7-Pat1 complex. RNA. *18*, 936-944.

Chung,S., Jiang,L., Cheng,S., and Furneaux,H. (1996). Purification and properties of HuD, a neuronal RNA-binding protein. J. Biol. Chem. *271*, 11518-11524.

Chung,S.Y. and Wooley,J. (1986). Set of novel, conserved proteins fold pre- messenger RNA into ribonucleosomes. Proteins. *1*, 195-210.

Collart,M.A. and Panasenko,O.O. (2012). The Ccr4—not complex. Gene. *492*, 42-53.

Dai,W., Zhang,G., and Makeyev,E.V. (2012). RNA-binding protein HuR autoregulates its expression by promoting alternative polyadenylation site usage. Nucleic Acids Res. *40*, 787-800.

Davidson,B.L. and McCray,P.B. Jr. (2011). Current prospects for RNA interference-based therapies. Nat. Rev. Genet. *12*, 329-340.

Dickson,A.M., Anderson,J.R., Barnhart,M.D., Sokoloski,K.J., Oko,L., Opyrchal,M., Galanis,E., Wilusz,C.J., Morrison,T.E., and Wilusz,J. (2012). Dephosphorylation of HuR protein during alphavirus infection is associated with HuR relocalization to the cytoplasm. J. Biol. Chem. *287*, 36229-36238.

Dean,J.L., Wait,R., Mahtani,K.R., Sully,G., Clark,A.R., and Saklatvala,J. (2001). The 3′ untranslated region of tumor necrosis factor alpha mRNA is a target of the mRNA-stabilizing factor HuR. Mol. Cell Biol. *21*, 721–730.

Devaux,A., Colegrove-Otero,L.J., and Standart,N. (2006). Xenopus ElrB, but not ElrA, binds RNA as an oligomer: possible role of the linker. FEBS Lett. *580*, 4947-4952.

Doller,A., Schlepckow,K., Schwalbe,H., Pfeilschifter,J., and Eberhardt,W. (2010). Tandem phosphorylation of serines 221 and 318 by protein kinase Cdelta coordinates mRNA binding andnucleocytoplasmic shuttling of HuR. Mol. Cell. Biol. *30,* 1397-1410.

Doller,A., Winkler,C., Azrilian,I., Schulz,S., Hartmann,S., Pfeilschifter,J., and Eberhardt,W. (2011). High-constitutive HuR phosphorylation at Ser 318 by PKC{delta} propagates tumorrelevant functions in colon carcinoma cells. Carcinogenesis *32,* 676-685.

Epis,M.R., Barker,A., Giles,K.M., Beveridge,D.J., and Leedman,P.J. (2011). The RNA-binding protein HuR opposes the repression of ERBB-2 gene expression by microRNA miR-331-3p in prostate cancer cells. J. Biol. Chem. 286, 41442-41452.

Fabian,M.R., Cieplak,M.K., Frank,F., Morita,M., Green,J., Srikumar,T., Nagar,B., Yamamoto,T., Raught,B., Duchaine,T.F., and Sonenberg,N. (2011). miRNA-mediated deadenylation is orchestrated by GW182 through two conserved motifs that interact with CCR4-NOT. Nat. Struct. Mol. Biol. *18*, 1211-1217.

Fan,X.C. and Steitz,J.A. (1998a). HNS, a nuclear-cytoplasmic shuttling sequence in HuR. Proc. Natl. Acad. Sci. U. S. A *95*, 15293-15298.

Fan,X.C. and Steitz,J.A. (1998b). Overexpression of HuR, a nuclear-cytoplasmic shuttling protein, increases the *in vivo* stability of ARE-containing mRNAs. EMBO J. *17*, 3448-3460.

Fialcowitz-White,E.J., Brewer,B.Y., Ballin,J.D., Willis,C.D., Toth,E.A., and Wilson,G.M. (2007). Specific protein domains mediate cooperative assembly of HuR oligomers on AU-rich mRNA-destabilizing sequences. J. Biol. Chem. *282*, 20948-20959.

Filipowicz,W., Bhattacharyya,S.N., and Sonenberg,N. (2008). Mechanisms of post-transcriptional regulation by microRNAs: are the answers in sight? Nat. Rev. Genet. *9*, 102-114.

Ford,L.P., Watson,J., Keene,J.D., and Wilusz,J. (1999). ELAV proteins stabilize deadenylated intermediates in a novel *in vitro* mRNA deadenylation/degradation system. Genes Dev. *13*, 188–201.

Frolov,I., Agapov,E., Hoffman,T.A., Jr., Pragai,B.M., Lippa,M., Schlesinger,S., and Rice,C.M. (1999). Selection of RMA replicons capable of persistent noncytopathic replication in mammalian cells. J. Virol. *73*, 3854-3865.

Fros,J.J., Domeradzka,N.E., Baggen,J., Geertsema,C., Flipse,J., Vlak,J.M., and Pijlman,G.P. (2012). Chikungunya virus nsP3 blocks stress granule assembly by recruitment of G3BP into cytoplasmic foci. J. Virol. *86*, 10873-10879.

Gantt,K.R., Cherry,J., Richardson,M., Karschner,V., Atasoy,U., and Pekala,P.H. (2006). The regulation of glucose transporter (GLUT1) expression by the RNA binding protein HuR. J. Cell Biochem. *99*, 565-574.

Gao,F., Carson,C., Levine,T.D., and Keene,J.D. (1994). Selection of a subset of mRNAs from 30UTR combinatorial libraries using neuronal RNA-binding protein, Hel-N1. Proc. Natl. Acad. Sci. USA. *91*, 11207-11211.

Gao,F.B. and Keene,J.D. (1996). Hel-N1/Hel-N2 proteins are bound to polyA + mRNA in granular RNP structures and are implicated in neuronal differentiation. J. Cell. Sci. *109*, 579-589.

Garmashova,N., Gorchakov,R., Frolova,E., and Frolov,I. (2006). Sindbis virus nonstructural protein nsP2 is cytotoxic and inhibits cellular transcription. J. Virol. *80*, 5686-5696.

Garneau,N.L., Sokoloski,K.J., Opyrchal,M., Neff,C.P., Wilusz,C.J., and Wilusz,J. (2008). The 3' untranslated region of sindbis virus represses deadenylation of viral transcripts in mosquito and mammalian cells. J. Virol. *82*, 880-892.

George,J. and Raju,R. (2000). Alphavirus RNA genome repair and evolution: molecular characterization of infectious Sindbis virus isolates lacking a known conserved motif at the 3’ end of the genome. J. Virol. *74*, 9776-9785.

Gherzi,R., Chen,C.Y., Trabucchi,M., Ramos,A., and Briata,P. (2010). The role of KSRP in mRNA decay and microRNA precursor maturation. Wiley Interdiscip. Rev. RNA. *1*, 230-239.

Glisovic,T., Bachorik,J.L., Yong,J., and Dreyfuss,G. (2008). RNA-binding proteins and post-transcriptional gene regulation. FEBS Lett. *582*, 1977–1986.

Good,P.J. (1995). A conserved family of elav-like genes in vertebrates. Proc. Natl. Acad.Sci. U. S. A *92*, 4557-4561.

Gorchakov,R., Frolova,E., and Frolov,I. (2005). Inhibition of transcription and translation in Sinbis virus-infected cells. J. Virol. *79*, 9397-9409.

Gorchakov,R., Frolova,E., Williams, B.R., Rice,C.M., and Frolov,I. (2004). PKR-dependent and –independent mechanisms are involved in translation shutoff during Sindbis virus infection. J. Virol. *78*, 8455-8467.

Gratacós,F.M. and Brewer,G. (2010). The role of AUF1 in regulated mRNA decay. Wiley Interdiscip. Rev. RNA. *1*, 457-473.

Hardy,R.W. (2006). The role of the 3' terminus of the Sindbis virus genome in minus-strand initiation site selection. Virology *345*, 520-531.

Hardy,R.W. and Rice,C.M. (2005). Requirements at the 3' end of the Sindbis virus genome for efficient synthesis of minus-strand RNA. J. Virol. *79*, 4630-4639.

Hardy,W.R. and Strauss,J.H. (1989). Processing the nonstructural polyproteins of Sindbis virus: nonstructural proteinase is in the C-terminal half of nsP2 and functions both in *cis* and *trans*. J. Virol. *63*, 4653-4664.

Hinman,M.N. and Lou,H. (2008). Diverse molecular functions of Hu proteins. Cell. Mol. Life Sci. *65*, 3168-3181.

Hutin,S., Lee,Y., and Glaunsinger,B.A. (2013). An RNA element in human interleukin 6 confers escape from degradation by the gammaherpesviral SOX protein. J. Virol. *13*, [Epub ahead of print].

Ibrahim,F., Rohr,J., Jeong,W.J., Hesson,J., and Cerutti,H. (2006). Untemplated oligoadenylation promotes degradation of RISC-cleaved transcripts. Science. *314*, 1893.

Jain,R.G., Andrews,L.G., McGowan,K.M., Gao,F., Keene,J.D., and Pekala,P.P. (1995). Hel-N1, an RNA-binding protein, is a ligand for an A + U rich region of the GLUT1 30 UTR. Nucleic Acids Symp. Ser. *33*, 209-211.

Jain,R.G., Andrews,L.G., McGowan,K.M., Pekala,P., and Keene,J.D. (1997). Ectopic expression of Hel-N1, an RNA-binding protein, increases glucose transporter (GLUT1) expression in 3T3-L1 adipocytes. Mol. Cell. Biol. *17*, 954-962.

Jones,P.H., Maric,M., Madison,M.N., Maury,W., Roller,R.J., and Okeoma,C.M. (2013). BST-2/tetherin-mediated restriction of Chikungunya (CHIKV) VLP budding is counteracted by CHIKV non-structural protein 1 (nsP1). Virology. *438*, 37-49.

Joshi,R.L., Ravel,J.M., and Haenni,A.L. (1986). Interaction of turnip yellow mosaic virus Val-RNA with eukaryotic elongation-factor EF-1[alpha]. Search for a function. EMBO J. *5*, 1143–1148.

Kasashima,K., Sakashita,E., Saito,K., and Sakamoto,H. (2002). Complex formation of the neuron-specific ELAV-like Hu RNA-binding proteins. Nucleic Acids Res. *30*, 4519-4526.

Katsanou,V., Papadaki,O., Milatos,S., Blackshear,P.J., Anderson,P., Kollias,G., and Kontoyiannis,D.L. (2005). HuR as a negative posttranscriptional modulator in inflammation. Mol. Cell. *19*, 777–789.

Kawai,T., Lal,A., Yang,X., Galban,S., Mazan-Mamczarz,K., and Gorospe,M. (2006). Translation control of cytochrome c by RNA-binding proteins TIA-1 and HuR. Mol. Cell Biol. *26*, 3295-3307.

Keene,J.D. (1999) Why is Hu where? Shuttling of early-response gene messenger RNA subsets. Proc. Natl. Acad. Sci. USA. *96*, 5-7.

Khabar,K.S., Bakheet,T., and Williams,B.R. (2005). AU-rich transient response transcripts in the human genome: expressed sequence tag clustering and gene discovery approach. Genomics *85*, 165-175.

Khan,A.H., Morita,K., Parquet,M.C., Hasebe,F., Mathenge,E.G., and Igarashi,A. (2002). Complete nucleotide sequence of Chikungunya virus and evidence for an internal polyadenylation site. J. Gen. Virol. *83*, 3075-3084.

Kim,D.Y., Atasheva,S., Frolova,E.I., and Frolov,I. (2013). Venezuelan equine encephalitis virus nsP2 protein regulates packaging of viral genome into infectious virions. J. Virol. [Epub ahead of print].

Kim,H.H., Abdelmohsen,K., Lal,A., Pullmann,R., Jr., Yang,X., Galban,S., Srikantan,S., Martindale,J.L., Blethrow,J., Shokat,K.M., and Gorospe,M. (2008a). Nuclear HuR accumulation through phosphorylation by Cdk1. Genes Dev. *22*, 1804-1815.

Kim,H.H., Kuwano,Y., Srikantan,S., Lee,E.K., Martindale,J.L., and Gorospe,M. (2009). HuR recruits let-7/RISC to repress c-Myc expression. Genes Dev. *23*, 1743-1748.

Kim,H.H. and Gorospe,M. (2008b). Phosphorylated HuR shuttles in cycles. Cell Cycle *7*, 3124-3126.

Kim,H.H., Yang,X., Kuwano,Y., and Gorospe,M. (2008c). Modification at HuR(S242) alters HuR localization and proliferative influence. Cell Cycle *7*, 3371-3377.

van Kouwenhove,M., Kedde,M., and Agami,R. (2011). MicroRNA regulation by RNA-binding proteins and its implications for cancer. Nat. Rev. Cancer. *11*, 644-656.

Kratochvill,F., Machacek,C., Vogl,C., Ebner,F., Sedlyarov,V., Gruber,A.R., Hartweger,H., Vielnascher,R., Karaghiosoff,M., Rülicke,T., Müller,M., Hofacker,I., Lang,R., and Kovarik,P. (2011). Tristetraprolin-driven regulatory circuit controls quality and timing of mRNA decay in inflammation. Mol. Syst. Biol. *7*, 560.

Lebedeva,S., Jens,M., Theil,K., Schwanhäusser,B., Selbach,M., Landthaler,M., and Rajewsky,N. (2011). Transcriptome-wide analysis of regulatory interactions of the RNA-binding protein HuR. Mol. Cell. *5*, 340-352.

Lemm,J.A., Bergqvist,A., Read,C.M., and Rice,C.M. (1998). Template-dependent initiation of Sindbis virus RNA replication *in vitro*. J. Virol. *72*, 6546-6553.

Levine,T.D., Gao,F., King,P.H., Andrews,L.G., and Keene,J.D. (1993). Hel-N1: an autoimmune RNA-binding protein with specificity for 3' uridylate-rich untranslated regions of growth factor mRNAs. Mol Cell Biol. *13*, 3494-3504.

Levy,N.S., Chung,S., Furneaux,H., and Levy,A.P.(1998). Hypoxic stabilization of vascular endothelial growth factor mRNA by the RNA-binding protein HuR. J. Biol. Chem. *273*, 6417-6423.

Li,X.Y., Andersen,J.B., Ezelle,H.J., Wilson,G.M., and Hassel,B.A. (2007). Post-transcriptional regulation of RNase-L expression is mediated by the 3'-untraslated region of its mRNA. J. Biol. Chem. *16*, 7950-7960.

Li,Y., Song,M., and Kiledjian,M. (2011). Differential utilization of decapping enzymes in mammalian mRNA decay pathways. RNA. *17*, 419-428.

Ligon,B.L. (2006). Reemergence of an unusual disease: the Chikungunya epidemic. Semin. Pediatr. Infect. Dis. *17*, 99-104.

Lin,J.Y., Shih,S.R., Pan,M., Li,C., Lue,C.F., Stollar,V., and Li,M.L. (2009). hnRNP A1 interacts with the 5' untranslated regions of enterovirus 71 and Sindbis virus RNA and is required for viral replication. J. Virol. *83*, 6106-6114.

Liu, L., Rao, J.N., Zou, T., Xiao, L., Wang, P.Y., Turner, D.J., Gorospe, M., and Wang, J.Y. (2009). Polyamines regulate c-Myc translation through Chk2-dependent HuR phosphorylation. Mol. Biol. Cell. *20*, 4885-4898.

Liu,S.W., Rajagopal,V., Patel,S.S., and Kiledjian,M. (2008). Mechanistic and kinetic analysis of the DcpS scavenger decapping enzyme. J. Biol. Chem. *283*, 16427-16436.

López de Silanes,I., Zhan,M., Lal,A., Yang,X., and Gorospe,M. (2004). Identification of a target RNA motif for RNA-binding protein HuR. Proc. Natl. Acad. Sci. U. S. A *101*, 2987-2992.

Lu,L., Wang,S., Zheng,L., Li,X., Suswam,E.A., Zhang,X., Wheeler,C.G., Nabors,L.B., Filippova,N., and King,P.H. (2009). Amyotrophic lateral sclerosislinked mutant SOD1 sequesters Hu antigen R (HuR) and TIA-1-related protein (TIAR): implications for impaired post-transcriptional regulation of vascular endothelial growth factor. J. Biol. Chem. *284*, 33989-33998.

Luers,A.J., Adams,S.D., Smalley,J.V., and Campanella,J.J. (2005). A phylogenomic study of the genus alphavirus employing whole genome comparison. Comp Funct. Genomics *6*, 217-227.

Lykke-Andersen,S., Tomecki,R., Jensen,T.H., and Dziembowski,A. (2011). The eukaryotic RNA exosome: same scaffold but variable catalytic subunits. RNA Biol. *8*, 61-66.

Ma,W.J., Cheng,S., Campbell,C., Wright,A., and Furneaux,H. (1996). Cloning and characterization of HuR, a ubiquitously expressed Elav-like protein. J. Biol. Chem. *271*, 8144-8151.

Ma,W.J., Chung,S., and Furneaux,H. (1997). The Elav-like proteins bind to AU rich elements and to the poly(A) tail of mRNA. Nucleic Acids Res. *25*, 3564-3569.

Mandel,C.R., Kaneko,S., Zhang,H., Gebauer,D., Vethantham,V., Manley,J.L., and Tong,L. (2006). Polyadenylation factor CPSF-73 is the pre-mRNA 3'-end-processing endonuclease. Nature *444*, 953-956.

Meisner,N.C., Hackermuller,J., Uhl,V., Aszodi,A., Jaritz,M., and Auer,M. (2004). mRNA openers and closers: modulating AU-rich element-controlled mRNA stability by a molecular switch in mRNA secondary structure. Chembiochem. *5*, 1432-1447.

Mellman,D.L., Gonzales,M.L., Song,C., Barlow,C.A., Wang,P., Kendziorski,C., and Anderson,R.A. (2008). A Ptdlns4,5P2-regulated nuclear poly(A) polymerase controls expression of select mRNAs. Nature. *21*, 1013-1017.

Moon,S.L., Barnhart,M.D., and Wilusz,J. (2012). Inhibition and Avoidance of mRNA Degradation by RNA Viruses. Current Opinion in Micro. *15*, 500-505.

Moucadel,V., Lopez,F., Ara,T., Benech,P., and Gautheret,D. (2007). Beyond the 3'end: experimental validation of extended transcript isoforms. Nucleic Acids Res. *35*, 1947-1957.

Murray,K.E., Roberts,A.W., and Barton,D.J. (2001). Poly(rC) binding proteins mediate poliovirus mRNA stability. RNA. *7*, 1126–1141.

Mukherjee,N., Corcoran,D.L., Nusbaum,J., Reid,D., Georgiev,S., Hafner,M., Ascano,M.Jr., Tuschl,T., Ohler,U., and Keene,J.D. (2011). Integrative regulatory mapping indicates that RNA-binding protein HuR (ELAVL1) couples pre-mRNA splicing and mRNA stability. Mol. Cell. *43*, 327-339.

Nagaoka,K., Suzuki,T., Kawano,T., Imakawa,K., and Sakai,S. (2006). Stability of casein mRNA is ensured by structural interactions between the 3'-untranslated region and poly(A) tail via the HuR and poly(A)-binding protein complex. Biochem. Biophys. Acta *1759*, 132-140.

Nickens,D.G. and Hardy,R.W. (2008). Structural and functional analyses of stem-loop 1 of the Sindbis virus genome. Virology. *370*, 158-172.

Nguyen,C.M., Chalmel,F., Agius,E., Vanzo,N., Khabar,K.S., Jegou,B., and Morello,D. (2009). Temporally regulated traffic of HuR and its associated ARE containing mRNAs from the chromatoid body to polysomes during mouse spermatogenesis. PloS. One. *4*, e4900.

Ou,J.H., Trent,D.W., and Strauss,J.H. (1982). The 3'-non-coding regions of alphavirus RNAs contain repeating sequences. J. Mol. Biol. *156*, 719-730.

Pearson,L., Chen,C.-h.B., Gaynor,R.P., and Sigman,D.S. (1994). Footprinting RNA-protein complexes following gel retardation assays: application to the R-17-procoat-RNA and tat-TAR interactions. Nuc. Acids Res. *22*, 2255-2263.

Peng,S.S., Chen,C.Y., Xu,N., and Shyu,A.B. (1998). RNA stabilization by the AU-rich element binding protein, HuR, an ELAV protein. EMBO J. *17*, 3461-3470.

Perlewitz,A., Nafz,B., Skalweit,A., Fahling,M., Persson,P.B., and Thiele,B.J. (2010). Aldosterone and vasopressin affect I- and I-EnaC mRNA translation. Nucleic Acids Res. *38*, 5746-5760.

Powers,A.M., Brault,A.C., Shirako,Y., Strauss,E.G., Kang,W., Strauss,J.H., and Weaver,S.C. (2001). Evolutionary relationships and systematics of the alphaviruses. J. Virol. *75*, 10118-10131.

Rathore,A.P., Nq,M.L., and Vasudevan,S.G. (2013). Differential unfolded protein response during Chikungunya and Sindbis virus infection: CHIKV nsP4 suppresses eIF2alpha phosphorylation. Virol. J. *10*, 36. [Epub ahead of print].

von Roretz,C. and Gallouzi,I.E. (2010). Protein kinase RNA/FADD/caspase-8 pathway mediates the proapoptotic activity of the RNA-binding protein human antigen R (HuR). J. Biol. Chem. *285,* 16806-16813.

Saleh,S.M., Poidinger,M., Mackenzie,J.S., Broom,A.K., Lindsay,M.D., and Hall,R.A. (2003). Complete genomic sequence of the Australian south-west genotype of Sindbis virus: comparisons with other Sindbis strains and identification of a unique deletion in the 3'-untranslated region. Virus Genes. *26,* 317-327.

Sanchez-Diaz,P. and Penalva,L.O. (2006). Post-transcription meets post-genomic: the saga of RNA binding proteins in a new era. RNA Biol. *3,* 101–109.

Sawicki,D., Barkhimer,D.B., Sawicki,S.G., Rice,C.M., and Schlesinger,S. (1990). Temperature sensitive shut-off of alphavirus minus strand RNA synthesis maps to a nonstructural protein, nsP4. Virology *174,* 43-52.

Schaeffer,D. and van Hoof,A. (2011). Different nuclease requirements for exosome-mediated degradation of normal and nonstop mRNAs. Proc. Natl. Acad. Sci. *108,* 2366-2371.

Schoenberg,D.R. (2011). Mechanisms of endonuclease-mediated mRNA decay. Wiley Interdiscip. Rev. RNA. *2,* 582-600.

Schwartz,O. and Albert,M.L. (2010). Biology and pathogenesis of Chikungunya virus. Nat. Rev. Microbiol. *8,* 491-500.

Sheets,M.D. and Wickens,M. (1989). Two phases in the addition of a poly(A) tail. Genes Dev. *3,* 1401-1412.

Simone,L.E. and Keene,J.D. (2013). Mechanisms coordinating ELAV/Hu mRNA regulons. Current Opinion in Genetics and Development. *23,* 1-9.

Sokoloski,K.J., Dickson,A.M., Chaskey,E.L., Garneau,N.L., Wilusz,C.J., and Wilusz,J. (2010). Sindbis virus usurps the cellular HuR protein to stabilize its transcripts and promote productive infections in mammalian and mosquito cells. Cell Host Microbe. *8,* 196-207.

van Solingen,C., Seghers,L., Bijkerk,R., Duijs,J.M., Roeten,M.K., van Oeveren-Rietdijk,A.M., Baelde,H.J., Monge,M., Vos,J.B., de Boer,H.C., Quax,P.H., Rabelink,T.J. and van Zonneveld,A.J. (2009). Antagomir-mediated silencing of endothelial cell specific microRNA-126 impairs ischemia-induced angiogenesis. J. Cell. Mol. Med. *13,* 1577-1585.

Soller,M. and White,K. (2005). ELAV multimerizes on conserved AU4-6 motifs important for ewg splicing regulation. Mol. Cell Biol. *25,* 7580-7591.

Song,M.,G., Bail,S., and Kiledjian,M. (2013). Multiple Nudix family proteins possess mRNA decapping activity. RNA. *19*, 390-399.

Spangberg,K., Wiklund,L., and Schwartz,S. (2001). Binding of the La auto-antigen to the hepatitis C virus 3′ untranslated region protects the RNA from rapid degradation in vitro. J Gen. Virol. *82*, 113–120.

Sreejith,R., Rana,J., Namrata,D., Kumar,K., Gabrani,R., Sharma,S.K., Gupta,A., Vrait,S., Chaudhary,V.K., and Gupta,S. (2012). Mapping interactions of Chikunguya virus nonstructural proteins. Virus Res. *169*, 231-236.

Strauss,J.H. and Strauss,E.G. (1994). The alphaviruses: gene expression, replication, and evolution. Microbiol. Rev. *58*, 491-562.

Strauss,J.H., Wang,K.S., Schmaljohn,A.L., Kuhn,R.J., and Strauss,E.G. (1994). Host-cell receptors for Sindbis virus. Arch. Virol. Suppl *9*, 473-484.

Thiboutot,M.M., Kannan,S., Kawalekar,O.U., Shedlock,D.J., Khan,A.S., Sarangan,G., Srikanth,P., Weiner,D.B., and Muthumani,K. (2010). Chikungunya: a potentially emerging epidemic? PLoS Negl. Trop. Dis. *4*, e623.

Tian,B., Hu,J., Zhang,H., and Lutz,C.S. (2005). A large-scale analysis of mRNA polyadenylation of human and mouse genes. Nucleic Acids Res. *33*, 201-212.

Toba,G. and White,K. (2008). The third RNA recognition motif of Drosophila ELAV protein has a role in multimerization. Nucleic Acids Res. *36*, 1390-1399.

Tomar,S., Hardy,R.W., Smith,J.L., and Kuhn,R.J. (2006). Catalytic core of alphavirus nonstructural protein nsP4 possesses terminal adenylyltransferase activity. J. Virol. *80*, 9962-9969.

Tominaga,K., Srikantan,S., Lee,E.K., Subaran,S.S., Martindale,J.L., Abdelmohsen,K., and Gorospe,M. (2011). Competitive regulation of nucleolin expression by HuR and miR-494. Mol. Cell Biol. *31*, 4219-4231.

Wang,K.S., Kuhn,R.J., Strauss,E.G., Ou,S., and Strauss,J.H. (1992). High affinity laminin receptor is a receptor for Sindbis virus in mammalian cells. J. Virol. *66*, 4992-5001.

Wang,L., Dowell,R.D. and Yi,R. (2013). Genome-wide maps of polyadenylation reveal dynamic mRNA 3'-end formation in mammalian cell lineages. RNA. *19*, 413-425.

Wang,W., Furneaux,H., Cheng,H., Caldwell,M.C., Hutter,D., Liu,Y., Holbrook,N.J., and Gorospe,M. (2000). HuR regulates p21 mRNA stabilization by UV light. Mol. Cell. Biol. *20*, 760-769.

Wang,W., Lin,S., Caldwell,C.M., Furneaux,H., and Gorospe,M. (2000). HuR regulates cyclin A and cyclin B1 mRNA stability during cell proliferation. EMBO J. *19*, 2340-2350.

Wang,Y.F., Sawicki,S.G., and Sawicki,D.L. (1991). Sindbis virus nsP1 functions in negative-strand RNA synthesis. J. Virol. *65*, 985-988.

Xin,Z., Han,W., Zhao,Z., Xia,Q., Yin,B., Yuan,J., and Peng,X. (2011). PCBP2 enhances the antiviral activity of IFN-α against HCV by stabilizing the mRNA of STAT1 and STAT2. PLoS One. *6*, e25419.

Yepiskoposyan,H., Aeschimann,F., Nilsson,D., Okoniewski,M., and Mühlemann,O. (2011). Autoregulation of the nonsense-mediated mRNA decay pathway in human cells. RNA. *17*, 2108-2118.

Yoneyama,M., Kikuchi,M., Natsukawa,T., Shinobu,N., Imaizumi,T., Miyagishi,M., Taira,K., Akira,S., and Fujita,T. (2004). The RNA helicase RIG-I has an essectial function in double-stranded RNA-induced innate antiviral responses. Nat. Immunol. *5*, 730-737.

Yoon,J.H., Abdelmohsen,K., Srikantan,S., Yang,X., Martindale,J.L., De,S., Huarte,M., Zhan,M., Becker,K.G., and Gorospe,M. (2012). LincRNA-p21 suppresses target mRNA translation. Mol. Cell. *47*, 648-655.

Yu,T.X., Wang,P.Y., Rao,J.N., Zou,T., Liu,L., Xiao,L., Gorospe,M., and Wang,J.Y. (2011). Chk2-dependent HuR phosphorylation regulates occludin mRNA translation and epithelial barrier function. Nucleic Acids Res. *39*, 8472-8487.

Zhenghe,L., Nagy,P.D. (2011). Diverse roles of host RNA-binding proteins in RNA virus replication. RNA Biol. *8*, 305-315.

Zhu,H., Zhou,H., Hasman,R.A., Lou,H. (2006). Hu proteins regulate polyadenylation by blocking sites containing U-rich sequences. J. Biol. Chem. *262*, 2203-2210.

APPENDIX A

List of Author's Publications

Dickson,A.M., Anderson,J.R., **Barnhart,M.D.**, Sokoloski,K.J., Oko,L., Opyrchal,M., Galanis,E., Wilusz,C.J., Morrison,T.E., and Wilusz,J. (2012). Dephosphorylation of HuR protein during alphavirus infection is associated with HuR relocalization to the cytoplasm. J. Biol. Chem. *287*, 36229-36238.

Moon,S.L., **Barnhart,M.D.**, Wilusz,J. (2012). Inhibition and Avoidance of mRNA Degradation by RNA Viruses. Current Opinion in Micro. *15*, 500-505.

APPENDIX B

Scatchard Plots to Determine Dissociation Constant

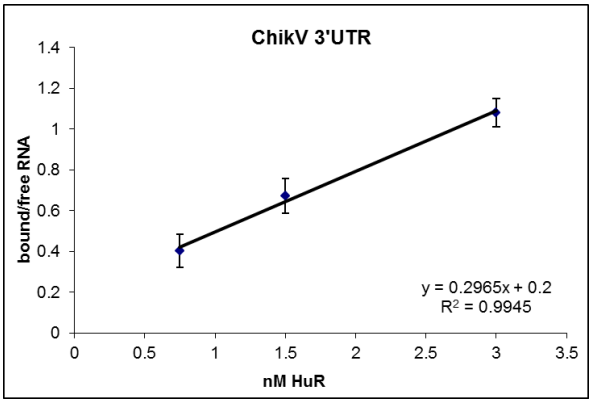

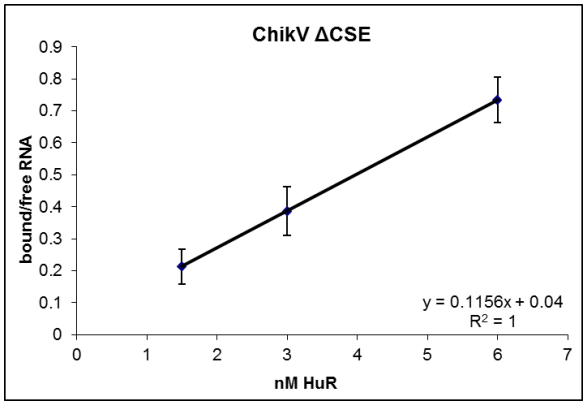

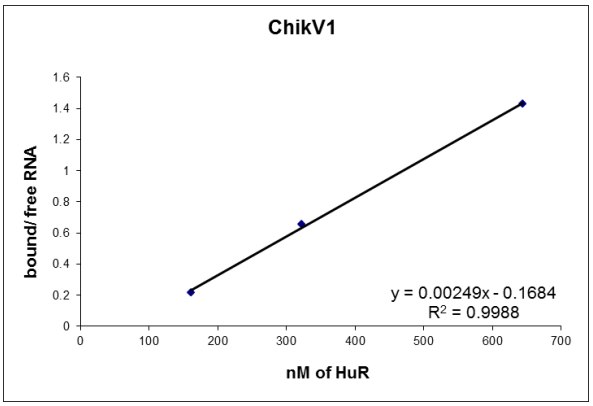

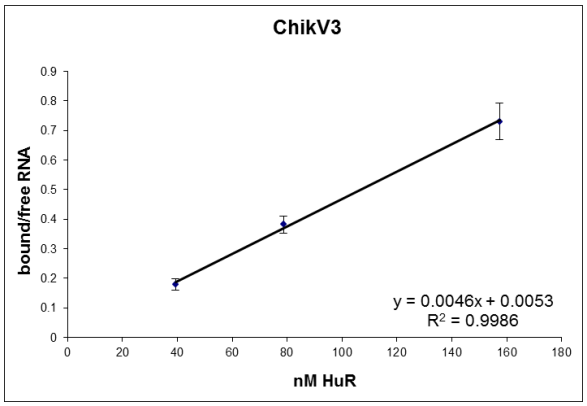

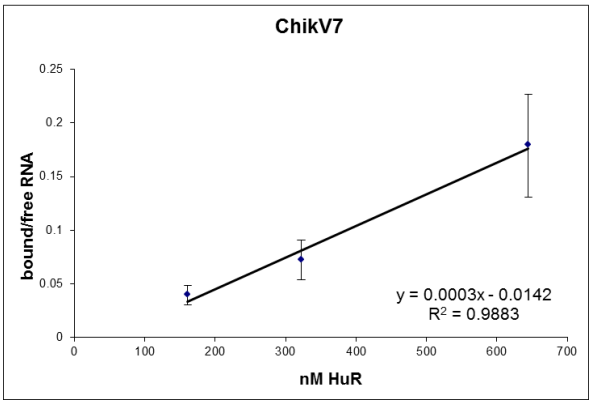

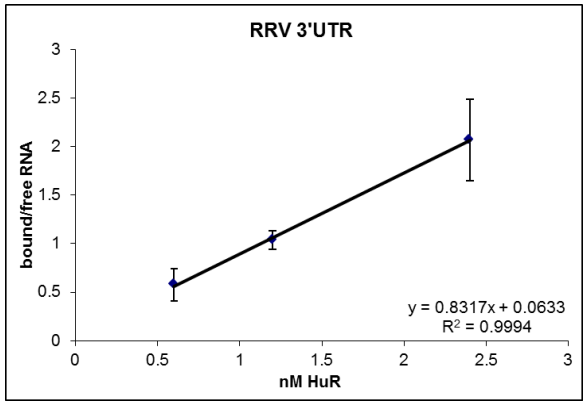

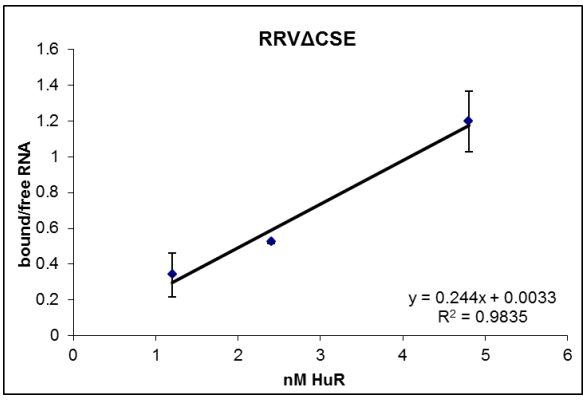
RRVΔCSE
bound/free RNA
nM HuR
y = 0.244x + 0.0033
R² = 0.9835

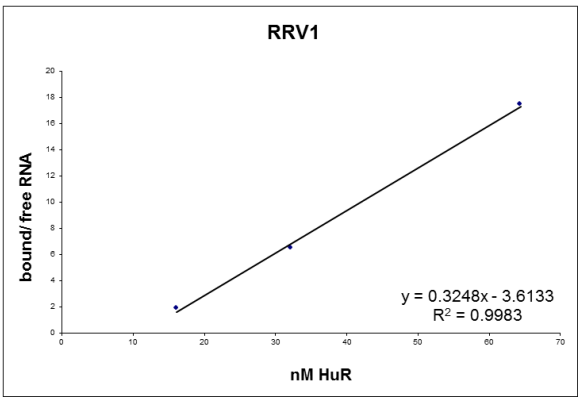
RRV1
bound/ free RNA
nM HuR
y = 0.3248x - 3.6133
R² = 0.9983

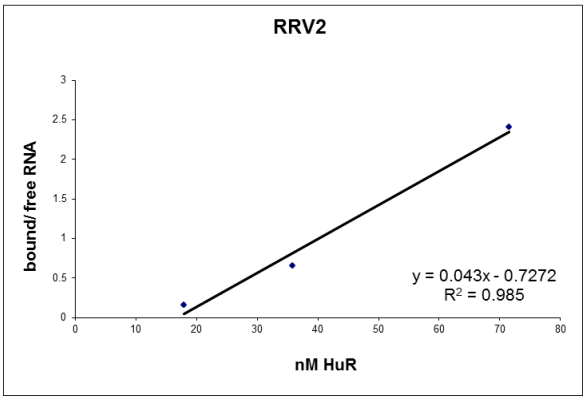
RRV2
bound/ free RNA
nM HuR
y = 0.043x - 0.7272
R² = 0.985

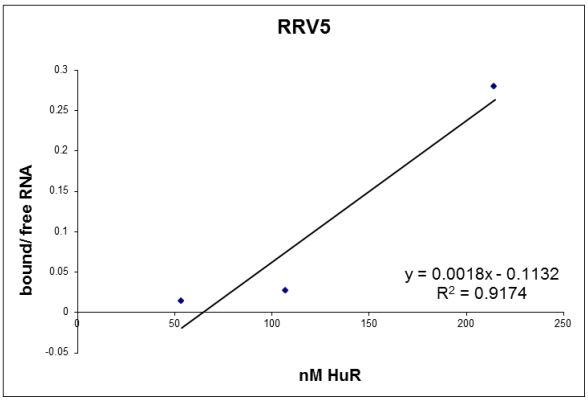
RRV5
bound/ free RNA
nM HuR
y = 0.0018x - 0.1132
R² = 0.9174

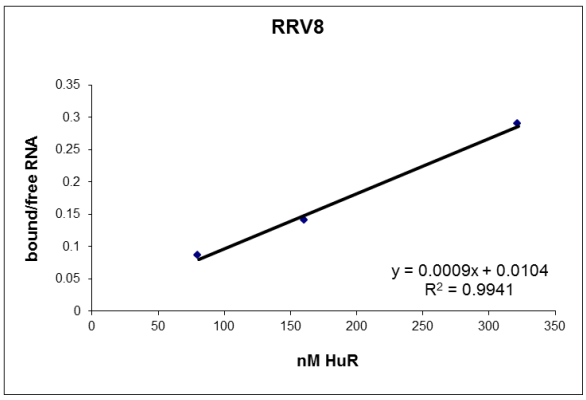
RRV8
bound/free RNA
nM HuR
y = 0.0009x + 0.0104
R² = 0.9941

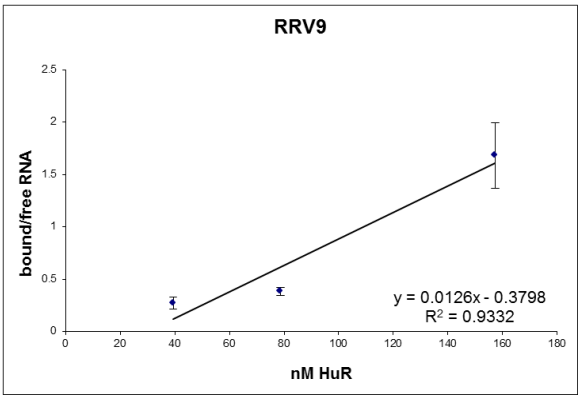
RRV9
bound/free RNA
nM HuR
y = 0.0126x - 0.3798
R² = 0.9332

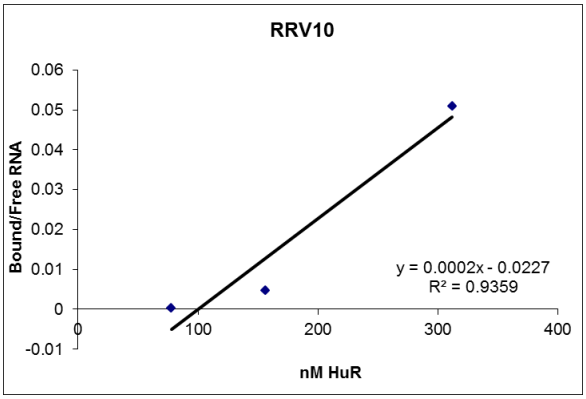
RRV10
Bound/Free RNA
nM HuR
y = 0.0002x - 0.0227
R² = 0.9359

LIST OF ABBREVIATIONS

293T	Human embryonic kidney cell line, T-antigen transformed
ARE	A-rich element
ATP	Adenosine triphosphate
BHK-21	Baby hamster kidney cell line
BSA	Bovine serum albumin
^{o}C	Degrees Celsius
CAF1	CCR4-associated factor 1
CCR4	Carbon catabolite repressor 4
cDNA	Complementary DNA
ChikV	Chikungunya virus
CHX	Cycloheximide
COX-2	Cyclooxygenase 2
CPM	Counts per minute
CSE	Conserved Sequence Element
CTP	Cytidine triphosphate
CUGBP1	CUG-binding protein 1
Da	Daltons
DCP2	Decapping protein 2
DCPS	Decapping protein scavenger
DNA	Deoxyribonucleic acid
dsRNA	Double stranded ribonucleic acid

DTT	Dithiothreitol
E1	Envelope protein1
E2	Envelope protein 2
E3	Envelope protein 3
EDTA	Ethylenediaminetetraacetic acid
EEEV	Eastern equine encephalitis virus
eIF2α	Eukaryotic initiation factor 2α
ELAV	Embryonic lethal abnormal vision
EMSA	Electrophoretic mobility shift assay
FBS	Fetal bovine serum
Fig	Figure
GAPDH	Glyceraldehyde 3-phosphate dehydrogenase
GRE	G-rich element
GTP	Guanidine triphosphate
HCV	Hepatitis C virus
hnRNP	Heterogeneous nuclear ribonucleoprotein particle
hpi	Hours post infection
hr	Hours
HSCB	High salt column buffer
HRP	Horseradish peroxidase
HuR	Human antigen R
IL	Interleukin
K_d	Dissociation constant

kDa	Kilodalton
L	Liter
LB	Luria broth
LSm1-7	Like SM protein complex
mL	Milliliter
MOI	Multiplicity of infection
mRNA	Messenger ribonucleic acid
mRNP	Messenger ribonucleoprotein
NEB	New England Biolabs
NGD	No-go decay
nm	Nanometer
NMD	Nonsense-mediated decay
NSD	Non-stop decay
nsP	Nonstructural protein
OD	Optical density
ONNV	O'nyong-nyong virus
ORF	Open reading frame
PAGE	Polyacrylamide gel electrophoresis
PAN	Poly(A) binding protein-dependent poly(A) nuclease
PARN	Poly(A)-specific ribonuclease
PBS	Phosphate buffered saline
PCBP	Poly(rC)-binding protein
PCI	Phenol chloroform iso-amyl alcohol

PCR	Polymerase chain reaction
RBP	Ribonucleic acid binding protein
RBPDB	RNA Binding Protein DataBase
RdRP	RNA-dependent RNA polymerase
RISC	RNA induced silencing complex
RIG-I	Retinoic acid inducible gene 1
RIPA	Radioimmunoprecipitation assay
RNA	Ribonucleic acid
RNase	Ribonuclease
RNase L	Ribonuclease L
RRM	RNA recognition motif
RSE	Repeat sequence element
RT	Reverse transcriptase
RT-qPCR	Quantitative reverse transcription polymerase chain reaction
SDS	Sodium dodecyl sulfate
SFV	Semliki Forest virus
SinV	Sindbis virus
SKI	Superkiller
SP6	Bacteriophage SP6
T4	Bacteriophage T4
TNF	Tumor necrosis factor
TTP	Tristetraprolin
TUT1	Terminal uridylyl transferase 1

TYMV	Turnip yellow mosaic virus
U	Units
μCi	Microcurie
μg	Microgram
μL	Microliters
URE	Uridine rich element
UTP	Uridine triphosphate
UTR	Untranslated region
v	Volume
v/v	Volume per volume
VEEV	Venezuelan equine encephalitis virus
WEEV	Western equine encephalitis virus
w/v	Weight per volume
XRN1	5’-to-3’ exoribonuclease 1
ZAP	Zinc-finger antiviral protein